

Functional Analysis of Mouse *Wdr13* Gene through Transgenic and Gene Knockout Approaches

SUBMITTED FOR THE DEGREE OF

DOCTOR OF PHILOSOPHY

TO

JAWAHARLAL NEHRU UNIVERSITY
NEW DELHI

BY

Vijay Pratap Singh



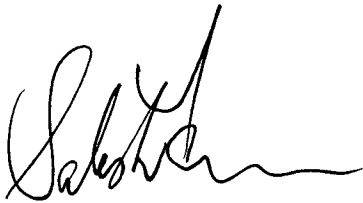
CCMB

Centre for Cellular & Molecular Biology
A constituent laboratory of CSIR

2011

CERTIFICATE

The research work presented in this thesis has been carried out at the Centre for Cellular and Molecular Biology (CCMB), Hyderabad, India. This work is original and has not been submitted in part or full to any other university for any other degree or diploma. The contribution of others has been clearly indicated.



Dr. Satish Kumar
(Thesis Supervisor)



Vijay Pratap Singh
(Student)

To My Family

Acknowledgment

My heartiest gratitude to my mentor Dr. Satish Kumar for all the encouragement, support and the freedom he gave me to plan my research. His supervision and patience has been invaluable in keeping the morale high under trying situations. His guidance and support has helped me to see the finish line of my PhD and I am eternally grateful to him.

My sincere thanks to the Director CCMB, Dr. Ch. Mohan Rao and former Director Dr. Lalji Singh for providing excellent facilities at CCMB to carry out my PhD.

I would like to acknowledge Ms. Jyothi Lakshmi for all her help in conducting animal experiments. My special thanks to Dr. Archana for her guidance in doing some vital experiments.

I thank Mr. D. Partha Sarathi for his help in cell culture and Dr. Jomini Liza Alex, Dr. Sachin Singh and Ms. Purnima Sailasree for their help in embryo manipulation experiments. A special thanks to Dr. Jerald Mahesh Kumar, Jedy Jose and all other Animal House staff for maintaining excellent facilities in the Animal House for conducting experiments smoothly.

I would like to thank Dr. Anant B. Patel, Dr. Sashi Singh and Ms. Uma Prasad for their help and suggestions in various aspects of my work. A word of thanks to Ms. Varalaxmi for helping me in generation of antibody.

I acknowledge Dr. Nandini Nagrajan for her help in microscopy and Mr. Avinash for helping me in tissues sectioning.

I would like to thank all dissertation and summer students- Anand, Ravindra, Shubham, Anupama and Krishna for their contributions in various molecular biology experiments.

I thank all my lab seniors- Chandrashekar, Bony, Rakesh, Vineet, Pushpa, and Sudhamani for their encouragement and support during my PhD. My sincere thanks to all my labmates- Suneesh, Shiladitya, Swathi, Arun, Naireen, Roshan, Chandrashekar, Alok, Shalu and Gopal. Every body has been very nice, helpful and created a joyful environment in and outside the lab.

I would like to thank Rajshekar, Venkatesh and Martha for their sincere efforts in maintaining the cleanliness of the lab. Without their help, it would have been very difficult to conduct experiments.

I am grateful for the cooperation of Mr. Kishore Joshi and all the staff of fine bio-chemicals for providing chemicals on a timely basis. I also thank the instrumentation group and other non-technical groups for making research life smooth at CCMB.

My heartfelt thanks to my close friends Narendra and Anurag, for their interesting discussions that have broadened my views on science in general, and for their queries and suggestions that have influenced my thinking. I extend my thanks to Jaya, Sheikh Nizamudeen, Shameem and Sayantane for their help in many occasions.

I also acknowledge all my batchmates- Pankaj, Anoop, Madhavi, Saurav, Pushpendra, Abhishek, Purnima, Pavan, Aninda, Priyanka for making my stay at CCMB memorable.

It was my M.Sc. Professor, Dr. B.K. Bajaj, who instigated me to pursue a research career in science. His inspiration is duly acknowledged.

It was my father's support, which instilled confidence in me and encouraged me to pursue my PhD to the logical end. I thank my mother, sisters and uncle for their support and encouragement. The love and affection of my wife, Archana has changed my life for the better. I thank Archana for her patience and she always kept my morale high.

I would like to thank CSIR-UGC for providing me fellowship during my PhD.

I am sure that this is not the complete list. I thank one and all for their help.

TABLE OF CONTENTS

LIST OF CHAPTERS
LIST OF FIGURES
LIST OF TABLES
LIST OF ABBREVIATIONS
APPENDIX
LIST OF REFERENCES

LIST OF CHAPTERS

Page No.

CHAPTER 1: INTRODUCTION

| | |
|--|----|
| 1.1 The WD repeat proteins | 2 |
| 1.2 Functional diversity in WD repeat proteins | 4 |
| 1.3 WD repeat proteins in human diseases | 7 |
| 1.4 The <i>Wdr13</i> gene | 8 |
| 1.5 Mouse models to study gene function | 12 |
| 1.6 Generation of <i>Wdr13</i> knockout mice | 14 |
| 1.7 Objectives of the current study | 15 |

CHAPTER 2: MATERIALS AND METHODS

| | |
|---|----|
| 2.1 Isolation of genomic DNA | 16 |
| 2.1.1 Isolation of genomic DNA from mouse tail | 16 |
| 2.1.2 Isolation of genomic DNA from ES cells and MEFs | 16 |
| 2.1.3 Southern analysis of DNA | 17 |
| 2.1.4 PCR analysis of DNA | 19 |
| 2.1.4.1 Primer designing | 19 |
| 2.1.4.2 PCR amplification | 19 |

| | |
|---|----|
| 2.2 RNA analysis | 20 |
| 2.2.1 Northern blot analysis | 20 |
| 2.2.2 Real time PCR analysis | 21 |
| 2.3 DNA manipulation | 23 |
| 2.3.1 Plasmid DNA isolation | 23 |
| 2.3.1.1 Plasmid miniprep | 23 |
| 2.3.1.2 Endotoxin free plasmid maxiprep | 24 |
| 2.3.2 Preparation of ultra competent cells and transformation | 25 |
| 2.3.3 Restriction digestion of plasmid DNA | 26 |
| 2.3.4 Isolation of DNA from agarose gel | 26 |
| 2.3.5 End filling reactions | 27 |
| 2.3.6 Ligation reactions | 27 |
| 2.3.7 Screening of recombinant clones by cracking method | 28 |
| 2.4 Protein analysis | 28 |
| 2.4.1 Western blot analysis | 28 |
| 2.4.2 Immunocytochemistry | 30 |
| 2.5 Phenotypic analysis of mice | 32 |
| 2.5.1 Breeding of <i>Wdr13</i> knockout mice | 32 |
| 2.5.2 Sperm analysis of mice | 32 |
| 2.5.2.1 Isolation of sperm from epididymas | 32 |
| 2.5.2.2 Sperm motility analysis by CASA | 33 |
| 2.5.2.3 Acrosomal reaction | 33 |
| 2.5.3 Weight measurement of mice | 33 |
| 2.5.4 Feed consumption | 34 |
| 2.5.5 Organ weight measurement | 34 |
| 2.5.6 Insulin and triglyceride measurement | 34 |

| | | |
|--------|---|----|
| 2.5.7 | Glucose measurement | 35 |
| 2.5.8 | Histopathological examination of various tissues | 35 |
| 2.5.9 | Cell proliferation assay in pancreas and testis | 36 |
| 2.5.10 | Apoptosis analysis in pancreas and testis | 36 |
| 2.5.11 | Islet isolation and purification | 37 |
| 2.5.12 | MTT assay | 37 |
| 2.6 | <i>In vitro</i> adipogenesis of mouse embryonic fibroblast (MEFs) | 37 |
| 2.6.1 | Isolation and culturing of MEFs | 37 |
| 2.6.2 | Induction of adipogenesis | 40 |
| 2.6.3 | Oil red O staining | 40 |
| 2.7 | Immunoprecipitation and LC-MS/MS | 40 |
| 2.7.1 | Construction of overexpression vectors | 40 |
| 2.7.2 | Transfection of mammalian cells | 46 |
| 2.7.3 | Lysis of mammalian cells and immunoprecipitation | 47 |
| 2.7.4 | Trypsin digestion and LC-MS/MS | 47 |
| 2.8 | Overexpression of <i>wdr13</i> protein in ES cells | 49 |
| 2.8.1 | Construction of pCMV-LNL- <i>Wdr13</i> vector | 49 |
| 2.8.2 | Construction of pHPRT-CMV-LNL- <i>Wdr13</i> vector | 49 |
| 2.8.3 | ES cells culture, electroporation and screening of clones | 49 |

CHAPTER 3: PHENOTYPIC ANALYSIS OF *Wdr13* KNOCKOUT MICE

| | | |
|-------|---|----|
| 3.1 | INTRODUCTION | 56 |
| 3.2 | RESULTS | 60 |
| 3.2.1 | Screening of <i>Wdr13</i> knockout mice | 60 |

| | |
|--|----|
| 3.2.2 Targeting of <i>Wdr13</i> gene leads to null allele | 60 |
| 3.2.3 Effect of <i>Wdr13</i> genotype on litter size | 63 |
| 3.2.4 Unaltered sperm number and motility in <i>Wdr13</i> knockout mice | 63 |
| 3.2.5 Unaltered acrosome reaction of <i>Wdr13</i> knockout mice | 63 |
| 3.2.6 <i>Wdr13</i> knockout mice gained more weight on normal chow in age dependent manner | 66 |
| 3.2.7 Obesity of <i>Wdr13</i> knockout mice gets preponed on high fat diet | 66 |
| 3.2.8 <i>In vitro</i> adipogenesis of mouse embryonic fibroblasts | 66 |
| 3.2.8.1 <i>In vitro</i> differentiation of MEFs to adipocytes | 66 |
| 3.2.8.2 Delayed expression of adipogenic marker during differentiation in knockout fibroblasts | 67 |
| 3.2.9 Hyperinsulinemia in <i>Wdr13</i> knockout mice | 72 |
| 3.2.10 Metabolic parameters in <i>Wdr13</i> knockout mice | 72 |
| 3.2.11 Better glucose clearance in <i>Wdr13</i> knockout mice | 75 |
| 3.2.12 Unaltered insulin sensitivity in <i>Wdr13</i> knockout mice | 75 |
| 3.2.13 Histopathological examination of various tissues | 75 |
| 3.2.14 Increased pancreatic beta cell and spermatogonial cell proliferation in <i>Wdr13</i> knockout mice | 78 |
| 3.2.15 Apoptotic index of pancreatic beta cell and spermatogonial cell | 81 |
| 3.2.16 Cell cycle marker analysis in <i>Wdr13</i> knockout mice | 81 |
| 3.2.17 Overexpression of <i>wdr13</i> causes cell growth retardation | 83 |
| 3.2.18 Overexpression of <i>wdr13</i> causes down regulation of cyclin D2 and cyclin E1 | 83 |
| 3.2.19 Overexpression of <i>wdr13</i> protein in ES cells | 83 |

| | |
|--|-----|
| 3.3 DISCUSSION | 87 |
| 3.3.1 Hyperinsulinemia and obesity in <i>Wdr13</i> knockout mice | 87 |
| 3.3.2 Increased pancreatic islet mass and beta cell proliferation in <i>Wdr13</i> knockout mice | 91 |
| 3.3.3 Overexpression of <i>wdr13</i> causes cell growth retardation | 93 |
| | |
| CHAPTER 4: IDENTIFICATION OF INTERACTING PARTNER OF <i>wdr13</i> PROTEIN | |
| | |
| 4.1 INTRODUCTION | 94 |
| | |
| 4.2 RESULTS | |
| 4.2.1 Overexpression of <i>wdr13</i> protein in mammalian cells | 97 |
| 4.2.2 Immunoprecipitation of interacting proteins with <i>wdr13</i> and their identification by LC-MS/MS | 97 |
| 4.2.3 PHIP1 Interact with <i>wdr13</i> by co-immunoprecipitation and colocalization | 100 |
| 4.2.4 HDAC1, 3 and 7 Interact with <i>wdr13</i> | 103 |
| 4.2.5 HDAC1 and 3 do not interact with PHIP1 | 103 |
| 4.2.6 <i>wdr13</i> protein contains nuclear receptor box (LxxLL) | 104 |
| | |
| 4.3 DISCUSSION | 106 |
| | |
| CHAPTER 5: OVERVIEW | 110 |

LIST OF FIGURES

CHAPTER 1

| | |
|--|----|
| Figure 1.1 The WD repeat protein | 3 |
| Figure 1.2 Evolutionary organization of <i>Wdr13</i> gene | 10 |
| Figure 1.3 Predicted domain structure and post translational modification site of <i>Wdr13</i> | 11 |

CHAPTER 2

| | |
|--|----|
| Figure 2.1 Construction of <i>Wdr13</i> overexpression vectors | 43 |
| Figure 2.2 Construction of pCMV- <i>Myc</i> -PHIP1 vector | 44 |
| Figure 2.3 Construction of adenoviral vector for overexpression of FLAG tag <i>wdr13</i> protein | 45 |
| Figure 2.4 Construction of HPRT targeting vector for <i>wdr13</i> overexpression in mouse | 52 |

CHAPTER 3

| | |
|---|----|
| Figure 3.1 Screening of <i>Wdr13</i> <i>-/0</i> mice | 61 |
| Figure 3.2 Targeting <i>Wdr13</i> gene lead to null allele | 62 |
| Figure 3.3 Sperm motility parameters of wild type and <i>Wdr13</i> <i>-/0</i> mice | 64 |
| Figure 3.4 Body weight, feed consumption and metabolic parameters of <i>Wdr13</i> mutant mice on normal chow and on high fat diet | 68 |
| Figure 3.5 Increased adipose tissue mass in <i>Wdr13</i> knockout mice | 69 |
| Figure 3.6 Adipogenesis in mouse embryonic fibroblast isolated from 13.5 dpc embryo from <i>Wdr13</i> <i>+/+</i> , <i>+/0</i> and <i>-/0,-/-</i> mice, induced by Insulin, IBMX and dexamethasone | 70 |
| Figure 3.7 Glucose homeostasis in <i>Wdr13</i> knockout mice | 74 |

| | |
|--|----|
| Figure 3.8 Glucose tolerance test (GTT) and insulin tolerance test (ITT) of <i>Wdr13</i> knockout mice | 76 |
| Figure 3.9 Histological examination of testis, liver, adipocytes and pancreas from <i>Wdr13</i> knockout mice (-/0) and their wild type littermates(+/0) | 77 |
| Figure 3.10 Pancreatic beta cell proliferation and apoptosis in <i>Wdr13</i> knockout mice | 79 |
| Figure 3.11 Spermatogonial cell proliferation and apoptosis in <i>Wdr13</i> -/0 mice | 80 |
| Figure 3.12 Relative expression of cell cycle regulators in pancreatic islet and testis of <i>Wdr13</i> knockout mice as compared to that of their wild type littermates | 82 |
| Figure 3.13 Overexpression of <i>wdr13</i> protein in MIN-6 and NIH3T3 cell lines and its effects on cell cycle regulation | 85 |
| Figure 3.14 Overexpression of <i>wdr13</i> protein in ES cells | 86 |

CHAPTER 4

| | |
|--|-----|
| Figure 4.1 Identification of interacting proteins of <i>wdr13</i> by Immunoprecipitation | 98 |
| Figure 4.2 Interaction of <i>wdr13</i> with PHIP1 by coimmunoprecipitation and immuno-colocalization | 101 |
| Figure 4.3 Interaction of <i>wdr13</i> , HDACs and PHIP1 | 102 |
| Figure 4.4 Presence of LxxLL motif in <i>wdr13</i> protein | 105 |

LIST OF TABLES

CHAPTER 2

| | |
|---|----|
| Table 2.1-Transfection of various cell lines using Xfect™ | 46 |
| Table 2.2- MEFs seeding density chart | 55 |

CHAPTER 3

| | |
|---|----|
| Table 3.1- Effect of <i>Wdr13</i> genotype on litter size | 65 |
| Table 3.2- Effect of <i>Wdr13</i> genotype on percent acrosome reaction | 65 |
| Table 3.3-Weight (in grams) of various organs of <i>Wdr13</i> mutant and their wild type littermates at the age of 12 months on normal chow | 71 |
| Table 3.4-Various metabolic parameters of <i>Wdr13</i> mutant and their wild type littermates at the age of 12 months on normal chow | 73 |

CHAPTER 4

| | |
|---|----|
| Table 4.1-List of proteins identified by LC-MS/MS | 99 |
|---|----|

LIST OF ABBREVIATIONS

| | |
|-------|---|
| bp | base pair |
| BCIP | 2-Bromo, 3-Chloro indolyl phosphate |
| BSA | bovine serum albumin |
| DAPI | 4',6-Diamidino-2-phenylindole dihydrochloride |
| DEPC | Diethylpyrocarbonate |
| DNA | Deoxyribonucleic acid |
| dNTP | deoxyribonucleotide phosphate |
| DMSO | Dimethyl sulfoxide |
| DTT | Dithiothreitol |
| EDTA | Ethylenediaminetetraacetic acid |
| ES | Embryonic stem |
| h | Hour |
| HCl | Hydrochloric acid |
| Kb | kilo base pair |
| kDa | kilo dalton |
| LB | Luria Bertani |
| LIF | Leukemia inhibitory factor |
| MEFs | Mouse embryonic fibroblasts |
| μg | microgram |
| μl | microliter |
| μM | micromolar |
| mM | millimolar |
| mm | millimeter |
| MCS | multiple cloning site |
| NaOAc | Sodium Acetate |
| OD | optical density |
| % | Percent |

| | |
|----------------|---|
| PAGE | polyacrylamide gel electrophoresis |
| PBS | phosphate buffered saline |
| PCR | polymerase chain reaction |
| PFA | Paraformaldehyde |
| RNA | Ribonucleic acid |
| RT | room temperature |
| SAP | Shrimp Alkaline Phosphatase |
| SDS | Sodium dodecyl sulphate |
| SSC | Sodium Citrate, Sodium Chloride |
| <i>Taq</i> | <i>Thermus aquaticus</i> |
| TBST | Tris buffered saline containing Tween -20 |
| TE | Tris EDTA |
| TEMED | N,N,N',N'-tetramethylene diamine |
| T _m | melting temperature |
| Tris | Tris(hydroxyl methyl) aminomethane |
| UTR | Un-translated region |
| WD | Tryptophan-Aspartate |
| X-gal | 5-Bromo-4-chloro-3-indolyl- <i>b</i> -D-galactosidase |

SYNOPSIS

Title: Functional Analysis of Mouse *Wdr13* Gene through Transgenic and Gene Knockout Approaches

Student Name: Vijay Pratap Singh

Thesis Supervisor: Dr. Satish Kumar

Introduction:

Over the past several years the massive collaborative efforts from all over the world helped to determine the complete genomic sequences of various organisms. The next challenge is to decipher the functional correlates of patterns embedded in these sequences. On the basis of DNA sequence similarities and predicted proteins, various proteins have been classified in different families. WD repeats protein family is an example of such families. WD repeats proteins contain 4-16 WD repeats. Each WD repeat contains 40-60 amino acids and four antiparallel beta strands. These WD repeats contain GH dipeptide at N-terminal and WD dipeptide at C-terminal. WD repeat proteins have diverse functions in various cell processes, including, signal transduction, cell cycle, chromatin organization, vesicular trafficking and apoptosis. Variation in number of WD repeats and sequence length of these repeats provide structural and functional diversity to WD repeat proteins (Li and Roberts, 2001; Smith et al., 1999).

wdr13 is a member of WD repeat protein family and contains five WD repeats with various putative posttranslational modification sites (D'Agata et al., 2003). This gene is present in all vertebrates examined thus far, and the genomic organization is conserved. In invertebrates, a homologue of this gene has been identified only in honeybee (Suresh et al., 2005). In mouse, the gene is expressed in most of the tissues with maximum expression in brain, testis,

ovary and pancreas. The complete ORF encodes for a protein of 485 amino acids and the same is localized into the nucleus. The conservation of *Wdr13* gene through evolution, expression in unfertilized egg, neural stem cells, and germ cells provides strong evidence that the protein has an essential role in development and fertility (Suresh et al., 2005). To understand the *in vivo* function(s) of *wdr13* protein, the knockout mouse strain lacking this gene was created using mouse embryonic stem cells.

Objective of the thesis:

The primary objective of the present study was to understand *in vivo* function(s) of *Wdr13* gene through the following approaches:

- 1) Analysis of the phenotype of *Wdr13* knockout mice
- 2) Overexpression of the *wdr13* protein in various cell lines and analysis of the resultant cellular phenotype
- 3) Identification of protein(s) interacting with *wdr13*, and therefore, understanding of the molecular mechanism(s) of *wdr13* action

Results:

The *Wdr13* knockout mice were viable and fertile without any overt phenotype till the age of sexual maturity. However, the mutant mice developed obesity in an age dependent manner. At eleven months of age, the knockout animals weighed significantly more than their wild type littermates when fed normal chow. However, the obesity phenotype was preponed to five months on high fat diet. *In vitro* adipogenesis using mouse embryonic fibroblasts (MEFs) from mutant and wild type mice did not reveal any differences in the extent of adipogenesis. The mutant mice developed hyperinsulinemia with age and this phenotype was preponed on high fat diet. The increase in insulin level was further accompanied by increased pancreatic islet mass and better glucose clearance in *Wdr13* knockout mice. However, insulin sensitivity of

mutant mice was similar to that of their wild type littermates, suggesting that the increased insulin level was not due to insulin resistance in mutant mice. The increased islet mass was due to increased beta cell proliferation as measured by *in vivo* BrdU labeling experiments. The enhanced cell proliferation property was not limited to beta cells only, but this was also observed in testicular spermatogonial cells of *Wdr13* knockout mice. However, the enhanced spermatogonial cells proliferation did not lead to increase in sperm numbers and it appeared that enhanced cell proliferation was being compensated by increased apoptosis. While the higher cell proliferation in pancreatic beta cells was due to upregulation of cyclin E1 and in case of spermatogonial cells it was caused by upregulation of cyclin D2. Consistent with these observations, the overexpression of *wdr13* caused suppression of cell proliferation in MIN-6 and NIH3T3 cells and the same was mediated through downregulation of cyclin D2 and cyclin E1.

The WD repeats in WD proteins provide platforms for protein-protein interaction (Li and Roberts, 2001). The immunoprecipitation experiments using FLAG tagged *wdr13* protein led to identification of PHIP1, HSPs, HDAC7 and NR2E1 as interacting proteins as revealed by LC-MS/MS. The interactions of PHIP1 and HDAC7 with *wdr13* were further confirmed by coimmunoprecipitation experiments. To identify interactions of *wdr13* with other repressor molecules like HDAC7, HDAC1 and HDAC3 were also identified as novel *wdr13* interacting proteins through coimmunoprecipitation experiments. The interactions of *wdr13* with various HDACs and the presence of LxxLL motif in this protein suggest that *wdr13* may function as a co-repressor of transcription.

Conclusions:

The *Wdr13* knockout mice are viable and fertile with no overt phenotype till the age of 2 months. However, the mutant mice gained more weight with age as compared to their wild type littermates. It appears that increase in body

weight is primarily due to increase in insulin level. The increase in cyclin E1 causes enhanced beta cell proliferation, which leads to the increased islet mass, and finally resulting into hyperinsulinemia and better glucose clearance in the mutant mice. Given the higher insulin levels and the lack of any evidence for insulin resistance in *Wdr13* knockout mice, this protein may be a potential candidate drug target for ameliorating the impaired glucose metabolism in diabetes. On the other hand overexpression on *wdr13* protein causes reduction in cell proliferation due to reduced levels of cyclin D2 and Cyclin E1 transcripts. Thus, *wdr13* agonists may be useful in reducing cell proliferation. The presence of five WD repeats, LxxLL motif and the interactions of this protein with various HDACs suggest that the *wdr13* may act as a co-repressor by recruiting various HDACs to the chromatin.

References:

D'Agata, V., Schreurs, B.G., Pascale, A., Zohar, O., and Cavallaro, S. (2003). Down regulation of cerebellar memory related gene-1 following classical conditioning. *Genes Brain Behav* 2, 231-237.

Li, D., and Roberts, R. (2001). WD-repeat proteins: structure characteristics, biological function, and their involvement in human diseases. *Cell Mol Life Sci* 58, 2085-2097.

Smith, T.F., Gaitatzes, C., Saxena, K., and Neer, E.J. (1999). The WD repeat: a common architecture for diverse functions. *Trends Biochem Sci* 24, 181-185.

Suresh, A., Shah, V., Rani, D.S., Singh, B.N., Prasad, G.U., Subramanian, S., Kumar, S., and Singh, L. (2005). A mouse gene encoding a novel member of the WD family of proteins is highly conserved and predominantly expressed in the testis (*Wdr13*). *Mol Reprod Dev* 72, 299-310.

Chapter 1

CHAPTER 1: INTRODUCTION

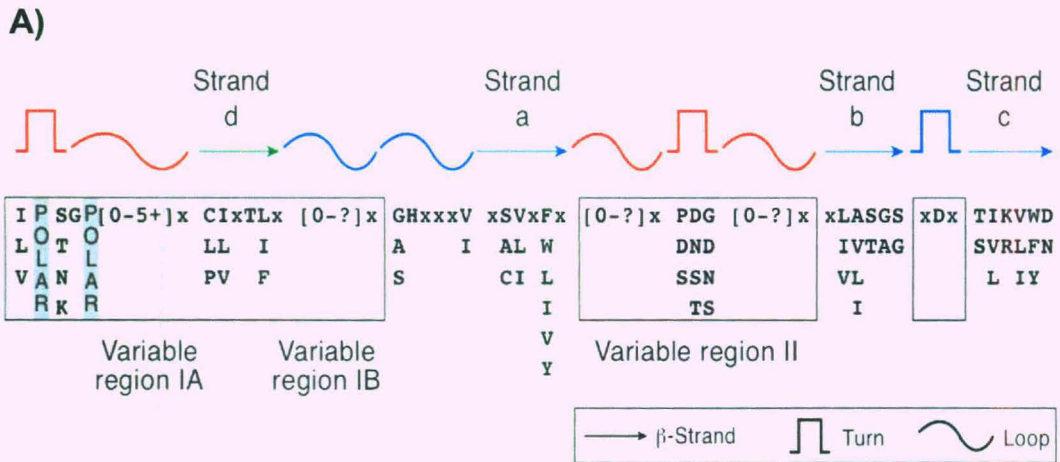
The massive collaborative effort from all over the world helped to determine the complete genomic sequences of various organisms over the past few years. One of the great achievements in this sequencing effort has been the complete sequencing of the human genome. However, the real challenge and the task that now lies ahead are to decipher functional correlates of the patterns embedded in these sequences. Comparative genomic studies between human and other organisms has already led to the discovery of a number of genes associated with various diseases. In post-genomic era, comparative genomic studies will further help determine the yet unknown function of thousands of other genes. Comparing the DNA sequences of entire genomes of different organisms will also help us understand human evolution and the common biology we share all of life. On the basis of DNA sequence similarities and predicted proteins, various genes have been classified among various families. These protein families serve similar biological function across different species or have adopted different function during evolution. The examples of protein families on basis of functional similarities are polycomb-group proteins family, MAP kinases family, immunoglobulin proteins family, and G-protein family where as on basis of sequence similarities are homeodomain proteins families, zinc-finger proteins families, bromodomain protein families, PHD domain families and WD domain family.

The WD repeat protein family has a large group of proteins, which are mainly present in eukaryotic organisms (Smith, 2008; Smith et al., 1999). However, some WD repeat proteins have been identified in prokaryotes like, *Cyanobacterium* and *Thermomonosora*, which are blue-green alga. The whole genome sequence analysis indicates that there are 136 WD-repeat proteins in humans, 98 in *Drosophila melanogaster*, 72 in *C. elegans* and 56 in *S. cerevisiae* (Li and Roberts, 2001). It would appear that the WD-repeat family either expanded in the ancestors of the eukaryotes or during the early diversification of eukaryotes.

1.1 The WD repeat proteins

These proteins contain 4 to 16 typical WD repeats and form beta propeller structure (Smith et al., 1999). Each WD repeat contains 40-60 amino acids. They typically have GH (Glycine-Histidine) dipeptide 11-24 residues from its N-terminus and WD (Tryptophan-Aspartic acid) dipeptide at the C-terminus (Figure 1.1A). Between these two conserved dipeptide motifs there is an approximately 40-amino acids core sequence and the latter is not conserved across various family members (Figure 1.1A). In each WD repeat there are four anti-parallel beta strands; namely, a, b, c and d. The sequence length between strand c of one WD repeat and strand a of the next repeat which includes strand d of the first repeat is variable (11 to 150 aa). This region is called as variable region I. The second variable region lies between strand a and strand b given as variable region II. The length of this region is 2-30 residues. The diversity in WD repeat proteins gets generated in two different ways- 1) the sequence variation within variable region I and II, and 2) the number of WD repeats within a given protein.

The WD repeat proteins form beta propeller structure. However, some non WD repeat proteins also form beta propeller structure. One major difference between WD repeat proteins and the non WD repeat propellers is that there is no evidence that WD repeat portion of any protein has enzymatic activity. By contrast, several non WD repeat propeller have enzymatic activity (methylamine dehydrogenase). As stated above each WD repeat contains four beta strands. However, the sequence repeat does not correspond to the four strands of a single blade of the propeller but, to the first three strands of one blade and fourth strand of the next blade. The last blade, which includes the C-terminal of the protein makes contact with N-terminal region of first WD repeat. This overlap forms the 'velcro snap' that fastens the propeller structure to form a close ring. All the known propeller proteins appear to have some mechanism for holding the ring shut. This sharing of one strand between two blades is believed to stabilize the molecule.



B)

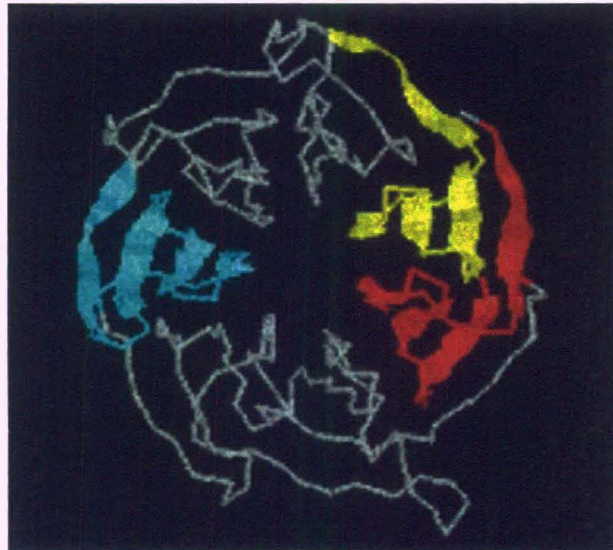


Figure 1.1 The WD repeat protein. A) The WD repeat consensus sequence. B) The structure of $G\beta$, the prototypical seven bladed WD repeat protein having a β -propeller structure. Each blade (one of which is shown in blue) of the propeller consists of a single four-stranded antiparallel β -sheet. The N-terminal and C-terminal WD repeats has been shown in red and yellow, respectively. (TIBS 24 –MAY 1999)

The crystal structure for G β protein is known (Wall et al., 1995). Each of the seven WD repeats of the G β protein folds into four strands of an antiparallel β sheet and these sheets are arranged around a central pseudosymmetrical axis into a circular β propeller with the inner most β strand being nearly parallel to the axis of central tunnel (Figure 1.1B).

The WD repeat motif can coexist with other motif in same protein. The WD repeat protein p57 contains a leucine zipper and actin binding motif (Liu et al., 2006). The other motif coexisting with WD repeat domain includes the zinc-binding motif (*COP1*) (Deng et al., 1992), F-box (*FBW7*) (Welcker and Clurman, 2008), a caveolin-binding motif, a coiled-coil structure, a calmodulin-binding domain (Zinedine, SG2NA, striatin) (Castets et al., 2000), the kinase catalytic domain (Steimle et al., 2001), bromodomain (Philipps et al., 2008; Podcheko et al., 2007), and a KEN box (Pfleger and Kirschner, 2000). *FBW7* is well characterised F-box and WD repeat containing protein. *FBW7* is the substrate recognition component of SCF (complex of *SKP1*, *CUL1* and F-box protein) type ubiquitin ligase. SCF^{*FBW7*} degrades several proto-oncogenes; namely, *myc*, cyclin E, notch and JUN and serve as tumour suppressor (Welcker and Clurman, 2008). These additional motifs provide more functional diversity to WD repeat proteins. WD repeat proteins can be found in various subcellular compartments and organelles of cells due to presence of signal sequences. The proteins that have role in chromatin assembly and transcription regulation are found in nucleus, while proteins involved in golgi vesicular trafficking are found in cytoplasm.

1.2 Functional diversity in WD repeat proteins

With conservative beta propeller structure WD repeat proteins have extremely diversified functions including signal transduction, RNA synthesis, vesicular trafficking, cytoskeleton assembly, cell cycle control, apoptosis and chromatin organization.

Signal transduction

In addition to the classical G proteins, there are many other WD repeat proteins involved in signal transduction, namely *RACK1*, *STE4*, *LIS1*, *MSI1*, *PR55*, *PLAP*, *rbAp-48* and *striatin*. RACKs (receptors for activated c-kinase) are necessary for the function of protein kinase C (*PKC*). *RACK1* is necessary for membrane anchorage of beta adrenergic receptor kinases suggesting role for *RACK1* in *PKC* mediated signalling (Ron et al., 1994). *Striatin*, a member of the WD repeat family is the first member known to bind with calmodulin in presence of Ca^{2+} and have role in Ca^{2+} signalling (Castets et al., 1996).

RNA synthesis and processing

Many WD repeat proteins have been reported that have role in RNA synthesis and processing. TFIID is a multiprotein complex containing the TATA box binding protein (*TBP*) and several tightly associated factors (*TAFs*). Majority of *TAFs* contain multiple WD repeat and help in transcription (Roberts, 2000). One of the multiple factors required for polyadenylation of mammalian pre-mRNA is cleavage stimulation factor (*CSF*), has three distinct subunits of 77, 64 and 50 kDa. The 50 kDa subunit has multiple WD repeats and required for mRNA processing (Takagaki and Manley, 1992).

Vesicular trafficking

Specific proteins involved in vesicular budding, translocation and fusion with target membranes mediate intracellular vesicular trafficking. The coated vesicles derived from golgi, called as coatamer contain a set of coat proteins of relative molecular mass 160 (α -*COP*), 110 (β -*COP*), 98 (γ -*COP*), 61 (δ -*COP*) kDa, and several smaller subunits. Most of the α - and β -*COP* proteins belong to WD repeat proteins. These *COPs* proteins are essential component of coatamers (Chow and Quek, 1996; Duden et al., 1991; Waters et al., 1991).

Cytoskeleton assembly

Many WD repeat proteins have been shown to be associated with actin and dyenin. The *Arp2/3* protein complex has been implicated in the control of

actin polymerization. This complex contains seven subunits known as actin related protein *Arp2*, *Arp3* and five other known as *p41-Arc*, *p34-Arc*, *P21-Arc*, *P20-Arc* and *P16-Arc*. *P41-Arc* is a member of WD repeat protein and have role in activity and/or localization of the complex (Welch et al., 1997).

Cell cycle regulation

The anaphase-promoting complex (*APC*), that governs sister chromatid separation to cytokinesis, is a multisubunit assembly that triggers the ubiquitin –dependent proteolysis of key regulatory proteins. Many of these regulatory factors are members of the WD repeat family. *APC* is activated during mitosis and G1 by two regulatory factors, *CDC20* and *HCDH1*. The WD repeat protein *CDC20* directly activates *APC* (Shirayama et al., 1998).

Programmed cell death

The apoptotic protease activating factor-1 (*Apaf-1*) was identified as a proximal activator of caspase-9 in cell death pathway that triggers mitochondrial damage and cytochrome c release and finally leads to cell death. The C-terminal of *Apaf-1* contains 12 WD repeat and has role in protein-protein interactions (Zou et al., 1997). The mechanism by which *Apaf-1* works is by clustering of caspase-9 molecule, thereby auto processing of adjacent zymozen.

Chromatin assembly

WD repeat proteins play essential roles in a variety of chromatin modifying complexes (Tyler et al., 1996; Verreault et al., 1996). Chromatin assembly factor-1 (*CAF-1*) is essential for chromatin assembly in eukaryotes and comprises of three subunits *p150*, *p60* and *p48*. The *p48* is a member of WD repeats proteins. Other Four WD repeat proteins – *WDR5*, *RbBp5*, *RbAp48/46* (each with seven repeats) and *Drosophila* homolog of *RbAp48/46*, *p55* are component of histone modifying complexes and have interaction with either histone H3 or H4 (Suganuma et al., 2008b).

1.3 WD repeat proteins in human diseases

Many disease-causing mutations have been identified in humans. Such knowledge does not only improve our understanding of the disease processes, but is also critical in delineating gene functions. Mutations in several WD repeat proteins have been implicated in various human diseases.

The lissencephaly-1 gene (LIS1) was the first WD-repeat gene identified as responsible for a human disease. In lissencephaly brain develops without convolutions or gyri. The point mutations or deletions of LIS1 gene have been identified by DNA sequencing of lissencephaly patients (Lo Nigro et al., 1997; Neer et al., 1993). The amino acid sequences of LIS1 shows significant homology with G protein beta subunit, with multiple WD repeats in their primary structure, suggesting that it may be involved in signal transduction pathway crucial for cerebral development (Reiner et al., 1993).

Cockayne syndrome (CS) is an autosomal recessive disease characterised by slow and abnormal development that becomes evident within a few year after birth. Two clinical types of cockayne syndrome (CS); namely, CSA and CSB have been identified and these are related to two diseases genes *CSA* and *CSB*, respectively. The *CSB* gene encodes for a protein with DNA unwinding function, i.e., a helicase (Troelstra et al., 1992). However, *CSA* gene encodes a 396-amino acid protein containing five WD repeats (Henning et al., 1995). The *CSA* protein interacts with *CSB*, and p44 - a subunit of human RNA polymerase II transcription factor IIH. These observations suggest that the products of these interactions are involved in transcription (Henning et al., 1995).

Triple-A syndrome is an autosomal recessive disorder characterized by adrenocorticotropin hormone (ACTH)-resistant adrenal insufficiency, achalasia of the oesophageal cardia, and alacrima. The syndrome is also known as Allgrove syndrome. The corresponding gene - *AAAS* encodes a protein of 547 amino acids with four WD repeats at the N-terminal, and mutations have been found in this gene in affected individuals. The predicted product of the *AAAS*

gene, aladin (alacrima-achalasia-adrenal insufficiency neurologic disorder), belongs to the WD repeat family of regulatory proteins (Handschug et al., 2001; Tullio-Pelet et al., 2000).

1.4 The *Wdr13* gene

Wdr13 is a member of WD-repeat protein family, isolated in a study aimed at identification of testis-specifying factors by screening of a testis cDNA library using a genomic sub-clone that hybridized with Banded Krait minor satellite DNA known to be associated with sex-determining chromosomes (Singh et al., 2003). The gene has been mapped on X-chromosome at position Xp11.23 in humans and at position XA1.1 in mouse (Suresh et al., 2005).

The genomic organization of the *Wdr13* is conserved across all the vertebrate phyla with the homologs from humans; chimpanzee, mouse, rat and puffer fish showed the presence of nine exons and eight introns arrangement. The gene is conserved through out evolution from fishes to mammals. The homolog of this gene has been identified from *Danio reeio*, *Fugu rubripipes*, *Xenopus tropicalis*, *xenopus laevis*, *Bos Taurus*, *Sus scrofa* and *Ciona intestinalis* (Suresh et al., 2005). In invertebrates this gene is present only in *Apis mellifera*, which has genomic organization of four exons and three introns spanning 2.2 kb of the genome, with 1.3 kb ORF which encodes 435 amino acids. In the vertebrates the coding sequences are highly similar that is evident by 99% identity between human, chimpanzee, rat and mouse. In the vertebrates in spite of same organization, the size of gene varies due to intronic size variation, which is evident by the variation in the size of complete gene; Apies ~ 2kb, Fugu ~ 4kb, mouse ~ 8 kb, Rat ~13 kb, chimpanzee ~ 7 kb and human ~ 7.3 kb (Figure 1.2). In spite of variation in intronic sequences there is identity between various homologs like; human – chimp (87-99%), mouse – rat (30-92%), Human – mouse (26-77%) and human – fugu (1-35%) (Suresh et al., 2005).

The *Wdr13* gene expresses ubiquitously in most of the tissues analyzed including brain, liver, heart, pancreas, kidney, lung, thymus, placenta, skeletal muscle, embryo, prostate, testis and ovary. The maximum expression is in brain, pancreas, testis and ovary. In human two types of transcript have been reported as a result of alternate splicing. The size of transcript is 3 kb and 2 kb in humans (Singh et al., 2003; Suresh et al., 2005). In the mouse the size of transcript is 4 kb from all tissues except from testis, where it is 2 kb as a result of variation in the 3' UTR region.

The complete ORF of *Wdr13* gene encodes a protein of 485 amino acids in mouse and human. The predicted structure of *wdr13* protein has five WD repeats; namely, 160-201, 206-245, 248-289, 394-437 and 442- 481 (Figure 1.3). In addition to WD repeats, there are putative cAMP-cGMP dependent protein kinase phosphorylation sites, casein kinase II phosphorylation sites, and N-glycosylation sites (D'Agata et al., 2003). These post-translational modification sites may have regulatory roles in *wdr13* function.

Agatha *et al.* (2003) have reported that down regulation of *Wdr13* following classical conditioning, which involve neutral stimulus along with stimulus of something significant (pre-orbital electrical stimulation and nictating membrane recording) and named this gene as cerebellar memory related gene-1 (D'Agata et al., 2003). In humans, X chromosomal deletions including this gene have been associated with mental retardation, obesity and xeroderma (Price et al., 2003; Whibley et al., 2010). Hattab et al., has reported that ~1.3 Mb tandem duplication at Xp11.23p11.3 in an 11-year-old boy with pleasant personality, hyperactivity, learning and visual-spatial difficulties, relative microcephaly, long face, stellate iris pattern, and periorbital fullness. The duplicated region contain three X-linked mental retardation gene; namely, *FTSJ1*, *ZNF81*, and *SYN1*. The authors have shown overexpression of *EBP*, *WDR13*, and *ZNF81* (El-Hattab et al., 2010). The multicopy gene *Slx* and *Slx1* knockdown using RNAi in mouse has shown in defects in spermatid differentiation and down regulation of *Wdr13* gene (Cocquet et al., 2010).

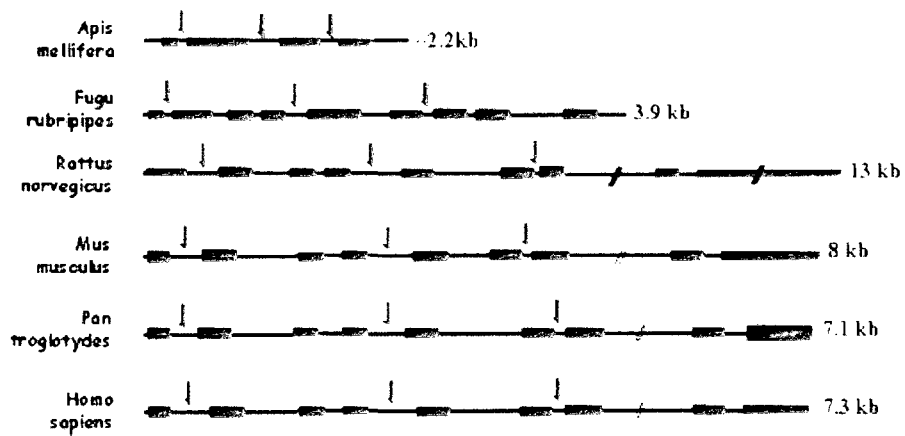


Figure 1.2 Evolutionary organization of *Wdr13* gene (Suresh et al., 2005). The boxes represent exons while black line represents intronic region. The arrows indicate the introns in the invertebrate gene (1, 2, and 3) that correspond to the positions 1, 4, and 6 in the chordate homologs. The invertebrate homolog shows different genomic organisation while chordate genes vary in the size of the gene.

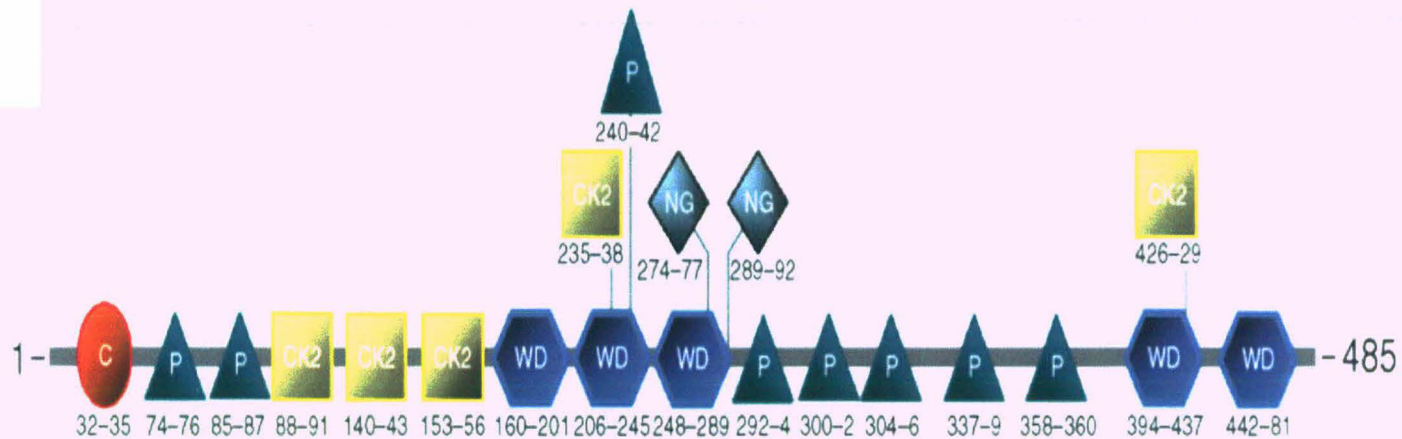


Figure 1.3 Predicted domain structure and post translational modification site of *Wdr13*.

Abbreviations: C, cAMP-cGMP dependent protein kinase phosphorylation site; CK2, casein kinase II phosphorylation site; NG, N-glycosylation site; p, Protein kinase C phosphorylation site; WD, WD repeat. (*Genes, Brain and Behaviour* (20003) 2: 231-237)

1.5 Mouse models to study gene function

A model organism is a species selected to either address a fundamental biological question (e.g. cell division) or to study a particular biological phenomenon (e.g. organismal development) or to recreate a non physiological scenario most commonly afflicting human beings (e.g. cancer, heart disease or neurodegeneration). A model organism is chosen due to its simplicity, inherent morphological features or oddities, past research history or technical advantages coupled with possibility of extrapolating the results obtained to other organisms especially humans.

Some of the popular model organisms used in research and development are *Escherichia coli*, *Saccharomyces cerevesiae*, *Arabidopsis thaliana*, *Caenorhabditis elegans*, *Drosophila melanogaster*, *Danio rerio*, and *Mus musculus*. The success of a scientific study does not only depend upon the choice of the right biological question but also on the choice of a suitable model system. *Mus musculus*- the laboratory mouse is the most commonly used mammalian model system. Mouse is an attractive mammalian model because of its small size, short life cycle, high fecundity and availability of various inbred and out-bred strains. Laboratory mice have large number of inbred strains in which individuals are genetically identical and homozygous at all loci. The coat colour genetics of mice is one of the most well studied fields in mouse genetics, which is utilized in breeding experiments. The laboratory mice have gestation period of 18 to 20 days depending on the strains. By three weeks of age the pups are developed completely and independent enough to be weaned away from the mother. Females attain sexual maturity by 6 weeks and males by 8 weeks.

Many genetics and molecular resources are available for mouse. Mouse Genome Information (MGI) maintains a database of mutant, transgenic and other variant mice, which have been published. Gene trap libraries of mutated genes in ES cells are generated by random integration of gene trap vector

DNA into ES cells. These serve as valuable resource to study loss of function of gene involved in particular process by generating knockout mice from gene trap ES cell lines. International gene trap consortium and the Texas Institute of Genomic Medicine are major repositories of gene trap libraries. Conditional gene trap libraries are also available from European conditional mouse mutagenesis (EUCOMM) program. BAC library clones for several mouse strains are available. Mutagenic insertion and chromosome Engineering Resources (MICER) is a resource of gene targeting vectors (Adams et al., 2004; Liu et al., 2011). Fully annotated sequence of mouse genome is a valuable tool for mouse genetists.

Generation of transgenic mice by microinjection or lentivirus vector is a well-established system in mouse. Until 2008 (Buehr et al., 2008; Li et al., 2008) mouse was the only mammal from which germ line competent ES cells were available (Evans and Kaufman, 1981). The mouse ES cells are able to efficiently support homologous recombination between chromosomes and extraneously introduced DNA fragments. ES cells can be propagated *in vitro* under conditions that inhibit differentiation and preserve pluripotency. When injected into developing mouse blastocyst, these cells can resume normal development and contribute to most or all cell lineages including germ line (Bradley et al., 1984). These cells can be genetically modified and be used to reconstitute animals (Baribault and Kemler, 1989; Capecchi, 1989). This ability of mouse ES cells has been exploited extensively by mouse geneticists to generate transgenic, knockout and conditional knockout mice, which have illuminated the role of many genes involved in developmental and physiological process in mammals. Moreover mouse development is extensively analyzed and mouse is routinely utilized as model system to study mammalian development.

Embryonic stem cells were isolated in 1981 by Evans and Kaufmann. The pluripotency of these cells was demonstrated by their ability to differentiate *in vitro* after with-drawl of feeder layers and formation of

teratomas in syngeneic mice (Evans and Kaufman, 1981). Bradley *et al.*, demonstrated that ES cells could contribute to germ line when injected into host blastocysts (Bradley *et al.*, 1984). Mouse ES cells are cultured in pluripotency state by addition of Leukemia inhibitory Factor (LIF) (Smith *et al.*, 1988). Removal of LIF from the ES cell culture media leads to spontaneous differentiation of ES cells. Pluripotency of the ES cells is attributed to transcription factor OCT4, NANOG and SOX2 that can induce reprogramming of terminally differentiated cells to pluripotent stem cells (Takahashi and Yamanaka, 2006).

1.6 Generation of *Wdr13* knockout mice

The function of *Wdr13* was not known. Given the conservation of *Wdr13* gene through out the evolution of vertebrates it was hypothesized that this gene would have a distinct role. To understand the *in vivo* function of this protein, the *Wdr13* gene was knocked out in mouse germ line (CCMB Annual Report - 2008). The targeting strategy has been given in figure 3.1A. Briefly, to construct a *Wdr13* gene-targeting vector, a 7.1 kb HindIII fragment of this gene including exon1 to exon7 was sub-cloned in pBluescript II KS vector (Stratagene) from a 13.3 kb genomic DNA fragment. A 1.35 kb region of this gene including exon 2 and exon 3 (partial) was replaced by XhoI-SalI fragment of pMC1neo Poly A (Stratagene). To further enrich the targeting efficiency, HSV-tk gene was placed before 5' end of the homologous sequences. The resulting vector had homologies of 1.6kb and 4.1kb at 5' and 3'end, respectively. Forty micrograms of linearized targeting vector DNA was electroporated into R1 ES cells. The ES cells were selected with G418 (0.25 mg/ml) and ganciclovir (2 μ M). To identify targeted clones, genomic DNA was isolated from ES cell clones and southern hybridization was performed using a 700bp EcoRV-BamHI fragment from 5' end of this locus. One of the targeted clones was injected into 3.5-dpc C57BL/6 blastocysts and the latter were transferred into the uteri of CD1 pseudopregnant females. To obtain germline

transmission of mutant allele, chimeric male mice were mated with CD1 female.

1.7 Objectives of the current study

The primary aim of the present study was to understand *in vivo* function(s) of *Wdr13* gene through the following approaches:

- 1) Analysis of the phenotype of *Wdr13* knockout mice
- 2) Overexpression of the *wdr13* protein in various cell lines and analysis of the resultant cellular phenotype
- 3) Identification of protein(s) interacting with *wdr13*, and therefore, understanding of the molecular mechanism(s) of *wdr13* action

Chapter 2

CHAPTER 2: MATERIALS AND METHODS

2.1 Isolation of genomic DNA

2.1.1 Isolation of genomic DNA from mouse tail

Mice were anesthetized with 1.25 % avertin (Sigma) according to their body weights to cut the tail tips for genomic DNA isolation. Tails were collected in micro centrifuge tubes kept on ice. Tails were lysed over night at 55°C in tail lysis buffer (20mM Tris- buffer pH8.0, 5mM EDTA, 400mM NaCl, 1% SDS and 400µg/ml proteinase K). Next morning one volume of phenol-chloroform-isoamyl mixture (25:24:1) was added to the lysed tails and mixed properly. Tubes were centrifuged at 10,000g for 5 minutes. The aqueous phase containing the DNA was transferred to separate tube and one volume of isopropanol was added to precipitate the DNA. Tubes were centrifuged at 10,000g for 5 min. DNA pellets were washed with 0.5ml of 70% alcohol once. Finally, the DNA was dissolved in 100 µl of ddH₂O and kept at 4°C till further use.

2.1.2 Isolation of genomic DNA from ES cells and MEFs

Genomic DNA was prepared by a simplified method described by Laird et al., (Laird et al., 1991). Once the cells were confluent in 24 well plates the medium was removed and the cells were washed with PBS twice. 0.5 ml lysis buffer (100 mM Tris.CL pH8.0, 5 mM EDTA, 0.2% SDS, 200 mM NaCl, 100 µg/ml proteinaseK) was added to the cells and the plates were incubated at 37°C overnight. Next day the lysate was transferred into fresh micro centrifuge tubes. The DNA was precipitated by addition of one volume of isopropanol. The DNA precipitates were collected by centrifugation at 10000g for 10 minutes. The DNA pellet was washed with 70% ethanol. About 100 µl of ddH₂O was added to the DNA pellet. The tubes were incubated at 4°C for 2-3 days for complete dissolution of DNA.

2.1.3 Southern analysis of DNA

Electrophoresis of DNA

Genomic DNA samples (~ 10 µg) were digested with appropriate restriction enzymes and size fractionated on 0.8% agarose gel at 2 volt/cm overnight in a continuous buffer system (40 mM Tris-acetate, 1 mM EDTA pH 8.0, with 0.5 µg/ml ethidium Bromide). Loading buffer (1/10 volume of a solution containing 40 mM EDTA, 0.1% SDS, 30% ficoll, and 0.25% bromophenol blue) was added to DNA samples before applying onto the agarose gels. After electrophoresis the gels were imaged in gel documentation system (Bio-Rad) at 302 nm.

Transfer of DNA onto hybond-N⁺ membrane

The DNA was transferred from the agarose gel onto hybond-N⁺ membrane (Amersham) using a VacuGene XL Vacuum Blotting System (Amersham) by modifying the method described by Southern (Southern, 1975) as per the instructions of the manufacturer. After gel documentation, high molecular weight DNA was depurinated by treatment of the gel in 0.2N HCl for 10 minutes with gentle shaking. The gel was washed at least twice with distilled H₂O to remove traces of HCl. Nylon membrane was pretreated with 2X SSC and placed on the porous screen. The plastic mask was placed on the membrane in a way that it overlaps on each side of the membrane by approximately 3mm. The top frame was fixed and secured by tightening the four locking clamps. The gel was loaded on VacuGene XL blotting unit by gradually sliding the gel on to the nylon membrane. Care was taken to avoid trapping of air bubbles. VacuGene XL pump was switched on and the vacuum was stabilized at 50-60 mbar. The gel was always covered with 0.4N NaOH solution. The transfer was carried out for 1.5 hours. After the transfer the gel was stained with ethidium bromide and visualized under transilluminator to confirm the transfer of DNA. The membrane was rinsed with excess of 2X SSC to wash away the NaOH, air dried and stored appropriately until used.

Preparation of radiolabeled DNA probe

Double-stranded DNA was radiolabeled using random primers using random labeling kit (BRIT) as per the manufacturer's instructions. About 50 ng of double-stranded DNA and 5 µl of random primers solution was denatured in a volume of 25 µl by boiling for 5 minutes and quick chilling on ice. This was followed by the sequential addition of 5 µl of 10X reaction buffer, 5 µl each of dCTP, dGTP, dTTP, 40 µCi of α - [³²P]-dATP and 2 units of klenow enzyme. The reaction volume was made up to 50 µl and the reaction was carried out at 37°C for 1 hours. The probe was separated from the unincorporated nucleotides by Sephadex G-50 spun column chromatography and denatured in boiling water for 5 minutes and rapidly chilled on ice.

Purification and measurement of radio labeled probe

Sephadex G-50 column chromatography was used to purify radio labeled probe. A sterile 2 ml disposable plastic syringe was plugged with sterile glass wool and filled with the Sephadex G-50 slurry previously equilibrated with TE pH 8.0. The column was packed by centrifugation at 1000g for 5 minutes in a Sorvall HB-4 rotor at room temperature. Then 100 µl of the DNA solution to be purified was loaded and the column was centrifuged at 1000g for 5 minutes at room temperature to elute the purified DNA. For routine checking of labeling efficiency, samples were counted by Cerenkov's method. An aliquot of 1 µl of labeled DNA was spotted on a Whatman 3 mm filter and activity was counted in scintillation counter.

Hybridization

Prehybridisation was carried out at 65°C for at least 2 hours in a hybridization bottle containing 0.5 M sodium phosphate buffer (pH 7.4), 1mM EDTA and 7% SDS. Then the membrane was hybridized at 65°C for 16 hours by the addition of denatured radio labeled probe (prepared by random primer labeling as described above). Post-hybridization, membrane was washed in

50 ml of 40 mM sodium phosphate buffer (pH 7.4), 0.5% SDS and 50 mM EDTA at 65°C for 10 minutes three washes each. The hybridized blot was wrapped in a saran wrap or a thin plastic bag, sealed and exposed for 4-12 hours in a Fuji phosphoimager cassette and the imaging plate was scanned using a phosphoimager from Fujifilm.

2.1.4 PCR analysis of DNA

2.1.4.1 Primer designing

All primers were designed by using Primer3 Software. The length of the amplicon was set as per the requirement in each case. The optimum T_m was set at 60°C, with minimum T_m at 55°C and maximum T_m at 65°C. The GC content of the primers ranged between 40%-60%. The optimal length of primers was set at 20 nucleotides for amplification.

2.1.4.2 PCR amplification

All PCR reactions were performed with *Taq* DNA polymerase (Invitrogen; Bioron) as per the guidelines of the manufacturer. A typical PCR reaction was carried out in 20 μ l containing 1X PCR buffer, 2.0 mM $MgCl_2$, 0.1 μ M of each primers, 50 ng of genomic DNA or 2-5 ng cDNA, 200 μ M dNTPs and one unit of *Taq* DNA polymerase. Typically the annealing temperature was set 5°C below the calculated T_m of the primers. For some primer sets, the annealing temperature was optimized by gradient PCR. PCR was carried out for 30-35 cycles with one minute/ kb elongation time and final extension time of 7 minutes in PTC-200 Peltier Thermal Cycler (MJ research). Amplicons exceeding three kb length were amplified with Phusion Hot Start (Finnzymes) as per the instructions of the manufacturer. PCR reactions were set as 20 μ l reactions containing 1X polymerase buffer, 0.5 μ M each primer, 5- 10 ng of cDNA, 200 μ M dNTPs and 1.0 units of DNA polymerase .

2.2 RNA analysis

2.2.1 Northern blot analysis

RNA isolation from mouse tissues

Mice were anesthetized with 1.25 % avertin (Sigma) according to their body weight and euthanized by cervical dislocation. Mice were dissected immediately and tissues were collected (~30mg) washed in PBS, stored in micro centrifuge tubes and snap frozen immediately in liquid N₂. For long term storage, the tubes were transferred to -80°C freezer. The tissues were lysed in 1 ml TRIzol reagent by homogenizing with hand homogenizer. About 0.1 ml of 1-Bromo-3-Chloropropane was added per ml TRIzol reagent used. The contents in the tubes were mixed vigorously by hand for 15-30 seconds and incubated at room temperature for 5 minutes. Tubes were centrifuged at 12000g for 15 minutes at 4°C. The upper aqueous phase, which contains the total RNA, was carefully transferred into fresh micro centrifuge tubes. About 0.5ml isopropyl alcohol per one ml of TRIzol reagent was added, mixed well and the tubes were incubated at room temperature for 10 minutes. RNA was pelleted by centrifugation at 13000g for 10 min at 4°C. The pellet was washed twice with atleast 1ml of 70% ethanol per ml TRIzol used, centrifuged at 13000g for 5 minutes at 4°C. RNA pellet was air dried at RT (care was taken not to dry completely) and RNA pellet was dissolved in 50µl DEPC treated ddH₂O. The quality of RNA was analyzed on 1.0% agarose gel in RNase free conditions and quantified by nanodrop.

RNA isolation from cell lines

Cells were washed with PBS and required amount (1ml for 30 mm dish, 2ml for T25 cm², and 6ml for T75 cm²) of TRIzol was added. The cells were lysed in TRIzol reagent by first swirling the flasks and then triturating the lysate through small bored glass pipette. The lysate was dispensed as 1ml aliquots into micro centrifuge tubes and stored at -80°C till further use.

TH-19776

Electrophoresis of RNA ,blotting and hybridization

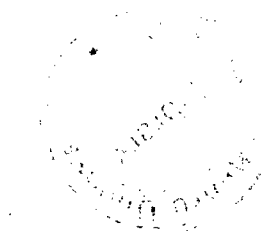
A total of 10 μ g RNA was denatured by deionized formamide (50%) at 85°C for 10 minutes, mixed with 1/10 volume of gel-loading buffer (50% glycerol, 10mM EDTA pH 8.0, 0.25% bromophenol blue, 0.25% xylene cyanol FF) and separated on 1% agarose gel containing 2.2M formaldehyde in MOPS buffer (0.02M MOPS-pH7.0, 2mM sodium acetate and 1mM EDTA) at 2 volts /cm. After electrophoresis the gels were imaged in gel documentation system (Bio-Rad) at 302 nm. The RNA was blotted with 40mM NaOH by VacuGene XL Vacuum Blotting System (Amersham) for 4 hours and hybridized with cDNA probes as mentioned in section 2.1.3.

2.2.2 Real time PCR analysis**Reverse transcription**

Total RNA was treated with RQ1 RNase-Free DNase (promega) in 1X DNase buffer for 30 min at 37°C, followed by inactivation of DNase by adding 1X DNase stop solution and incubating at 65°C for 15 minutes. Reverse transcription was performed using ImProm-II TM kit (Promega). The steps are following-

Step 1: RNA/primer mixtures were prepared in each tube as described below:

| | |
|----------------------------------|-----------|
| Total RNA | 5 μ g |
| Random hexamers (50 ng/ μ l) | 2 μ l |
| 10 mM dNTP mix | 1 μ l |



Step 2: The samples were incubated at 70°C for 5 minutes and then on ice for atleast a minute. Reaction master mixture was prepared for each reaction (50 μ l) as described below:

| | |
|--------------------------------------|-----------|
| 10x RT buffer | 5 μ l |
| 25 mM MgCl ₂ | 5 μ l |
| Reverse Transcriptase (50U/ μ l) | 1 μ l |
| RNAase inhibitor (40U/ μ l) | 1 μ l |

Step 3: The reaction mixture was added to the RNA/primer mixture, mixed briefly, and then placed at room temperature for 2 minutes. Then the tubes were incubated at 42°C for 90 minutes, heat inactivated at 70°C for 15 minutes and stored at -20°C until used for real-time PCR.

Real-time PCR

The real time PCR was performed using SYBR green 2X mix (Invitrogen). The primer concentrations were optimized for each gene and gene-specific forward and reverse primer pair was mixed. ABI Prism SDS 7000 was used to perform real time PCR. The steps are following:

Step 1: Real time PCR was set in 384 well plate as described below:

| | |
|---|-------------|
| SYBR Green Mix (2X) | 5 μ l |
| RT cDNA | 1-3 μ l |
| primer pair mix (2 pmol/ μ l each primer) | 1 μ l |
| ddH ₂ O | 3-1 μ l |

Step 2: Real time PCR program described below:

1. 50°C 2 min, 1 cycle
2. 95°C 10 min, 1 cycle
3. 95 °C 15sec, 58 °C 30sec, 72 °C 30sec, 40 cycles

4. 95 °C 15sec, 60 °C 15sec, 95 °C 15sec- dissociation stage

Step 3: After PCR was completed, the real-time PCR results were analyzed with the SDS 7000 software and graphs were plotted using Microsoft excel.

2.3 DNA manipulation

2.3.1 Plasmid DNA isolation

2.3.1.1 Plasmid miniprep

Plasmid DNA was prepared by alkali lysis method. Single bacterial colony was inoculated in 5 ml of LB broth containing appropriate antibiotics and incubated overnight at 37°C in a shaking incubator (Innova) at 180 rpm. Further QIAprep Spin Miniprep Kit (Qiagen) was used for isolation of plasmid DNA as per the instructions of the manufacturer. Briefly, overnight culture was transferred to a 15 ml centrifuge tube and centrifuged for five minutes at 6000g. Supernatant was poured off; pelleted bacterial cells were resuspended by vortexing in 250 µl buffer P1 and the suspension was transferred into 1.5 ml micro centrifuge tubes. 250 µl buffer P2 was added and mixed well by inverting tubes gently 4-6 times. 350 µl buffer N3 was added and tubes were inverted immediately 4-6 times. The tube was centrifuged for 10 minutes at 13000g. The supernatant was loaded on to the QIAprep column in a two ml collection tube by careful pipetting with cut tips and centrifuged for one minute at 10000g. The flow through was discarded; 750 µl of buffer PE was applied to the column and centrifuged for one minute at 10000g. The flow through was discarded and the column was centrifuged for two minutes at 10000g to remove the residual liquid. The column was transferred into a fresh clean sterile 1.5 ml micro centrifuge tube. DNA was eluted by addition of 50µl ddH₂O and centrifuging for one minute.

2.3.1.2 Endotoxin free plasmid maxiprep

Endotoxin free plasmid DNA from large scale bacterial culture was prepared using QIAGEN - EndoFree Plasmid Maxi Kit (Qiagen) except that the inoculation was done in 250 ml LB broth instead of 100 ml LB broth containing appropriate antibiotics and incubated overnight at 37°C in a shaking incubator (Innova) at 180 rpm.

Bacterial cells were harvested by centrifugation at 6000g for 15 minutes at 4°C and supernatant was discarded. Bacterial pellet was resuspended in 10 ml buffer P1 by vortexing. 10 ml buffer P2 was added and mixed gently but thoroughly by inverting 4–6 times and the tubes were incubated at room temperature for two minutes. During the incubation QIAfilter cartridges was prepared by first screwing the cap onto the outlet nozzle of the QIAfilter Maxi Cartridge. QIAfilter cartridge was placed into a tube. 10 ml chilled buffer P3 was added to the lysate, and mixed immediately by inverting 4–6 times. The lysate was poured into the barrel of the QIAfilter cartridge and incubated at room temperature for 10 minutes. Cap from the QIAfilter outlet nozzle was removed and the plunger was inserted into the QIAfilter maxi cartridge. The cell lysate was filtered into a 50 ml tube. 2.5 ml of buffer ER was added to the filtered lysate, mixed by inverting the tube 10 times and incubated on ice for 30 minutes.

During the incubation QIAGEN-tip 500 was equilibrated by applying 10 ml buffer QBT, and allowing the column to empty by gravity flow. After 30 minutes incubation the filtered lysate was applied to the QIAGEN-tip and allowed to enter the resin by gravity flow. QIAGEN-tip was washed with 2 x 30 ml buffer QC. DNA was eluted with 15 ml buffer QN and precipitated by adding 10.5 ml (0.7 volumes) room temperature isopropanol to the eluted DNA. The contents were mixed well and centrifuged immediately at 13000g for 30 minutes at 4°C. The supernatant was carefully decanted and DNA pellet was washed with 5 ml endotoxin-free, room-temperature 70% ethanol (prepared by adding 40 ml of 96–100% ethanol to the endotoxin-free water

supplied with the kit). Ethanol was removed by centrifugation at 13000g for 10 minutes. Supernatant was discarded without disturbing the pellet. The DNA pellet was air-dried for 5 -10 minutes and the DNA redissolved in 1 ml of endotoxin-free H₂O.

2.3.2 Preparation of ultra competent cells and transformation

E.coli DH5 α ultra competent cells were prepared as described by Inoue *et al.*, (Inoue *et al.*, 1990). Inoue transformation buffer was prepared as described in appendix; filter sterilized through a pre-rinsed 0.22 μ m filter and stored at -20°C.

A single bacterial colony of *E.coli* strain DH5 α was inoculated and cultured for 6–8 hours at 37°C in 25 ml of LB medium in a 250 ml flask with vigorous shaking (250–300 rpm). The starter culture was used to inoculate three one liter flasks, each containing 250 ml of LB broth. The first flask received 10 ml of starter culture, the second received four ml and the third received two ml. All three flasks were incubated for 14 hours at 18–22°C with moderate shaking. Optical Density (OD) was read at 600 nm. OD of all three cultures was monitored every 45 minutes. Once the OD₆₀₀ of one of the cultures reached exactly 0.55, the flask was transferred to an ice-water bath for 10 minutes. The other two cultures were discarded. Cells were harvested by centrifugation at 2500g (3900 rpm in a Sorvall SLC-1500 rotor) for 10 minutes at 4°C. The cells were gently resuspended in 80 ml of ice-cold transformation buffer. The cells were harvested by centrifugation at 2500g (3900 rpm in a Sorvall SLC-1500 rotor) for 10 minutes at 4°C. The transformation buffer was poured off and centrifuge tube was stored open on a stack of paper towels for 2 minutes. The cells were gently resuspended in 20 ml of ice-cold transformation buffer. 1.5 ml DMSO was added; the bacterial suspension was mixed by swirling and then stored in ice for 10 minutes. The competent cell suspension was dispensed as aliquots of 70 μ l into chilled,

sterile micro centrifuge tubes and snap-frozen in liquid nitrogen. Competent cells were stored at -70°C until used.

In a typical transformation reaction 4-5 μl of ligation mix or 1-2 ng of plasmid DNA was incubated on ice with 70 μl ultra competent cells for 25-30 minutes, followed by a heat shock at 42°C for 1.5 minutes. 900 μl of plane LB media was added and allowed to grow at 37°C for 45 minutes. The cells were plated on to LB agar plate containing appropriate antibiotics and incubated overnight at 37°C . For blue-white colony selection forty μl of 2% X-gal (Sigma) solution and 7 μl of 20% IPTG (Sigma) solution was spread on to the LB plate containing appropriate antibiotics.

2.3.3 Restriction digestion of plasmid DNA

Plasmid DNA was digested with various restriction endonucleases (New England Biolabs) as per the manufacturer's instructions, except that the enzymes were used 2 to 3fold excess of the recommended units.

2.3.4 Isolation of DNA from agarose gel

Fragments of DNA (From PCR or restriction digestion reactions) were isolated from the gel using Gel extraction kit (Qiagen) as per the manufacturer's instructions.

Briefly, gel fragments containing the DNA band were excised with clean sharp scalpel and weighed in micro centrifuge tube. Three volumes of buffer QG was added to one volume of gel and incubated at 50°C until the gel slice was completely dissolved. One gel volume of isopropanol was added to the sample and mixed by inverting the tube. The sample was applied on to the QIAquick/minelute column placed in two ml collection tube and centrifuged for one minute at $10000g$ to allow the DNA to bind to the column. Flow-through was discarded and the column was washed 0.75 ml of buffer PE and

centrifuged for one minute at 13000g. Flow-through was discarded and the column was centrifuged for an additional one minute to remove residual liquid. QIAquick/minelute column was placed in a clean 1.5 ml micro centrifuge tube. To elute DNA 50 μ l (for QIAquick column) or 20 μ l (for minelute column) of pre-warmed (65°C) ddH₂O was added to center of the membrane in the column and centrifuged for one minute at 13000g.

2.3.5 End filling reactions

Plasmid DNA digested with appropriate restriction enzymes was precipitated with 0.1 volume 3M NaOAc and two volumes of absolute alcohol. DNA was pelleted by centrifugation at 13000g for 30 minutes and was washed with 70% ethanol. The DNA pellet was dissolved in sterile ddH₂O. The end-filling was performed as described below:

| | |
|---------------------|----------------------------|
| Digested DNA | X μ l (~ 1 μ g) |
| NEB Buffer 1,2,3,4 | 2.5 μ l |
| dNTPs (2.5 mM each) | 1.0 μ l |
| Klenow | 0.2 μ l (10U/ μ l) |
| ddH ₂ O | Up to 25 μ l |

The above components were mixed well in micro centrifuge tube and the reaction was carried out at 25°C for 30 minutes.

2.3.6 Ligation Reactions

Ligation reaction was carried out at 22°C for 2 hours with following components:

| | |
|-------------------------|---|
| Vector DNA | ~25-40 ng |
| Insert DNA | 3-5 times molar concentration of vector DNA |
| 10X NEB ligation buffer | 1 μ l |
| T4 DNA ligase | 0.4 μ l (50U/ μ l) |
| ddH ₂ O | Up to 10 μ l |

2.3.7 Screening of recombinant clones by cracking method

The colonies were screened for the recombinant clones by a modified cracking method, which was adapted from protocol described by Maniatis *et al.* (1982). Individual colonies were picked with a sterile toothpick and smeared at the bottom of a micro centrifuge tube containing 200 μ l LB media with appropriate antibiotics and allowed it to grow for 12 hours at 37°C in shaking condition. 50 μ l of freshly prepared cracking buffer (refer to appendix) was added and the contents were vortexed for 1-2 minutes, incubated for 5 minutes at 70°C on a water bath and allowed to cool to room temperature. 50 μ l of chloroform and 10 μ l 6X loading dye were added to the tube and vortexed for a brief period. The contents were centrifuged at 10000g for 5 minutes and to analyze for shift, upper aqueous layer was loaded in 0.8% agarose gel along with the control plasmid and DNA size marker. The clones showing slow mobility were presumed to be recombinant and were cultured overnight in five ml LB broth containing appropriate antibiotics. Plasmids were isolated and quantified spectrophotometrically.

2.4 Protein Analysis

2.4.1 Western blot analysis

SDS-polyacrylamide gel electrophoresis

SDS-PAGE was carried out by the method described by Laemmli (Laemmli, 1970) in a discontinuous buffer system. Gel of 1.5 mm thickness was cast and run on a vertical gel apparatus (Broviga, India). The resolving gel (6%-12% acrylamide, 0.375 M Tris.HCl pH 8.8, 0.1% SDS) and stacking gel (5% acrylamide, 0.125 M Tris.HCl pH 6.8, 0.1% SDS) were polymerized by the addition of TEMED (12 μ l for a 15 ml gel) and freshly prepared ammonium persulphate solution (150 μ l of a 10% solution for 15 ml of gel mixture). The protein samples were boiled in 1X Laemmli buffer (50 mM Tris.HCl pH 6.8, 100 mM DTT, 7% SDS, 0.1% bromophenol blue, 10%

glycerol) for 5 minutes and loaded on the gel. Electrophoresis was carried out in electrophoresis buffer (0.025M Tris.HCl, 0.250 M glycine pH 8.3, 0.1% SDS) at a constant current of 20 mA till the samples entered the stacking gel and then at 40 mA through the resolving gel. After the run, the gels were stained with 0.25% Coomassie Brilliant Blue R250 in 100 ml of methanol: acetic acid: water (40:10:50) for 2-3 hours and destained in 200 ml of methanol: acetic acid: water (40:10:50) for 3-4 hours on a shaker, with several changes of the destaining solution.

For silver staining gel was fixed in methanol: acetic acid: water (40:10:50) for 1 hour, followed by 2 washes of 50% and 30% methanol for 30 minutes each. To remove methanol gel was washed with water. The gel was sensitized with 250 mg/L of $\text{Na}_2\text{S}_2\text{O}_3$ for one minute and washed with water. Gel was impregnated (2g/L AgNO_3 , 750 μl of 37% Para formaldehyde) for 20 minutes. Colour was developed in developer (60g/L Na_2CO_3 , 500 μl of 37% Para formaldehyde) for 10-20 minutes. Colour development was stopped by adding methanol: acetic acid: water (40:10:50) mixture. Finally gel was stored in 7% glycerol.

Western transfer of proteins

The protein lysates were separated on SDS-PAGE and gels were equilibrated for 10 minutes in transfer buffer (192 mM glycine, 25 mM Tris base, and 20% methanol) and electro blotted onto a PVDF membrane by wet transfer apparatus (Bio-red). The PVDF membrane was pre-wetted in methanol, rinsed in distilled water and equilibrated in transfer buffer. The gels were placed in contact with the membrane and sandwiched between 6 pieces of Whatman No. 1 paper on each side. The sandwich was then placed between electrodes with the membrane facing the anode. The proteins were transferred for 1.5 hour using a current of 0.8 mA/ cm^2 blot. After transfer the proteins were visualized by staining with Ponceau-S dye (0.1% Ponceau-S dissolved in 5% acetic acid) and the positions of the protein molecular mass

markers were marked on the membrane for immunodetection by chemiluminescence reaction.

The PVDF membrane containing electro blotted proteins was blocked with 5% BSA or 5% milk in TBS containing 0.05% Tween-20 (TBST) for one hour at room temperature. The blot was incubated in the primary antibody diluted in TBST for 3 hours at room temperature and washed for an hour with several changes of buffer. The blot was then incubated with HRP-conjugated anti-IgG antibody diluted in TBST for 1 hour and washed extensively as described above. Immunoreactivity was determined with the use of luminol as substrate and detected by chemiluminescence using an ECL detection kit as per the manufacturer's instructions.

Deprobing of protein blots

To reprobe the western blots, the bound antibodies were stripped off from the PVDF membrane by incubating the membrane in stripping buffer (0.1 M β -mercaptoethanol, 2% SDS, 62.5 mM Tris-HCl, pH: 6.7) at 50°C for 30 minutes with constant shaking in the water bath. This step was repeated twice if necessary. The blot was then washed thoroughly with distilled water initially and then with TBST with many changes till the β -mercaptoethanol smell disappeared.

2.4.2 Immunocytochemistry

Fixing of cells

The cells on cover slips were fixed directly in six well polystyrene plates. Cover slips containing cells were rinsed with PBS and incubated with 3.7% formaldehyde in PBS for 10 minutes at room temperature followed by permeabilisation with 0.5% Triton X-100 for 6 minutes at RT.

Blocking

The fixed cells were incubated with 3% BSA or 5% horse serum in PBS for one hour at room temperature in order to block non-specific binding during incubation with primary and secondary antibodies.

Antibody incubation

The blocked cells were incubated first with the primary antibody diluted appropriately in PBST or blocking buffer or 3% BSA in PBST for one hour at room temperature. The slides were washed for 5 minutes with PBST. The wash was repeated twice. This was followed by incubation with secondary antibody conjugated with fluorophor for 45 minutes to one hour at room temperature. Then slides were washed thrice with PBST for 5 minutes each. The cross-reactivity of the secondary antibody conjugates to non-specific proteins was tested prior to the experiments. Cover slips were mounted in Vectashield, a glycerol-based mounting medium containing anti-fade reagent, with DAPI added to a final concentration of 1 µg/ml.

Immunofluorescence microscopy

Confocal laser-scanning immunofluorescence microscopy (CLSM) was carried out with a Zeiss LSM510 META confocal microscope. Mercury arc lamp for Zeiss system was used for excitation and a 435-485 band pass filter for detection of the DAPI signal. The 488 nm laser was used for excitation and a 500-530 band pass filter was used for detection of FITC and Alexa-488, the 543 nm laser was used for excitation and a 565-615 band pass filter was used for detection of Cy3. The 633 nm laser was used for excitation and a 650-670 band pass filter was used for detection of Cy5. Images were analyzed using LSM510 META software (Carl Zeiss, Germany) and assembled using Adobe Photoshop CS2.

2.5 Phenotypic analysis of mice

2.5.1 Breeding of *Wdr13* knockout mice

Wdr13 ^{-/0} males were bred with wild type CD-1 females. In first generation all females were heterozygous (*Wdr13* ^{-/+}). In next generation the *Wdr13* ^{-/+} females were crossed with Wild type male. To get *Wdr13* ^{-/-} females, *Wdr13* ^{-/0} males were bred with *Wdr13* ^{-/+} females. Offsprings were analyzed by southern blot as well as by PCR. For all experiment littermates were used.

2.5.2 Sperm analysis of mice

2.5.2.1 Isolation of sperm from epididymas

Wdr13 knockout mice and their wild type mice were anesthetized with 2.5% avertin (Sigma) according to their body weight and euthanized by cervical dislocation. After dissecting the mice Epididymas was separated and kept in 1ml of Krebs Ringer bicarbonate media (Tulsiani et al., 1997).

Krebs Ringer Bicarbonate media-

| | |
|---------------------------------|---------|
| NaCl | 112.4mM |
| KCl | 4.8mM |
| CaCl ₂ | 1.7mM |
| KH ₂ PO ₄ | 1.2mM |
| Mg ₂ SO ₄ | 1.2mM |
| NaHCO ₃ | 4.0mM |
| HEPES | 21mM |
| Sodim lactate | 25mM |
| Sodium pyruvate | 1.0mM |
| Glucose | 5.6mM |
| Phenol Red | 28μM |
| BSA | 0.3% |

Media was filter sterilized with 0.22 μ m filter and stored at 4°C. Epididymas was dissected in Krebs Ringer bicarbonate media and sperm were allowed to release in media at 37°C. Various parameters were analyzed in this media.

2.5.2.2 Sperm motility analysis by computer assisted sperm analysis (CASA)

Sperms were diluted in Krebs Ringer bicarbonate media in 1:5 ratios. The motile swim up spermatozoa were then collected and counted in a Makler chamber using a HTM-CEROS (Hamilton Thorne, Beverly, MA, USA) Computer Assisted Semen Analyzer (CASA). Motility of sperms was recorded at 0h, 1h, 2h, 3h and 4h.

2.5.2.3 Acrosomal reaction

Acrosome reacted sperms were identified by Coomassie Brilliant Blue G-250 staining at various time point after collection (Abou-Haila and Tulsiani, 2003). Sperms were fixed in 4% Para formaldehyde containing 110mM NaHPO₄ and 2.5 mM NaH₂PO₄ for 10 minutes. After fixation, sperms were washed in 100mM ammonium acetate (pH-9.0) twice. Finally spermatozoa were stained in 0.2% G-250 prepared in 50% methanol, 10% acetic acid and 40% water for 2 minutes. Stained spermatozoa were mounted and examined using bright field microscope.

2.5.3 Weight measurement of mice

All mice were housed in proper condition of humidity, dark and light cycles on autoclaved normal chow or high fat diet. Mice were weighted fortnightly. Free access to food and water was provided.

Normal chow and High Fat Diet (HFD) Compositions

| Product | Normal Chow Kcal % | HFD Kcal% |
|--------------|-----------------------|--------------|
| Protein | 25.0 | 20 |
| Carbohydrate | 58.0 | 20 |
| Fat | 17.0 | 60 |
| Total | 100 | 100 |
| kcal/gm | 3.10 | 5.24 |

2.5.4 Feed consumption

Mice were kept in individual cages with free access to water and feed. Feed consumption was measured by weighing the feed weekly. Total feed consumption/day was calculated by feed consumed divided by total number of days.

2.5.5 Organ weight measurement

At the termination of growth experiment all the mice were euthanized and dissected. Brain, liver, lung, kidney, pancreas, spleen, heart, adipose mass, testis, ovary and uterus were collected and weighed separately.

2.5.6 Insulin and triglyceride measurement

Wdr13 knockout mice and their wild type mice were anesthetized with 1.5% avertin (sigma) according to their body weights and 0.5 ml of blood was collected from orbital sinus in fasting as well as in random fed condition. Blood was allowed to clot at room temperature and serum was separated by centrifugation at 3000g for 15 minutes and stored at -70°C for all the metabolic parameters. Insulin was measured by ELISA method using Rat/Mouse insulin ELISA kit (LINCO Research) as per manufacturer instructions. Triglycerides was measured by NAD kinetics method (Vijaya Diagnostics).

2.5.7 Glucose measurement

Glucose was measured by glucometer (Accucheck Sensor Strip) from blood. Glucose clearance was measured by Glucose tolerance test (GTT). Mice were kept on fasting for 16 hours and glucose was measured at fasting condition. Finally glucose was injected intraperitoneally (2.0 grams glucose /Kg body weight) (Wen et al., 2009) and blood was collected to measure glucose and insulin at 30, 60 and 120 minutes interval.

Insulin resistance was measured by insulin tolerance test (ITT). Human insulin was injected intraperitoneally (1U/kg) in random fed condition and blood glucose was measured by glucometer at 30, 60 and 120 minutes intervals (Wen et al., 2009).

2.5.8 Histopathological examination of various tissues

Wdr13 knockout mice and their wild type mice were anesthetized with 2.5% avertin and euthanized by cervical dislocation. At various age point tissues were collected and fixed in 4% para formaldehyde in PBS overnight. Next morning samples were washed in PBS and dehydrated by 30%, 60%, 80%, 95% and 100% ethanol gradients in shaking condition, each for one hours. After dehydration tissues were kept in chloroform for 1 hour. Finally tissues were dipped in paraplast tissue embedding medium (Fisher Health care) at 56°C for one hour and tissues blocks were prepared. Using microtome (*Leica*) 4.0µm thickness sections were taken in for each tissue and allowed to attach on positively charged slides (Fisher Scientific).

The slides were warmed for 10 minutes on a slide warmer at 45°C. Then the slides were immersed and washed in xylene for 10 minutes. The xylene wash was repeated thrice. The sections were rehydrated by soaking the slides in the following ethanol series: 100%, 95%, 80%, 60%, and 30% ethanol, for a minute at each concentration. Finally the slides were washed in

tap water for 2 minutes. The sections were stained in Gill's Hematoxylin for 2-3 minutes followed by a wash in tap water for 4 minutes. The slides were immersed in acidic alcohol solution for 5-10 seconds to reduce background and then in tap water for 5 minutes. The sections were further stained in Eosin solution for 10-20 seconds. Then the sections were dehydrated by passing three times through 95% ethanol for one minute each and then twice through 100% ethanol for 2-3 minutes each. Finally the slides were passed through xylene twice for 5 minutes each. Cover slips were mounted on the sections in the slides with DPX mountant and allowed to air-dry overnight in a hood. The sections were imaged in inverted phase contrast microscope (Leica).

2.5.9 Cell proliferation assay in pancreas and testis

100 mg/kg of body weight, BrdU (Sigma) was injected intraperitoneally 2h prior to sacrifices for spermatogonial cell proliferation and for beta cell proliferation, BrdU was given in drinking water (1mg/ml) for 7 days (deFazio et al., 1987). Tissues were sectioned as described in section 2.5.8. After rehydration, the slides were boiled in citrate buffer (9.9mM citric acid and 43 mM sodium citrate pH6.0) for 30 minutes to retrieve antigen. To denature the DNA, the slides were immersed in 2N HCl for 15 minutes and after that stabilized by 0.1M borax solutions for 10 minutes. Slides were washed in PBS and stained with insulin and BrdU and imaged, as described in section 2.4.2.

2.5.10 Apoptosis analysis in pancreas and testis

Tissues were sectioned as described in section 2.5.8. Apoptosis was performed by TUNEL staining (Song et al., 2008) using Dead end TM flurometric tunnel system (Promega) as per manufacturer instructions. After TUNEL staining slides were stained with insulin for beta cells and imaged, as described in section 2.4.2.

2.5.11 Islet isolation and purification

Islets were isolated from cervically dislocated mice by an initial injection of 2ml 0.5 mg/ml type XI collagenase (Sigma) dissolved in Hanks balanced salt solution (HBSS) (Gibco) into the pancreatic duct followed by a digestion with the same enzyme solution at 37°C for 20 minutes. The digested tissue was then washed twice with ice-cold HBSS and redistributed in 5ml HBSS. Islets were purified by adding 5ml Ficoll-paque PLUS solution (Amersham) to the bottom of the above tube and then centrifuged at 1000g for 15 minutes. The isolated islets were washed again with HBSS and used for RNA and protein isolation (Wen et al., 2009).

2.5.12 MTT assay

MTT assay was performed for cell proliferation analysis. 20,000 Min-6 cells were seeded in per well of 24 well plates (Meng et al., 2009). A total of 50 μ l of MTT (5mg MTT/ml in PBS) was added in each well containing 500 μ l DMEM complete media. Cells were incubated for three hours at 37 °C in incubator, followed by removal of media and addition of 500 μ l of acidified isopropanol (4mM HCl and 0.1% NP-40 in isopropanol) per well in shaking condition for 15 minutes to dissolve formazan. The 150 μ l of supernatant was transferred in 96- well plate and OD was recorded in ELISA reader @ 540nm wavelength.

2.6 *In vitro* adipogenesis of mouse embryonic fibroblast (MEFs)

2.6.1 Isolation and culturing of MEFs

Wdr13 *+/+* and *Wdr13* *-/-* females were crossed with *Wdr13* *+/-* and *Wdr13* *-/-* females respectively and females (~*d.p.c* 13.5) were euthanized and sprayed with 70% ethanol and swabbed with sterile cotton. Small cut was

made with sterile scissors through the belly skin at the median line just over the diaphragm. Skin was grasped with rat tooth forceps, on both sides, pulled in opposite directions to expose the untouched ventral surface of the abdominal wall. A longitudinal cut was made along the median line of the exposed abdominal wall with sterile scissors to reveal the viscera and uteri filled with embryos. The uterine horns were dissected out and placed into 100 mm petridish containing PBS with added antibiotics (2X). Embryos were separated from placenta and surrounding membranes with watchmaker forceps. Brain and dark red organs of the embryos were cut away and rinsed with fresh PBS to remove as much blood as possible. The embryos carcasses were transferred to a fresh dish and carefully minced with curved surgical scissors. About 2-3 ml of pre-warmed 0.25% trypsin/EDTA solution was added and triturated through a pipette. Embryos with trypsin solution were transferred from dish with a pipette to the barrel of a 10 ml syringe with an attached 18G needle. The syringe plungers were replaced and the embryo/trypsin suspension was pushed through the needle. This was repeated to obtain a cell suspension free of larger pieces of tissues. Suspended cells/tissue were incubated at 37°C for 15 minutes, briefly triturated after every 5 minutes and then equal volumes of fresh complete medium was added. The suspension was triturated vigorously with a pipette. Half an embryo equivalents were plated per 75cm² flasks and complete medium (13.3g/L DMEM, 3.7g/L NaHCO₃, 10% Serum, 50µg/ml ampicillin and 50µg/ml streptomycin) was added to make up a final volume of 10 ml. Next day medium was changed with an equal volume of fresh complete medium. After the culture attained 90% confluency (5-6 days), the MEFs were frozen as first passage (P1).

Harvesting/splitting of MEFs

MEFs cultured to confluence were washed with 7 ml PBS at least twice, and then cells were trypsinized using pre-warmed (37°C) trypsin/EDTA solution (one ml for 75cm² flask). Trypsin/EDTA solution was added; the flask was swirled to cover the culture completely and incubated in incubator (37°C)

for 120 seconds. Flasks were gently tapped from the sides to lift off the cells from the surface; approximately 5 ml of complete medium was added to neutralize the Trypsin/EDTA solution. Cell suspension was pipetted up and down several times to dissociate into single cells. Cells were centrifuged in 15 ml tubes at room temperature for 5 minutes at 1000g. Supernatant was removed and cells were resuspended in fresh medium. The cells were seeded at desired splitting ratio (generally 1:3) and cultured until confluent.

Freezing of MEFs

MEFs cultured to confluence were washed with 7 ml PBS at least twice, and then cells were trypsinized using pre-warmed (37°C) trypsin/EDTA solution (one ml for 75cm² flask). Trypsin/EDTA solution was added; the flask was swirled to cover the culture completely and incubated in incubator (37°C) for 120 seconds. Flasks were gently tapped from the sides to lift off the cells from the surface; approximately five ml of complete medium was added to neutralize the Trypsin/EDTA solution. Cell suspension was pipetted up and down several times to dissociate into single cells and counted by hemacytometer. Cells were centrifuged in 15 ml tubes at room temperature for 5 minutes at 1000g. Supernatant was removed and cells were resuspended in desired volume of prechilled freezing mix (10% DMSO in serum). One ml of this cell mixture was dispensed into pre-cooled and pre-labeled cryovials as per desired ratios. Vials were placed into pre-cooled Styrofoam box and transferred to -80°C freezers overnight. The next day cryovials were transfer to liquid N₂ tank (-196⁰ C) for long-term storage.

Thawing of MEFs

Required numbers of vials of MEFs were taken from the appropriate cryobox. Quickly, frozen MEFs were thawed in a warm water bath maintained at 37°C. The content of vials was transferred to a few ml of warm MEF medium and pelleted by centrifugation for 5 minutes at 1000g. The supernatant was discarded and cells were resuspended in MEF medium. Finally cells were plated in corresponding culture area flask. (See table 2.2)

2.6.2 Induction of adipogenesis

MEFs were genotyped by PCR and grown till passage 3. To induce differentiation MEFs at passage 3 were seeded in 60mm dish (0.35×10^6) in triplicate for each genotype (Tang et al., 2003). After confluency, cells were fed with DMEM containing 10% FBS, $1 \mu\text{g/ml}$ insulin, $1 \mu\text{M}$ dexamethasone and 0.5mM 3-isobutyl -1-methyl-xanthine (all from Sigma). Media was changed at interval for 48h till 8th day. Cells were lysed during differentiation by adding TRIzol to analyze the adipogenic markers at day 2, 4, 6 and 8. Level of *Wdr13*, PPAR γ and EBP α was checked by real time PCR as described in section 2.2.2.

2.6.3 Oil red O staining

After 8th day of MEFs were fixed in 4% formaldehyde for 15 minutes and stained with oil red O stain (0.5% Oil red O in 60 % isopropanol) for 10 minutes to observe the adipocytes. Stained MEFs were washed with 60% isopropanol to remove excess stain and finally submerged in PBS for storage. The 60mm dishes were imaged in inverted phase contrast microscope (Leica).

2.7 Immunoprecipitation and LC-MS/MS

2.7.1 Construction of overexpression vectors

Construction of pCMV-*Wdr13*

Wdr13 complete cDNA was constructed by cloning a 1.5 kb XhoI fragment from pCD7 (Suresh et al., 2005) at Xho I site of pCD1 and orientation was confirmed by restriction digestion with EcoRI and HindIII, named as pCD0. From pCD0 1.8 kb, EcoRI and SacI fragment was sub cloned at EcoRI and SacI site of pPOLY III named as pPOLY III-*Wdr13*. To

clone *Wdr13* cDNA in pCI vector, under control of CMV promoter, pPOLY III-*Wdr13* plasmid was digested with EcoRI and XbaI and cloned at EcoRI and XbaI of pCI vector named as pCI-*Wdr13* (Figure 2.1).

Construction of pCMV-FLAG-*Wdr13*

Wdr13 cDNA was amplified from pCI-*Wdr13* using Forward primer 5'CCGGAATTCCGGATGGCCGCGGTGTGG3' and reverse primer 5'GCTCTAGAGCAGCACAGGGTGACAGAACC3' containing EcoRI and XbaI primer site respectively and cloned at EcoRI and XbaI sites of vector containing FLAG peptide sequence at N terminal (Gift from Dr. Ghanshyam Swarup), named as pCMV-FLAG-*Wdr13* (Figure 2.1).

Construction of pAdTrack-CMV-FLAG-*Wdr13*

Wdr13 cDNA was amplified from pCMV-FLAG-*Wdr13* vector using T7 forward primer and *Wdr13* reverse primer 5'GCTCTAGAGCAGCACAGGGTGACAGAACC3', digested with PmeI and cloned at EcoRV digested and SAP treated pAdTrack-CMV vector. The orientation of insert was confirmed by HindIII and XhoI digestion. The resulting vector was linearized with PmeI and electroprated into *E. coli*. BJ5183 cells containing pEasy-1 vector. The recombinant clones were selected in kanamycin. Plasmid was isolated from clones and recombinants were confirmed by PacI digestion (Figure 2.3). The positive clones plasmid DNA was isolated and transfected in DH5 α cells to prepare 20 μ g of plasmid DNA to transfect in adenoviral packaging cells HEK293T. Adeno virus were generated according to He *et al.*, (He *et al.*, 1998) and used for *wdr13* overexpression studies.

Construction of pCMV-Myc-*Wdr13*

pFLAG-*Wdr13* plasmid was digested with EcoRI and XbaI to release *Wdr13* cDNA and cloned at EcoRI and XbaI sites of vector containing *Myc* peptide sequence at N terminal (Gift from Dr. Ghanshyam Swarup), named as pCMV-Myc-*Wdr13* (Figure 2.1).

Construction of pCMV-Myc-PHIP1

Pleckstrin homology domain interacting protein1 (*PHIP1*) was amplified from testis cDNA using forward primers 5'CTCGTGAGCACACACTGACA3' and reverse primer 5'TTCCATATCCCAAGGACTCA3' for N-terminal 3.4 kb fragment (WD domain) and 5'CCCAGGAGATGTCCATTTGT3' and 5'AATCCGTCATAGCAGCAAGG3' for C-terminal 2.8 kb fragment (Bromodomain). Both fragments were cloned in pMOSBlue vector (Promega) as per manufacturers guidelines and named as pMOS-*PHIP*-WD and pMOS-*PHIP*-Bromo respectively. Both fragments were cloned together to construct complete cDNA (Figure 2.2).

A 3.3 kb DNA fragment containing *PHIP* WD domain was released from pMOS-*PHIP*-WD vector by *Stu*I, *Xba*I digestion and cloned in pCMV-Myc vector, which was digested with *Eco*RI, end-filled by klenow, digested with *Xba*I. The resulting vector contain *PHIP1* WD domain with stop codon at C-terminal just after primer sequences and named as pCMV-Myc-*PHIP*-WD (Figure 2.2).

PHIP Bromodomain was cloned in pBluescript II KS at *Bam*HI site from pMOS-*PHIP*-Bromo plasmid by digesting with *Bgl*III and *Bam*HI, named as pBSKS-*PHIP*-Bromo. Further bromodomain containing 2.2kb fragment was released from pBSKS-*PHIP*-Bromo by digesting *Xba*I and *Eco*RI (Partially) and cloned at *Eco*RI and *Xba*I sites of pCMV-Myc vector named as pCMV-Myc-*PHIP*-Bromo (Figure 2.2).

Complete *PHIP1* expression vector was constructed by cloning *Nde*I and *Bam*HI (endfilled) fragment from pMOS-*PHIP*-Bromo plasmid in to *Xba*I (endfilled) and *Nde*I (Partially digested) sites of pCMV-Myc-*PHIP*-WD vector and named as pCMV-Myc-*PHIP1* (Figure 2.2).

Figure 2.1 Construction of *Wdr13* overexpression vectors

- A) pCD1:** This plasmid contains exon1, exon2 and exon3 of *Wdr13* in pBluescript II KS+.
- B) pCD7:** This plasmid contains exon2 to exon9 and 3' UTR of *Wdr13* in pBluescript II KS+.
- C) pCD0:** This plasmid contains exon1 to exon9 and 3' UTR of *Wdr13* in pBluescript II KS+. pCD0 contains a 1.5 kb XhoI fragment from pCD7, cloned at Xho I site of pCD1. EcoRI and SacI digestion releases the complete *Wdr13* cDNA.
- D) pPOLY III-*Wdr13*:** This plasmid contains a 1.8 kb EcoRI and SacI excised *Wdr13* cDNA fragment from pCD0, cloned at EcoRI and SacI sites of pPOLY III.
- E) pCI-*Wdr13*:** This plasmid contains a 1.8 kb EcoRI and XbaI excised *Wdr13* cDNA fragment from pPOLY III-*Wdr13*, cloned at EcoRI and XbaI sites of pCI vector.
- F) pCMV-FLAG-*Wdr13*:** This plasmid contains *Wdr13* cDNA at EcoRI and XbaI restriction sites, after amplification with Forward primer 5'CCGGAATTCCGGATGGCCGCGGTGTGG3' and reverse primer 5'GCTCTAGAGCAGCACAGGGTGACAGAACC3' containing EcoRI and XbaI restriction sites respectively.
- G) pCMV-*Myc-Wdr13*:** This plasmid contains EcoRI and XbaI excised *Wdr13* cDNA fragment from pCMV-FLAG-*Wdr13*, cloned at EcoRI and XbaI restriction sites of pCMV-*Myc* vector.

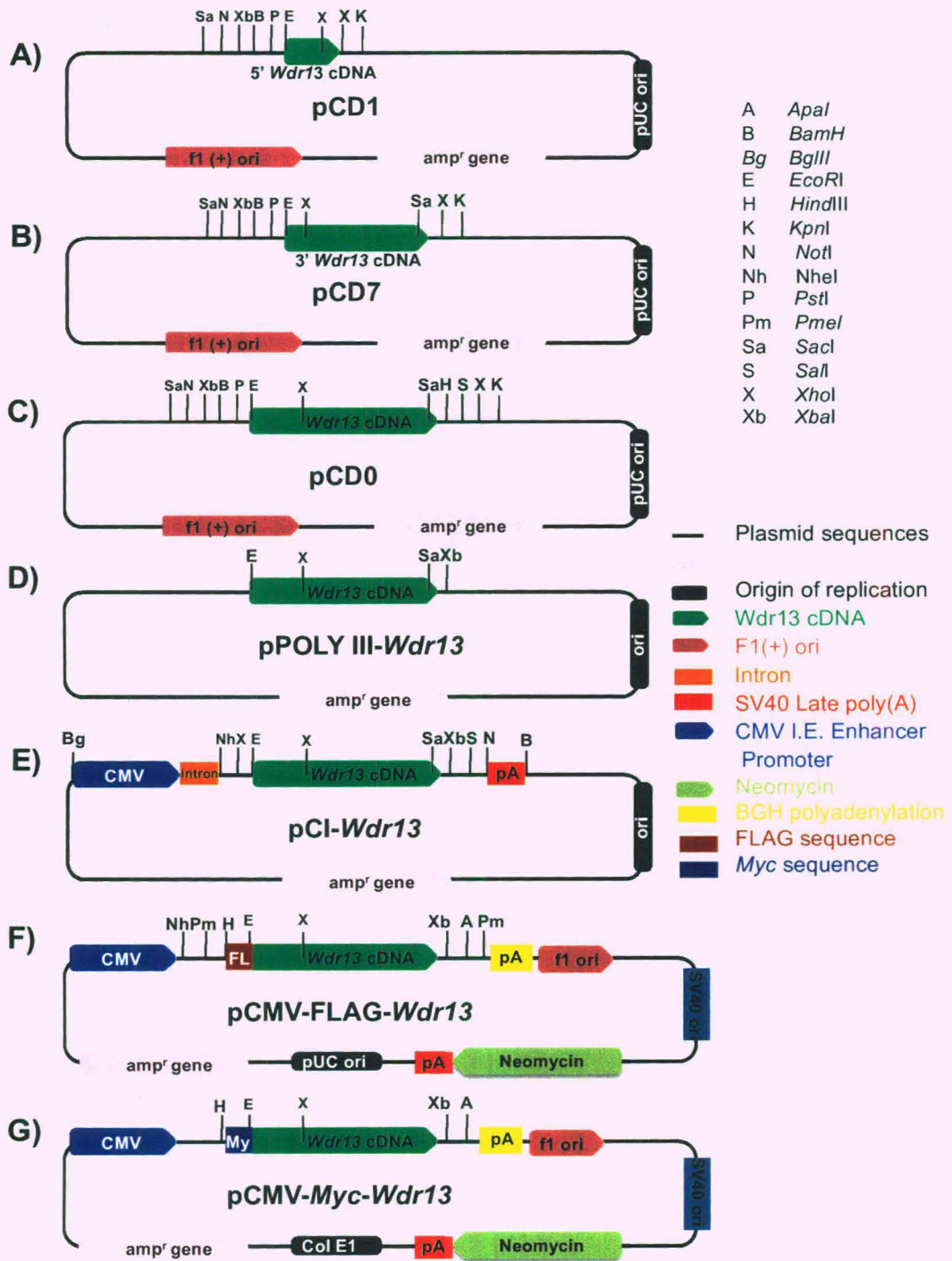


Figure 2.1 Construction of *Wdr13* overexpression vectors.

Figure 2.2 Construction of pCMV-Myc-PHIP1 vector

A) pMOS-PHIP-WD: This plasmid contains N-terminal WD domain DNA fragment of *PHIP1* at EcoRV site of pMOS-blue after amplification with forward primer 5'CTCGTGAGCACACACTGACA3' and reverse primer 5'TTCCATATCCCAAGGACTCA3'.

B) pMOS-PHIP-Bromo: This plasmid contains C-terminal bromodomain DNA fragment of *PHIP1* at EcoRV site of pMOS-blue after amplification with forward primer 5'CCCAGGAGATGTCCATTTGT3' and reverse primer 5'AATCCGTCATAGCAGCAAGG3'.

C) pBSKS-PHIP-bromo: This plasmid contains a 2.2 kb BglII and BamHI excised fragment of pMOS-PHIP-Bromo, cloned at BamHI site of pBluescript II KS+.

D) pCMV-Myc-PHIP-WD: This plasmid contains a 3.3 kb StuI and XbaI excised fragment from pMOS-PHIP-WD, cloned at EcoRI (end-filled) and XbaI sites of pCMV-Myc vector.

E) pCMV-Myc-PHIP-Bromo: This plasmid contains a 2.2 kb XbaI and EcoRI (partially digested) fragment from pBSKS-PHIP-Bromo, cloned at EcoRI and XbaI sites of pCMV-Myc vector.

F) pCMV-Myc-PHIP1: This plasmid contains a NdeI and BamHI (end-filled) fragment from pMOS-PHIP-Bromo plasmid, cloned at NdeI (partially digested) and XbaI (endfilled) of pCMV-Myc-PHIP-WD vector.

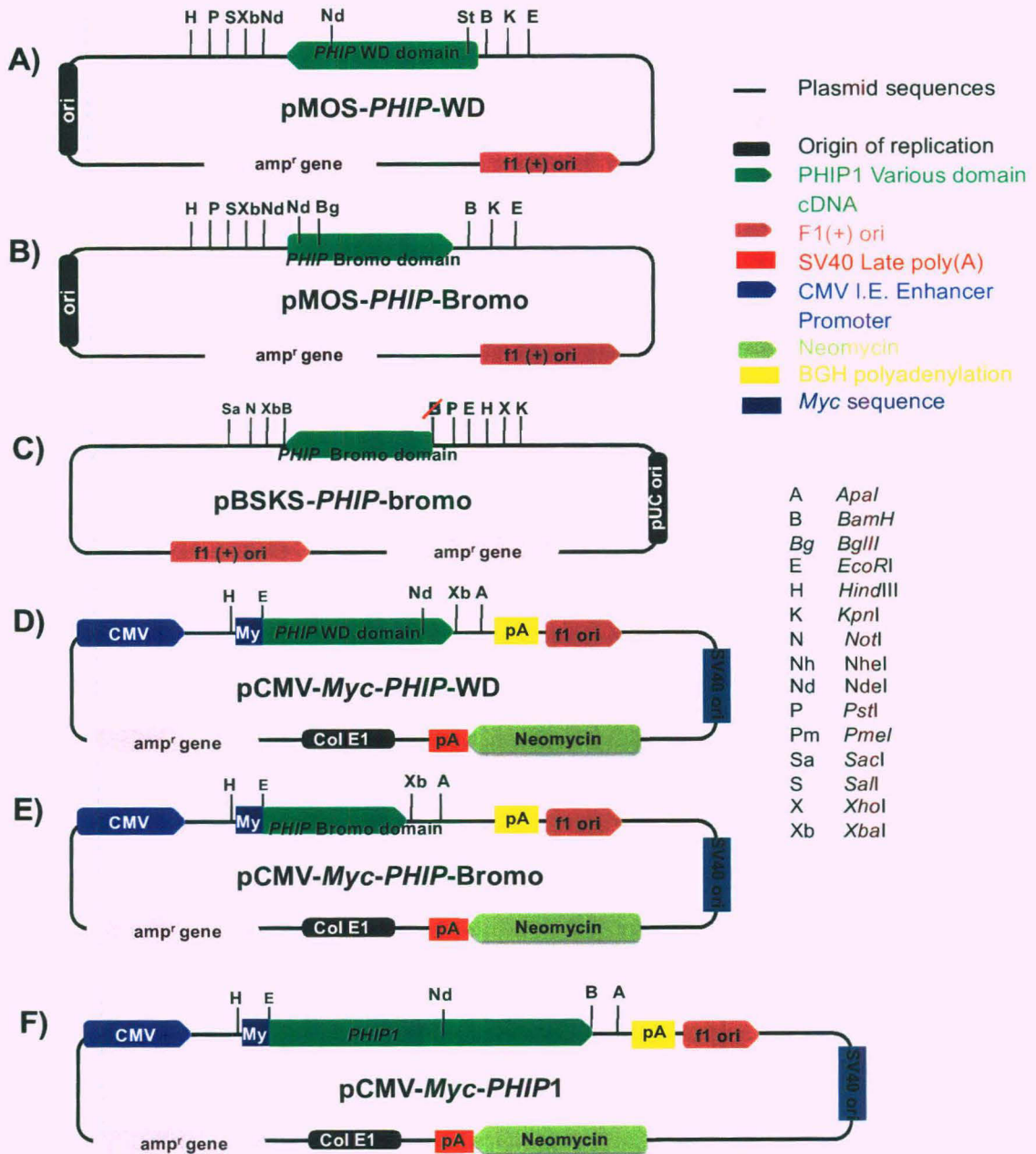


Figure 2.2 Construction of pCMV-Myc-PHIP1 vector

Figure 2.3 Construction of adenoviral vector for overexpression of FLAG tag wdr13 protein

A) pAdTrack-CMV: The basic shuttle vector contains multiple cloning sites for expression of gene of choice under CMV promoter with a built-in GFP tracer. It also contains right arm and left arm for recombination in pAdEasy-1 vector with kanamycin selection marker.

B) pAdTrack-CMV-FLAG-*Wdr13*: This plasmid contains FLAG tagged *Wdr13* cDNA at EcoRV of pAdTrack-CMV after amplification of *Wdr13* cDNA from pCMV-FLAG-*Wdr13* vector using T7 forward primer and *Wdr13* reverse primer 5'GCTCTAGAGCAGCACAGGGTGACAGAACC3'.

C) pAdEasy-1: The basic vector containing viral DNA and ampicillin selection marker. The pAdEasy-1 is an E1 and E3 double-deletion vector. Hence, the AdEasy-1 derived recombinant adenoviruses can be propagated in E1-expressing packaging cells, such as 293 or 911 cells.

D) pAdEasy-1-CMV-FLAG-*Wdr13*: The vector contains FLAG-*Wdr13* cDNA after recombination of AdEasy-1 and PmeI-linerialized pAdTrack-CMV-FLAG-*Wdr13* vectors in *E. coli* BJ5183 cells.

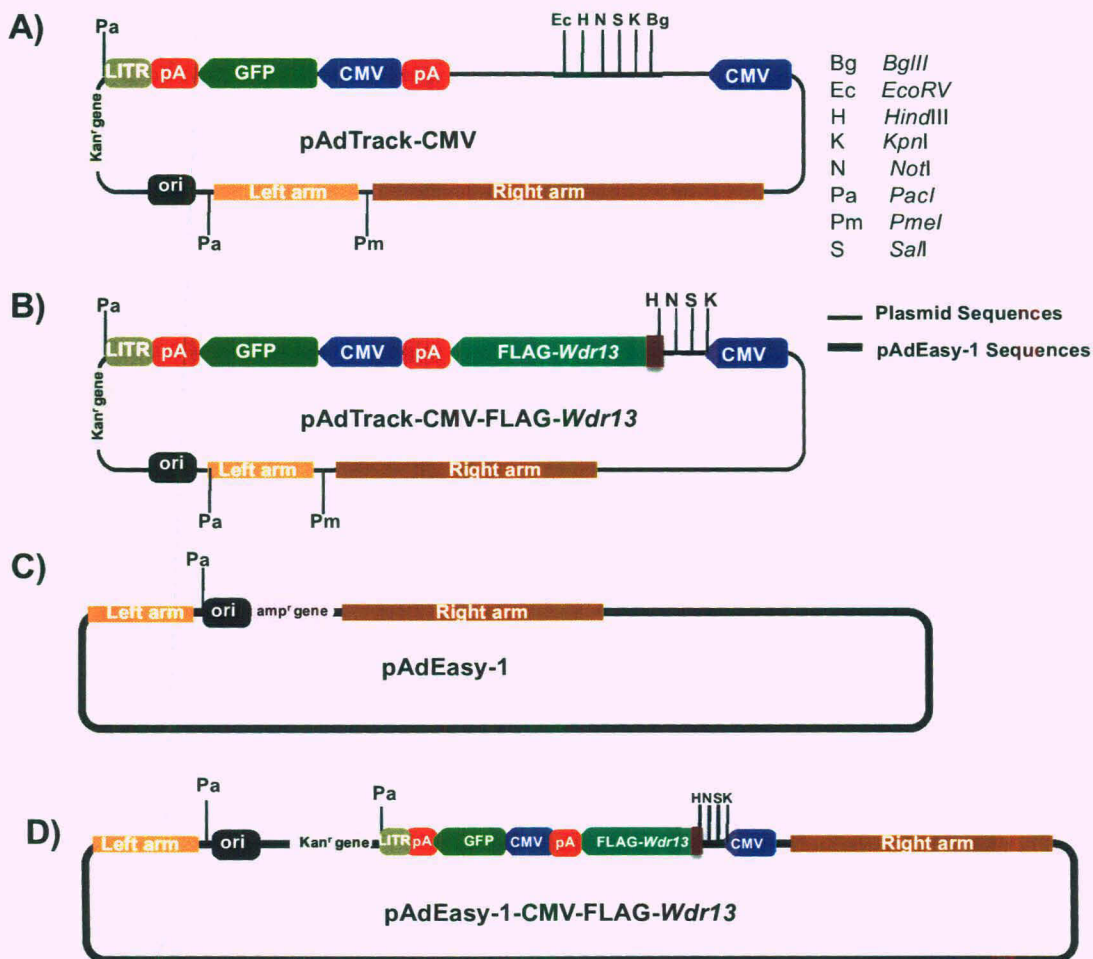


Figure 2.3 Construction of adenoviral vector for overexpression of FLAG tag wdr13 protein

2.7.2 Transfection of mammalian cells

Hela, HEK 293 and NIH3T3 cells were grown in complete media (13.3g/L DMEM, 3.7g/L NaHCO₃, 10% Serum, 50µg/ml ampicillin and 50µg/ml streptomycin). After reaching confluency cells were washed with 7 ml PBS at least twice, and then cells were trypsinized using pre-warmed (37°C) trypsin/EDTA solution (one ml for 75cm² flask), the flask was swirled to cover the culture completely and incubated in incubator (37°C) for 120 seconds. Flasks were gently tapped from the sides to lift off the cells from the surface; approximately 5 ml of complete medium was added to neutralize the Trypsin/EDTA solution. Cell suspension was pipetted up and down several times to dissociate into single cells. Cells were centrifuged in 15 ml tubes at room temperature for 5 minutes at 1000g. Supernatant was removed and cells were resuspended in fresh medium. The cells were seeded at desired splitting ratio (generally 1:9) and cultured until confluent. Cells were frozen and thawed as described in section 2.6.

Cells were transfected using Xfect™ (Clontech) as described by manufacturer instructions. Briefly cells were transfected at 60-80% confluency as described in table 2.1.

Table 2.1 - Transfected of various cell line using Xfect™

| Culture Vessel | Surface Area/Well | Complete Medium | DNA | DNA Dilution Volume | Xfect Polymer Volume | Polymer Dilution Volume |
|----------------|--------------------|-----------------|----------|---------------------|----------------------|-------------------------|
| 24-well plate | 2 cm ² | 250 µl | 0.75 µg | 25 µl | 0.23 µl | 25 µl |
| 12-well plate | 4 cm ² | 500 µl | 1.50 µg | 50 µl | 0.45 µl | 50 µl |
| 6-well plate | 10 cm ² | 01 ml | 5.00 µg | 100 µl | 1.50 µl | 100 µl |
| 10-cm dish | 60 cm ² | 10 ml | 30.00 µg | 600 µl | 9.00 µl | 600 µl |

DNA was diluted in dilution buffer, mixed with Xfect polymer and incubated for 10 minutes to form complex at room temperature. Finally DNA and Xfect mix was added to cells and swirled to mix with complete medium. The complex was incubated with cells for 3-4 hours and changed with fresh complete medium. The transfected cells were incubated at 37 °C for 48 to 72 hours.

2.7.3 Lysis of mammalian cells and immunoprecipitation

For immunoprecipitation, pCMV-FLAG-*Wdr13* vector and control pEF1GFP vector were transfected in ten 100mm dish of HELA cells each using Xfect reagent (Denis et al., 2006). After 48h of transfection cells were lysed in lysis buffer (50mM –Tris.HCl, 150mM-NaCl, 1mM-EDTA, 1%-Triton X-100 and Protease inhibitor cocktail). Cell lysate was centrifuged and pre-cleaned with Protein A. In pre cleaned lysate anti FLAG agarose beads (Sigma) was added and incubated for 4h at room temperature. Immuno complex was washed 4 times with wash buffer (50mM –Tris.HCl, 150mM-NaCl, 1mM-EDTA, 0.5%-Triton X-100 and Protease inhibitor cocktail). Immunocomplex was eluted using FLAG peptide (Sigma) and separated on 12% SDS PAGE for just 1cm. The gel was either stained with 0.1% Coomassie blue R-250 (in 40% methanol and 10% acetic acid) or blotted on PVDF membrane for western blot.

2.7.4 Trypsin digestion and LC-MS/MS

The entire gel was cut into 3 slices of roughly equal size and used for tryptic digestion as per manufacturers' instructions (Sigma). Peptide were separated using a capillary liquid chromatography system (Agilent HPLC 1100 Series, Agilent Technologies, Santa Clara, CA, USA) which was attached with a reversed-phase column (ZORBAX 300SB-C18, 75 µm × 150 mm, 3.5 µm, Agilent Technologies, Santa Clara, CA, USA) and coupled online to a MALDI target spotter (Probot, LC Packings, Dionex, Sunnyvale, CA, USA). The

mobile phase consisted of (A) 0.2% formic acid and (B) 0.2% formic acid in 90% acetonitrile. The peptides were dissolved in 10 μ L 0.1% TFA and samples were trapped on a short C18 reversed-phase column (300 mm id, 5 mm). Peptide separation was achieved with a 90 min linear gradient from 0 to 100% B at a flow rate of 200 nl/min. For MALDI analysis, the column effluent was directly mixed with MALDI matrix (5mg/ml α -cyano-4-hydroxycinnamic acid in 50% v/v acetonitrile/0.1% v/v TFA) at a flow rate of 3 μ L/min via a m-Tee fitting. Fractions were automatically deposited every 20 second onto a MALDI target plate (Applied Biosystems, Foster City, CA) using a Probot micro fraction collector. A total of 240 spots were collected from each HPLC run.

Mass-spectrometric analysis was performed on a 4800 MALDI TOF/TOF Analyzer (Applied Biosystems, Foster City, CA, USA) equipped with an Nd:YAG laser operating at 200 Hz. MS-spectra were acquired by accumulation of 1500 laser shots using the positive reflector mode. First, MS spectra were recorded from peptide standards on each of the 13 calibration spots and the default calibration parameters were updated. Second, MS spectra were recorded for all sample spots on the MALDI target plate (240 spots per sample per plate). MS/MS was performed using Information dependent acquisition (IDA) and spectral peaks that met the threshold criteria were included in the acquisition list for the MS/MS spectra. The following threshold criteria and settings were used: Mass range: 800–4000 m/z; minimum S/N for MS/MS acquisition: 100; maximum number of peaks/spot: 14. Peptide CID was performed at a collision energy of 1 kV and a collision gas pressure of approximately 2.5×10^6 Torr. During MS/MS data acquisition, 2000 laser shots were allowed for each spectrum. All obtained MS/MS-spectra were searched against the NCBI Homo sapiens protein sequence database. MASCOT Server (version 2.0) in combination with the GPS-ExplorerTM 3.6 software (Applied Biosystems, Foster City, CA, USA) was used for analysis.

2.8 Overexpression of *wdr13* protein in ES cells

2.8.1 Construction of pCMV-LNL-*Wdr13* vector

pMC1neo Poly A vector was digested with XhoI BamHI, endfilled and 1.1 kb neomycin fragment was cloned at endfilled HindIII, BamHI site of pBS246 (containing LoxP) by blunt end ligation, to destroy BamHI site for further cloning steps, named as pLNL. To construct the pCMV-LNL-*Wdr13* vector, pLNL was digested with NotI, XmnI, endfilled and 1.2 kb neomycin fragment was cloned at endfilled NheI site of pCMV-*Wdr13* vector by blunt end ligation method. The resulting vector was named as pCMV-LNL-*Wdr13* (Figure 2.4).

2.8.2 Construction of pHPRT-CMV-LNL-*Wdr13* vector

p18.6 containing HPRT gene was digested with EcoRV and 5kb EcoRV fragment containing exon2 and exon3 was cloned at EcoRV site of pBluescript II KS (XhoI site of pBluescript II KS was destroyed), named as pHPRT. pCMV-LNL-*Wdr13* plasmid was digested with BglII, BamHI, endfilled and 4.1 kb fragment (containing LNL and *Wdr13* cDNA) was cloned at endfilled XhoI site of pHPRT, named as pHPRT-CMV-LNL-*Wdr13*. The resulting vector was linearized with ApaI before electroporation into ES cells (Figure 2.4).

2.8.3 ES cells culture, electroporation and screening of clones

Preparation of feeders from MEFs

MEFs were cultured to confluence, medium was discarded and fresh pre-warmed complete medium was added. About 120 μ l of thawed Mitomycin C (50X stock) was added at final concentration 10 μ g /ml. Culture flasks were incubated for three hours at 37°C and 5% CO₂. After three hours, Mitomycin C containing medium was discarded and washed twice with PBS. Cells were

trypsinized and harvested as described above. Approximately 10 ml of cell suspension was placed to Neubauer haematocytometer with cover glass over and the cells were counted using the microscope. The number of cells per ml was calculated, and the total number of cells in the original culture was calculated as follows:

$$\text{Cells/ml} = \text{average count per square} \times 10^4$$

Total cells = cells per ml X dilution factor X total volume of cell preparation from which the sample was taken.

Thawing of mouse ES cells

Feeders were seeded in appropriate culture area at least 12 hours before seeding ES cells as given in table 2.2. For feeder free ES cell culture, culture plates were treated with 0.1% gelatin for atleast half an hour before seeding of ES cells. Gelatin was later aspirated completely just before seeding of ES cells. Vials of ES cells were taken out from liquid N₂ container and quickly thawed in 37°C water bath. Aseptically the cell suspension was transferred into a sterile centrifuge tube containing several ml of warm ES cell medium (13.3g/L DMEM, 3.7g/L NaHCO₃, 15% Serum, Minimum Non Essential amino acids 0.1mM/ml, β Mercaptoethanol 0.1mM/ml, Maurine Leukemia inhibitory factor 1000U/ml, Glutamax 2.0mM/ml, 50µg/ml ampicillin and 50µg/ml streptomycine). Cells were pelleted by centrifugation at 1000g for 5 minutes. Supernatant was aspirated and cells were resuspended into required quantity of fresh medium. Culture medium from the flasks containing feeders was aspirated; ES cells were seeded into the flasks and cultured in incubator (at 37°C and 5% CO₂).

Passage/expansion of ES cells

ES cell cultures were passaged at sub-confluence. ES cell medium was changed three hours before passaging them. Medium was aspirated and washed twice with PBS. Appropriate quantity of pre-warmed Trypsin/EDTA solution was added, swirled and placed in incubator at 37°C for 1-2 minutes.

The flask was gently tapped to lift off the colonies from the surface. Trypsin activity was neutralized by adding appropriate volume of ES cell medium. Colonies were dissociated into single cells by pipetting up and down for several times. Cells were pelleted by centrifugation at 1000g for 5 minutes. Medium was aspirated and the cells were resuspended in appropriate volume of fresh ES cell medium and cells were seeded in 1:6 ratios in to the flasks. Flasks were tilted several times to distribute the cells evenly and placed in the incubator.

Freezing of ES cells

ES cell cultures were passaged at sub-confluence and medium was changed three hours before freezing of ES cells. ES cells were harvested as described above. Medium was aspirated and the cells were resuspended in appropriate volume of ice-cold freezing medium (10% DMSO, 90% FBS). Cell suspension was transferred into pre-labeled cryovials. Vials were placed into pre-cooled Styrofoam box and transferred to -80°C freezers overnight. The next day cryovials were transfer to liquid nitrogen tank (-196°C) for long term storage.

Electroporation of ES cells

Growing ES cells from a sub-confluent culture were harvested by trypsinisation, pelleted by centrifugation and resuspended at high density in PBS. The cells were counted using a Neubauer haematocytometer. The cell concentration was adjusted to 10^8 cells/ml. About 0.8 ml cell suspensions containing 25-40 μg of targeting vector DNA was placed in a Bio-Rad Gene Pulser cuvette (width 0.4 cm). The mixture was given a single pulse of 240V and 500 μF . The electroporated cells were incubated at room temperature for 10 minutes, transferred into complete medium and plated in suitable dishes containing feeders. After 24 hours, medium was changed to complete medium containing G418 (250 $\mu\text{g}/\text{ml}$) to select for neomycin resistance gene marker. Medium was changed every 24-36 hours, 6-thioguanine (6-TG) was added five days onwards to kill HPRT positive ES cells. After 10 days of selection individual ES cell colonies were isolated for expansion and DNA analysis.

Figure 2.4 Construction of HPRT targeting vector for *wdr13* overexpression in ES cells.

- A) pLNL :** The vector contains 1.1kb XhoI (end-filled) and BamHI (end-filled) neomycin fragment from pMC1neo Poly A, cloned at HindIII (end-filled) and BamHI (end-filled) sites of pBS246 (containing LoxP).
- B) pCMV-LNL-*Wdr13*:** This vector contains a 1.2 kb NotI (end-filled) and XmnI (end-filled) neomycin fragment from pLNL, cloned at end-filled NheI site of pCMV-*Wdr13*.
- C) pHPRT-CMV-LNL-*Wdr13*:** This vector contains a 4.1 kb BglII (end-filled) and BamHI (end-filled) fragment (containing LNL and *Wdr13* cDNA) from pCMV-LNL-*Wdr13* vector, cloned at XhoI (end-filled) site of pHPRT.

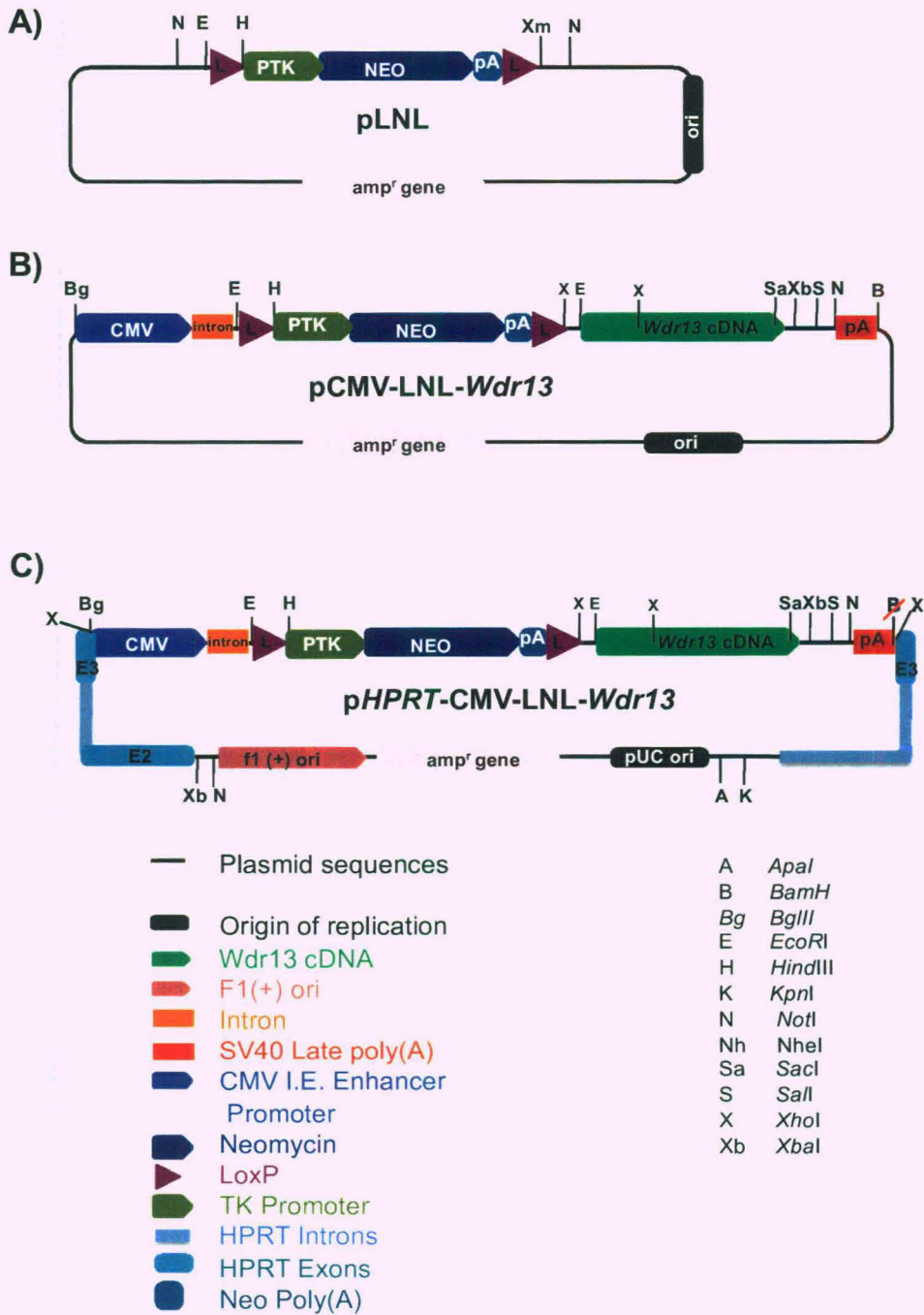


Figure 2.4 Construction of *HPRT* targeting vector for *wdr13* overexpression in ES cells.

Isolation and expansion of individual ES cell clones

Following electroporation and selection, individual ES cell colonies with undifferentiated phenotype were picked up using p2-p10 pipette tips while working under inverted microscope in laminar airflow cabinet. Each colony was incubated for a brief period in small drop (50 μ l) of 0.05 % trypsin/EDTA. Trypsin activity was neutralized with 200 μ l complete medium and colony was disintegrated by trituration with p20-p200 pipette tips. The cell suspension was plated in a well of 24 well plate containing 0.5 ml complete medium and cultured in CO₂ incubator. The following day the cells were fed with fresh medium. At confluency (3-4 days), cells were trypsinized, around 50% of the cells were frozen for future retrieval and the rest of the cells were left behind in the wells to be cultured for DNA preparation.

Chromosome Analysis of ES Cells

Chromosome spreads of the targeted ES cells were analyzed by the method described by Robertson (1987) except that the cells were not treated with colcemid. Cells from a sub-confluent T25 cm² flask were trypsinized, pelleted and washed with PBS two times. Pelleted cells were resuspended by continuous flicking in 3 ml pre-warmed (37°C) hypotonic solution (0.56% w/v KCl) and incubated at 37°C for 15-20 minutes. An equal volume of ice cold Carnoy's fixative (three volumes of absolute methanol: one volume of glacial acetic acid; freshly prepared) was added by continuous flicking to avoid formation of clumps. Cells were pelleted at 1000g for 5 minutes and resuspended in 5 ml fixative and pelleted again. The cells were washed atleast twice with the fixative and finally suspended in 0.5 ml of fixative. The metaphase spreads were prepared on pre-cleaned slides. The slides were air dried and stained in 3% (v/v) Gurr's Giemsa stain in PBS for 10-15 minutes and the chromosome number was analyzed by examination of slides under oil immersion objective (~ 1000 X total magnification).

Excision of neomycin resistance gene by transient expression of Cre-Recombinase using pNCP

The targeted ES cells were cultured in T25 cm² flask to sub-confluence; cells were trypsinized and counted. Around 2 million ES cells were electroporated with 5 µg of super coiled pNCP and plated into appropriate culture dishes with feeders as described in sub-section 2.5.5. Approximately 0.5×10^6 cells were plated per 100 mm culture dish to ensure growth of individual separate colonies. Six hours post electroporation, equal volume of complete ES cell medium containing 4 µg/ml puromycin drug was added to the culture dishes to achieve final concentration of 2 µg/ml puromycin. The medium containing puromycin was replaced with complete ES cell medium after 30 hours of electroporation. After five days of culture, separate individual colonies were picked, plated as replicas in 48 well plates for further analysis to confirm neomycin sensitivity.

Table 2.2 – MEFs seeding density chart

| S. No. | Type of Vessels | Area/well (cm ²) | Total culture Area (cm ²) | Total no. of feeder (PMEF) cells | Volume of Working media required | Volume of Trypsin / EDTA required |
|--------|-----------------------------|------------------------------|---------------------------------------|----------------------------------|----------------------------------|-----------------------------------|
| 1 | Flask (T25) | | 25 | 0.31x10 ⁶ | 3 - 4 ml | 500 µl – 800 µl |
| 2 | Flask (T75) | | 75 | 0.93x10 ⁶ | 10 ml | 1.0 ml |
| 3 | Flask (T150) | | 150 | 1.86x10 ⁶ | 20 ml | 2.0 ml |
| 4 | Flask (T175) | | 175 | 2.11x10 ⁶ | 25 ml | 2.5 ml |
| 5 | Flask (T225) | | 225 | 2.79x10 ⁶ | 30 ml | 3.0 ml – 4.0 ml |
| 6 | Small Dish (35 mm x10 mm) | | 9.6 | 0.12x10 ⁶ | 2 ml | 200 µl – 300 µl |
| 7 | Small Dish (40 mm x 10 mm) | | 12.5 | 0.15x10 ⁶ | 2 ml | 300 µl- 500 µl |
| 8 | Medium Dish (60 mm x 15 mm) | | 28.2 | 0.35x10 ⁶ | 3 - 4 ml | 500 µl – 800 µl |
| 9 | Large Dish (100 mm x 20 mm) | | 78.5 | 0.98x10 ⁶ | 10 ml | 1.0 ml |
| 10 | 96well plate | 0.35 | 37 | 0.46x10 ⁶ | 50 µl / well (Approx. 5 ml) | 10 µl – 20 µl/ well |
| 11 | 48 well plate | 0.85 | 40 | 0.5x10 ⁶ | 250 µl /well (Approx. 12 ml) | 25 µl /well |
| 12 | 24 well plate | 1.77 | 42.4 | 0.53x10 ⁶ | 500 µl /well (Approx. 12 ml) | 50 µl /well |
| 13 | 12 well plate | 3.50 | 41.6 | 0.52x10 ⁶ | 1 ml /well (Approx. 12 ml) | 100 µl/well |
| 14 | 6 well plate | 9.60 | 57.6 | 0.72x10 ⁶ | 2 ml / well (Approx. 12 ml) | 200 µl – 300 µl /well |
| 15 | 4 well plate | 1.77 | 7.08 | 0.09x10 ⁶ | 500 µl / well (Approx. 2 ml) | 50 µl /well |

Chapter 3

CHAPTER 3: PHENOTYPIC ANALYSIS OF *Wdr13* KNOCKOUT MICE

3.1 INTRODUCTION

After sequencing of the whole human genome, the next logical goal for biologists has been to understand the functions of these sequences. Loss-of-function and gain-of-function mutational studies have been extensively used to study gene function in various model systems. Mouse is an excellent mammalian system to study gene function. Availability of several resources and techniques for manipulation of genome makes it an obvious choice to study the developmental, molecular and physiological processes in mammals. The discovery of mouse embryonic stem cells (Evans and Kaufman, 1981) made it possible to create loss-of-function and gain-of-function mutations in mouse. The gene knockout technology in mouse involves targeting of a gene or locus in the mouse ES cell genome to genetically modify the ES cell genome. Such genetically altered or engineered ES cells are used to generate chimeric mice by either blastocyst injection or morula aggregation of ES cells. The chimeric mice are bred further to transmit the mutation to the next generation. These mutations lead to phenotypic effects on various aspects of mouse development, physiology and susceptibility to various diseases. To study the gene function, several gene-knockout and overexpression mouse strains have been created and the resultant phenotypes have been analyzed. This approach has also been successful in developing mouse models of various human diseases. The examples include neurological disorders, cardiovascular diseases, developmental disorders, diabetes, obesity and infertility (Francia et al., 2011; Lijnen, 2011; Roy and Matzuk, 2006).

In constitutive gene knockout strategy, a gene or part of the gene is replaced with selection markers (e.g. neomycin, puromycin) thereby ablating the expression of the gene. This approach is appropriate when the phenotype defects appear in the post-natal stages. Most gene knockout mice are generated by this approach. When a gene is likely to an essential role in

mouse embryogenesis, the mutant embryos would abort due to developmental arrests. In such a scenario, it becomes difficult to understand the molecular mechanisms underlying the phenotype and impossible to see the effect of loss of the gene in the adult mice. To overcome these limitations, conditional targeting of the gene can be achieved by utilizing Cre-lox system (Gu et al., 1994). A conditional knockout mouse can be constructed by introducing loxP sequences on either sides of an exon (floxed exon) of the gene without disturbing the expression and function of the gene. These conditional knockout mice are then bred with suitable transgenic mice expressing cre-recombinase in a tissue specific or developmental stage specific/ inducible promoters to achieve control over the tissue and the timing of knockout of the floxed exon.

Phenotypes of targeted mouse mutants are not always those predicted from expression data and the presumed function of a given gene product. In some cases, unexpected phenotype such as lethality due to inflammatory bowel disease in interleukin-2 knockout mice (Sadlack et al., 1993) has been observed, whereas other null mutations revealed either very minor, or no apparent defect such as HPRT-deficient mice (Wu and Melton, 1993). The absence of phenotype may be due to functional redundancy between genes and/ or at the genetic pathway level. In several cases different independent groups have knocked out the same gene but disparate phenotypes have been reported. The phenotypic discrepancies may be due to variation in genetic background or different targeting construct which may affect adjacent or overlapping genes (Muller, 1999).

The majority of targeted mouse mutants to date have been generated using ES cell derived from 129 substrains and in many cases initial analysis was performed with mixed genetic background (129 X C57BL/6 or 129 X BALB/c). The mixed genetic background may affect the phenotype of a mutant gene. To eliminate the confounding effect caused by mixed genetic backgrounds, mutant mice can be maintained on pure genetic background. This is achieved by breeding of chimera with the same genetic background as

of the ES cells or by backcrossing for several generations to the desired mouse strains. Apart from the effect of genetic background, functional redundancy in genes and genetic pathways can affect the phenotype. Within gene families, related proteins may functionally compensate for the deficits associated with the loss of one of the family members. The example of functional compensation has been seen in β -APP gene family consisting of ubiquitously expressed APP-protein and two closely related APP-like proteins, APLP1 and APLP2. Knockout of individual gene resulted in very minor phenotypes whereas deletion of various combination of these genes at the same time has resulted in postnatal lethality (Muller, 1999).

Various genes have been implicated in different stages of germ cell differentiation, but the complete process, which affects reproduction, is still unknown (DeJong, 2006; Matzuk and Lamb, 2002; Roy and Matzuk, 2006). Reproduction is essential for the propagation of species and continuation of life. It is a complex biological process and is regulated by multiple factors during the reproductive lifespan of an organism. About 300 knockout mouse strains have been shown to have defects in the reproductive process (Roy and Matzuk, 2006) along with other abnormalities. Among the earliest mouse knockouts generated, that were found to affect different aspects of reproduction were *inhibin α* (Matzuk et al., 1992), *leukemia inhibitory factor (LIF)* (Stewart et al., 1992), and *estrogen receptor knockout α* (Lubahn et al., 1993). The LIF deficient females had defect in implantation, while *inhibin α* knockout males and females were infertile and developed gonadal tumor. The female knockout mice for *estrogen receptor knockout α* were infertile while males had reduced fertility. Other than altered reproduction these knockout mice developed various complex phenotypes; namely, cancer, neurological disorders, diabetes and obesity. The *estrogen receptor knockout α* male and female mice developed obesity in age dependent manner (Heine et al., 2000). The knockout of cell cycle inhibitor p21 and p27 developed normally with increased sertoli cells number in testis along with increased testis mass (Holsberger et al., 2005). However, these knockout mice developed obesity

and tumors in various tissues with age (Naaz et al., 2004; Philipp et al., 1999). These examples indicate that knockout of a gene may have a limited effect or may result into a complex phenotype.

Wdr13 is a member of WD repeats protein family, which expresses in unfertilized egg, neural stem cells and germ cells during development. The predominant expression of *Wdr13* in germ cells suggests the necessity of the gene during their differentiation or maintenance (Suresh et al., 2005). Given the conservation of *wdr13* protein throughout evolution in vertebrates and its ubiquitous expression, the *Wdr13* knockout mice was generated (CCMB annual report - 2008). The *Wdr13* gene was constitutively knocked out in mouse ES cells by replacing exon2 and exon3 (partially) with neomycin containing poly A. The engineered mouse ES cells were injected in C57BL/6 blastocysts to generate chimera. The chimeras were bred with CD1 mice strain to get the germ line transmission. The germ line transmission was analysed by southern blot analysis.

This chapter describes the phenotypic analysis of *Wdr13* knockout mice. The mutant mice are viable and fertile. Further, overexpression of *wdr13* protein using adenoviral system in MIN6 and NIH3T3 cells and the resultant phenotypes have been described in this chapter.

3.2 RESULTS

3.2.1 Screening of *Wdr13* knockout mice

The genotyping of *Wdr13* knockout and wild type mice was done by southern blot analysis. The strategy for screening is given in Figure 3.1A. A 700bp DNA fragment containing 5' region of *Wdr13* gene was used as probe. After EcoRI digestion of genomic DNA, *Wdr13* +/0 and +/+ allele showed 9.3kb band size, where as *Wdr13* -/0 and -/- showed 3.8kb band size (Figure 3.1B). The *Wdr13* -/+ mice showed both wild type (9.3kb) as well as mutant band (3.8kb). Further PCR was performed to screen the *Wdr13* knockout mice to make it easy for next generations. Since exon 2 of *Wdr13* gene was replaced by neomycin gene, two primer pairs, each from exon 2 and neomycin had been used to differentiate *Wdr13* +/0, +/+ (193bp), *Wdr13* +/- (193bp and 345bp) and *Wdr13* -/0, -/- (345bp) allele (Figure 3.1C).

3.2.2 Targeting of *Wdr13* gene leads to null allele

The targeting of *Wdr13* gene was further confirmed by northern blot as well as by western blot analysis. Using *Wdr13* cDNA as probe, northern blot analysis was performed from brain, testis tissues of *Wdr13* +/0 and *Wdr13* -/0 mice. As expected, 4kb *Wdr13* transcript from brain tissues and 2kb *Wdr13* transcript from testis tissues were not detected in knockout mice, suggesting that there is no transcription of *Wdr13* mRNA in knockout mice (Figure 3.2A). To further strengthen our targeting results, western blot analysis was performed from various tissues like brain, testis, liver and pancreas using anti *wdr13* antibody (Sigma). None of the tissues examined showed *wdr13* protein expression in knockout mice (Figure 3.2B). In pancreas, the predominant expression of *wdr13* protein was observed in purified pancreatic islet but not in the acinar cells (Figure 3.2B), suggesting role of *wdr13* protein in islet cells.

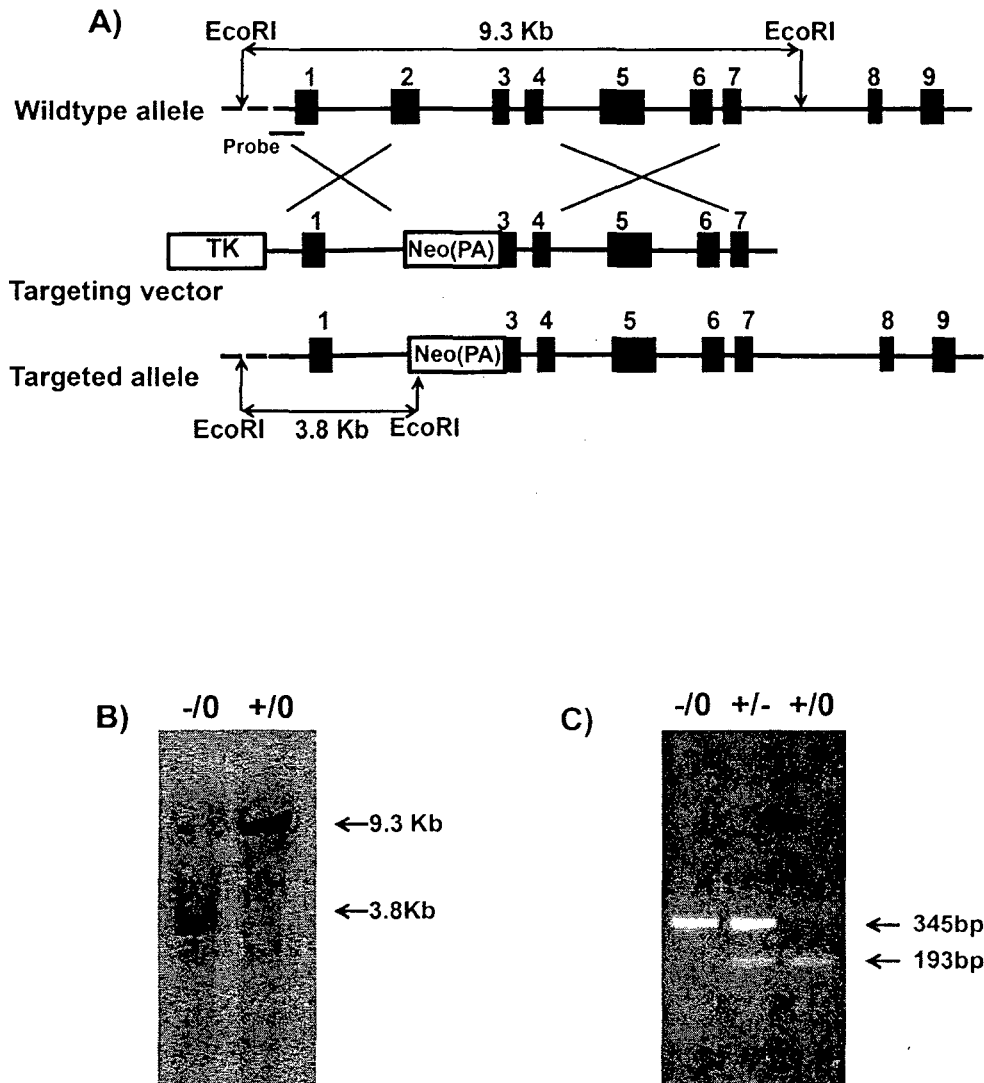


Figure 3.1 Screening of *Wdr13* $-/0$ mice. A) Upon targeting exon2 and exon3 (partial) of *Wdr13* gene are replaced by neomycin resistant marker gene. B) Southern blot analysis shows 9.3 kb EcoRI fragment from wild type allele and 3.8 kb fragment from mutant allele using a 700 bp 5' probe. C) Genotyping of *Wdr13* knockout mice by PCR screening shows 345bp amplicon in knockout mice and 193bp amplicon in wild type mice whereas heterozygous shows both bands.

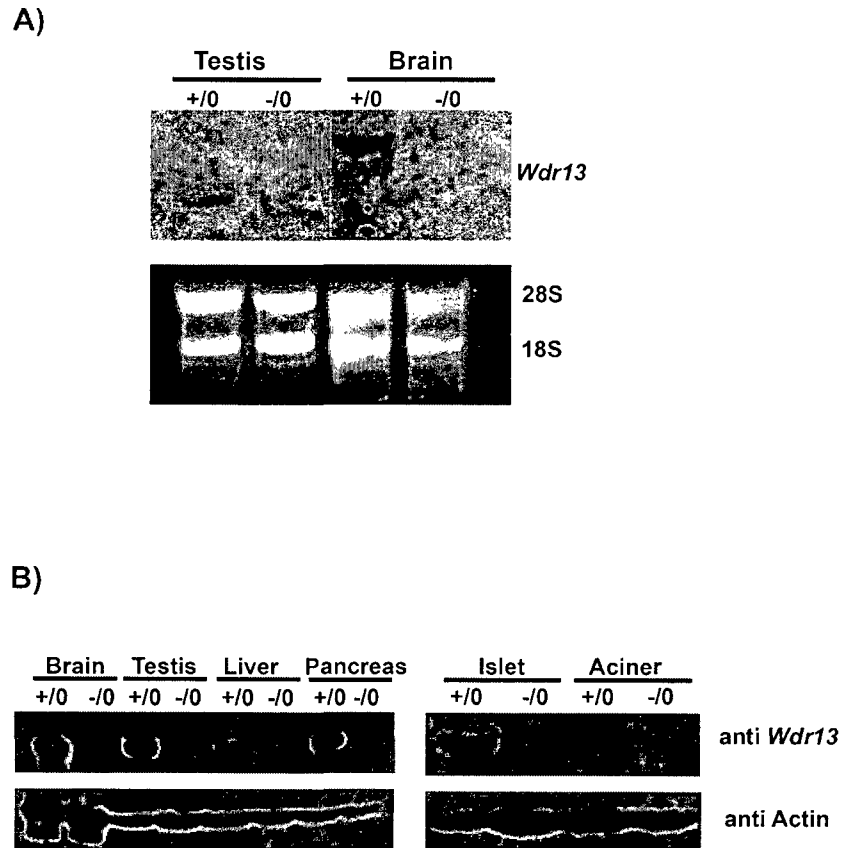


Figure 3.2 Targeting *Wdr13* gene lead to null allele. A) Northern blot analysis by *Wdr13* cDNA probe shows absence of *Wdr13* transcript in *Wdr13* *-/-* mice (upper panel) and ethidium bromide staining as loading control (lower Panel). B) Western blot analysis from Brain, testis, liver, pancreas, purified islet and acinar cells using anti-*wdr13* rabbit polyclonal antibody (upper panel) shows absence of *wdr13* protein in *Wdr13* *-/-* mice and anti-beta actin as loading control (lower panel).

3.2.3 Effect of *Wdr13* genotype on litter size

Wdr13 Knockout males and females are viable and fertile. They were born in expected mendelian ratio, suggesting no lethality or gross abnormality during development. Given the relatively high expression of *wdr13* protein in testis and ovary, the litter size from matings involving different possible *Wdr13* parental genotypes were analyzed (Table 3.1). The parental genotypes did not affect the litter sizes and sex ratios in the progeny from such various mating types.

3.2.4 Unaltered Sperm number and motility in *Wdr13* knockout mice

Various fertility parameters of *Wdr13* +/0 and *Wdr13* -/0 male mice were analysed. The sperm number was 37.96 ± 3.05 million/ml for *Wdr13* +/0 and 40.68 ± 5.49 million/ml for *Wdr13* -/0 genotype, indicating no significant difference between the wildtype and knockout mice. To further study the sperm properties, various sperm motility parameters such as straight line velocity (VSL), straightness, lateral head movement (ALH), beat cross frequency (BCF), curvilinear velocity (VCL) and linearity (LIN) were performed using CASA (Figure 3.3) from *Wdr13* +/0 and *Wdr13* -/0 mice. All the sperm motility parameters of *Wdr13* knockout mice were comparable with those of wild type.

3.2.5 Unaltered acrosome reaction of *Wdr13* knockout mice

Acrosomal reaction of sperms occurs during their movement in female reproductive track. To study the effect of *Wdr13* genotype on acrosome reaction, sperms were cultured in Krebs Ringer Bicarbonate media for four hours and stained with Coomassie Brilliant Blue G-250 at various time points for number of reacted sperms. Spermatozoa with intact acrosome showed blue stain at head while such stain was not present on sperm that had undergone the acrosome reaction. The percentages of reacted sperms were similar in *Wdr13* -/0 mice and their wild type littermates at various time points (Table 3.2).

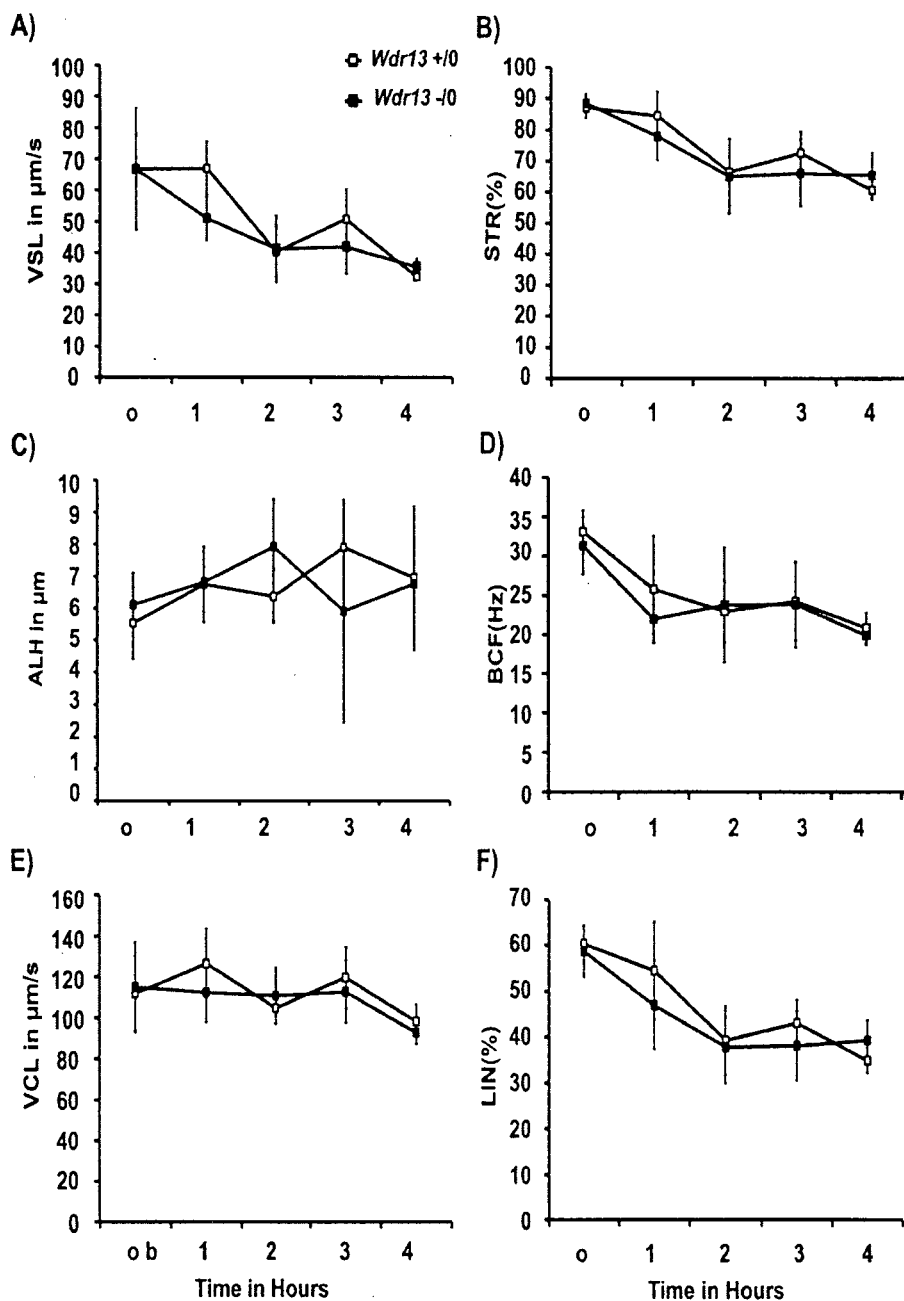


Figure 3.3 Sperm Motility parameters of Wild type (○) and *Wdr13* ^{-/-} (●) mice. A) Straight Line velocity (VSL), B) Straightness, C) Lateral head movement (ALH), D) Beat cross frequency (BCF), E) Curvilinear Velocity (VCL) and F) Linearity (LIN). Various sperm motility parameters of *Wdr13* ^{-/-} are similar to their wildtype littermates.

Table 3.1- Effect of *Wdr13* genotype on litter size

| Mating type | Number of matings | Average litter size |
|-------------------------------------|-------------------|---------------------|
| <i>Wdr13</i> -/0 X <i>Wdr13</i> -/+ | 6 | 11.66 |
| <i>Wdr13</i> +/0 X <i>Wdr13</i> -/+ | 7 | 10.57 |
| <i>Wdr13</i> -/0 X <i>Wdr13</i> +/+ | 5 | 10.40 |
| <i>Wdr13</i> -/0 X <i>Wdr13</i> -/- | 6 | 09.83 |

Table 3.2- Effect of *Wdr13* genotype on % acrosome reaction

| Time | <i>Wdr13</i> +/0 | <i>Wdr13</i> -/0 |
|------|------------------|------------------|
| 0h | 8.75±2.59 | 8.50±3.40 |
| 1h | 22.00±7.22 | 21.00±1.47 |
| 2h | 56.00±5.04 | 43.75±7.75 |
| 3h | 59.25±5.49 | 45.25±10.92 |
| 4h | 66.66±7.63 | 59.66±9.64 |

3.2.6 *Wdr13* knockout mice gained more weight on normal chow in age dependent manner

Weight of *Wdr13* deficient mice was similar to their wildtype littermates at age of one month. However *Wdr13* deficient mice differentiated in body weight from their wild-type littermates around nine months of age and at 11 months, the mutant male mice had 13% higher weights than their littermates ($P \leq 0.05$) and this value was 11% in females (Figure 3.4A). Thus *Wdr13* mutant mice are mildly obese compared to their wild type littermates (Figure 3.5). The weight of adipose tissues at 11 months was compared and the weight of epididymal fat pad was 2.5 fold more in *Wdr13* $-/-$ mice in comparison to wild type, whereas the weight of ovarian fat pad was 2 fold more in *Wdr13* $-/-$ in comparison to the wild type (Figure 3.4C). Various organs including, brain, lung, heart, liver, pancreas, spleen and testis of mutant and wild type mice were weighed at 12 months. Mutant mice had significantly higher pancreatic weight, while there were no difference in the weights of any other organs (Table 3.3).

3.2.7 Obesity of *Wdr13* knockout mice gets preponed on high fat diet

The mild obesity of *Wdr13* knockout mice got preponed when mutant mice and their wild type littermates were kept on 60% high fat diet. The weight of mutant mice was significantly more compared to their wild type littermates at age of 6 months (Figure. 3.4B), which was significantly higher at age of 11 months on normal chow.

3.2.8 *In vitro* adipogenesis of mouse embryonic fibroblasts (MEFs)

3.2.8.1 *In vitro* differentiation of MEFs to adipocytes

To understand whether the obesity in *Wdr13* knockout mice was due to enhanced adipogenesis, we isolated embryonic fibroblast (MEFs) from 13.5

days old embryos of both mutant mice and their wild type littermates. The MEFs were grown in normal DMEM media with 10% serum till passage 3. At passage 3, cells were seeded in 60mm dish (0.35×10^6) in triplicates for each genotype. After confluency cells were fed with DMEM containing 10% FBS, 1 μ g/ml insulin, 1 μ M dexamethasone and 0.5mM 3-isobutyl -1-methyl-xanthine (hormonal cocktail) to induce adipogenesis in MEFs and the same was assayed by oil red O staining at 8th day. The oil red O staining did not show any significant difference in the extent of adipogenesis in mutant MEFs (Figure 3.6A).

3.2.8.2 Delayed expression of adipogenic marker during differentiation in knockout fibroblasts

Adipogenic markers; namely, PPAR γ and EBP α were assayed by real time PCR at day-0, day-4 and day-8 during the induction of adipogenesis to quantify the extent of adipogenesis. The expression level of PPAR γ was similar in both wildtype and *Wdr13* knockout MEFs during differentiation. However, there was an evidence of delayed expression of EBP α in *Wdr13* knockout MEFs (Figure 3.6B,C).

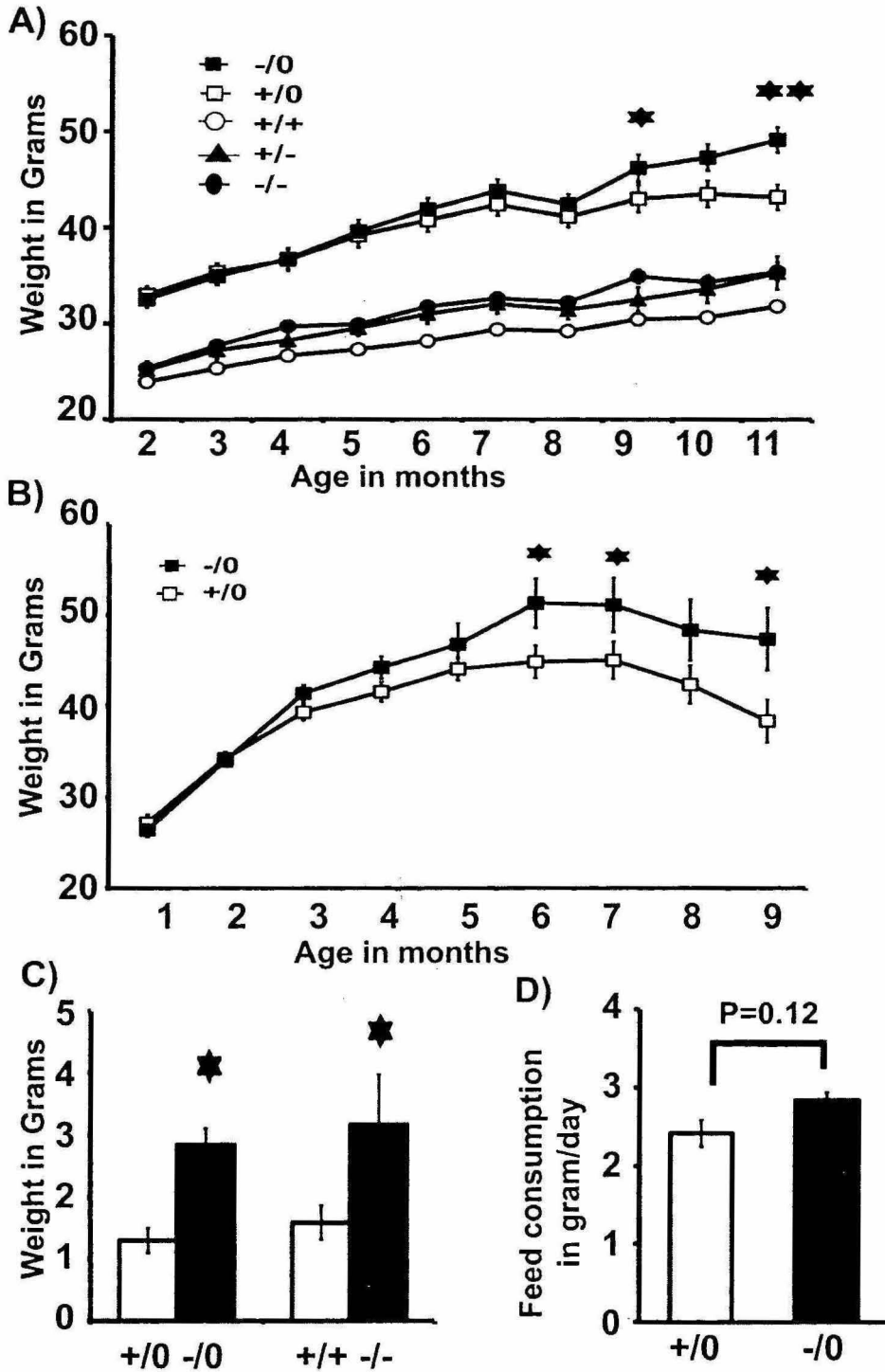
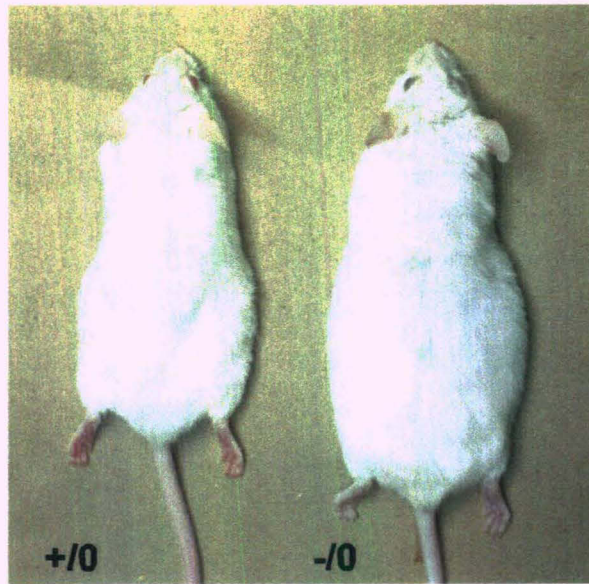


Figure 3.4 Body weight, feed consumption and metabolic parameters of *Wdr13* mutant mice on normal chow and on high fat diet. A) Growth curve of *Wdr13* +/0 male, *Wdr13* -/0 male, *Wdr13* +/+ female, *Wdr13* +/- female and *Wdr13* -/- female (n=12) on normal chow. B) Weight of *Wdr13* +/0 and -/0 on high fat diet (n=10) C) Weight of epididymal fat pad in male and ovarian fat pad in female at 12 months. D) Feed consumption in grams per day of *Wdr13* -/0 mice.

A)



B)

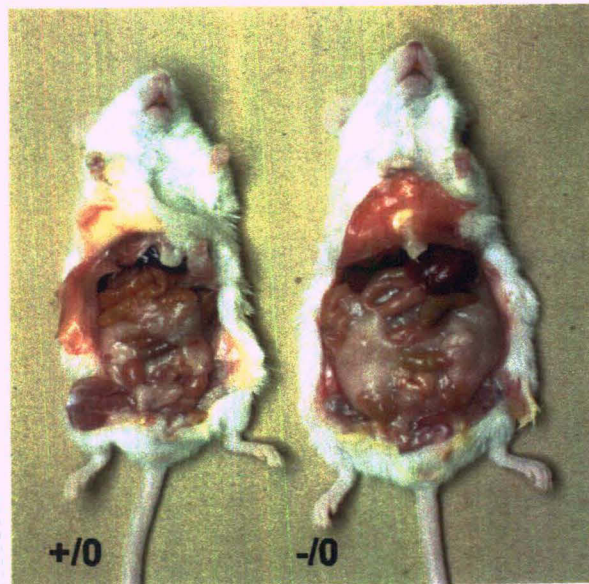


Figure 3.5 Increased adipose tissue mass in *Wdr13* knockout mice. A) Phenotype of *Wdr13* knockout mice and their wild type litter mates. B) Increased adipose tissue mass in *Wdr13* knockout mice.

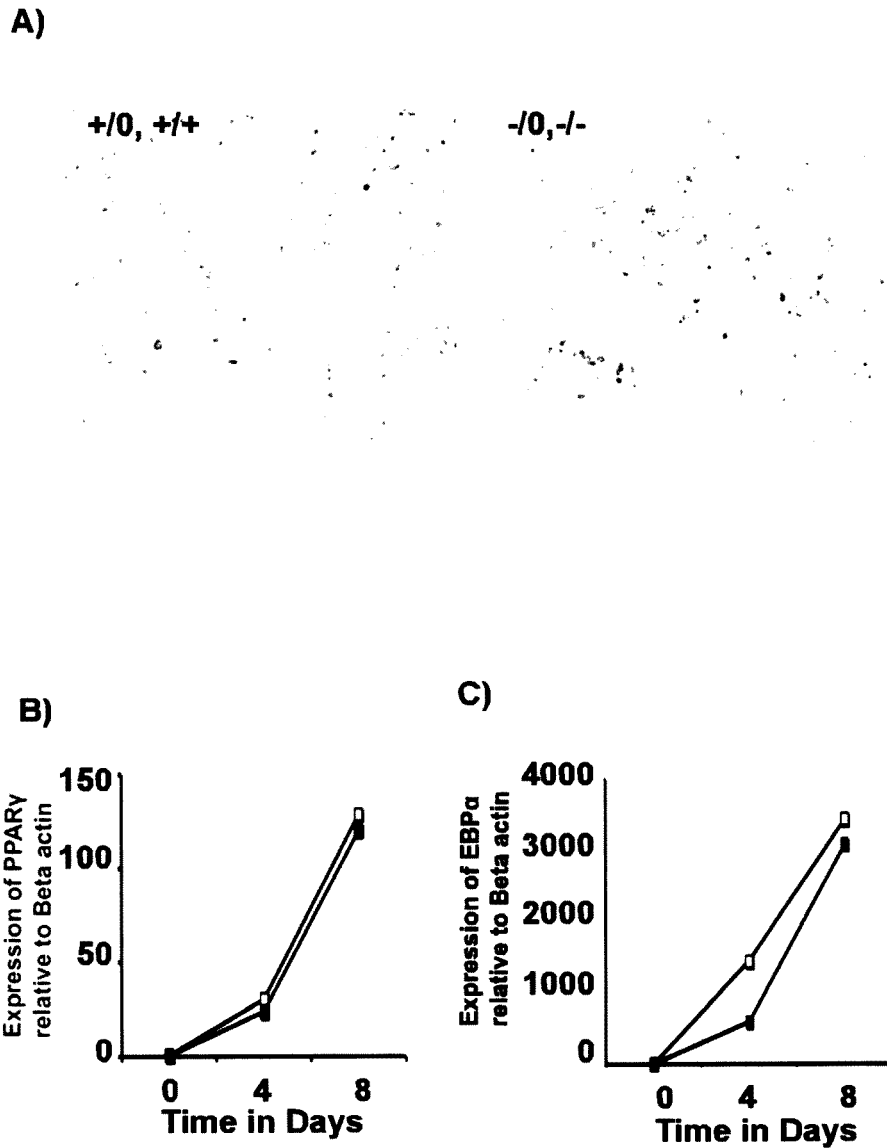


Figure 3.6 Adipogenesis in mouse embryonic fibroblast isolated from 13.5 dpc embryo from *Wdr13* +/+, +/0 and -/0, -/- mice, induced by Insulin, IBMX and dexamethasone. A) Oil red O staining of *Wdr13* +/0, +/+ and -/0, -/- MEFs. B) PPAR γ expression during adipogenesis in *Wdr13* +/0, +/+ (□) and *Wdr13* -/0, -/- (■) MEFs. C) EBP α expression during adipogenesis in *Wdr13* +/0, +/+ (□) and *Wdr13* -/0, -/- (■) MEFs.

Table 3.3 - Weight (in grams) of various organs from *Wdr13* mutant and their wild type littermates at the age of 12 months on normal chow

| Genotype/ Tissues | Pancreases | Testis / ovary | Liver | Brain | Heart | Kidney | Spleen | Lung |
|------------------------|------------|----------------|-----------|-----------|-----------|-----------|------------|-----------|
| <i>Wdr13</i> +/0 (n=8) | 0.22±0.01 | 0.18±0.01 | 1.67±0.05 | 0.48±0.01 | 0.20±0.01 | 0.58±0.02 | 0.06±0.005 | 0.25±0.01 |
| <i>Wdr13</i> -/0 (n=8) | 0.30±0.01* | 0.18±0.01 | 1.85±0.10 | 0.49±0.01 | 0.21±0.01 | 0.62±0.02 | 0.08±0.004 | 0.27±0.01 |
| <i>Wdr13</i> +/+ (n=6) | 0.33±0.02 | 0.87±0.29 | 1.46±0.07 | 0.49±0.01 | 0.18±0.01 | 0.41±0.01 | 0.11±0.008 | 0.22±0.01 |
| <i>Wdr13</i> -/- (n=6) | 0.41±0.06* | 0.63±0.12 | 1.50±0.07 | 0.52±0.01 | 0.18±0.01 | 0.45±0.03 | 0.12±0.007 | 0.31±0.11 |

3.2.9 Hyperinsulinemia in *Wdr13* knockout mice

Given the age dependent obesity phenotype of *Wdr13* knockout mice, the random and fasting blood glucose levels were measured at different age points. There was no effect of *Wdr13* genotype on random glucose levels at various age points (Figure 3.7A). Similarly, the fasting glucose levels at 2 months did not differ between the mutant and wild type mice. However, the mutant mice showed hypoglycemia under fasting conditions at 12 months on normal chow and this phenotype got preponed when the mice were fed high fat diet (Figure 3.7B).

In the light of hypoglycemia, serum insulin levels at various age points were estimated. At age of 2 months mutant mice were having similar insulin levels in both fasting and fed conditions. However, interestingly, *Wdr13* deficient mice had 2.13 fold more random insulin level at 12 months when fed on normal chow. Similarly, the random insulin level was 2 fold more in mutant mice at 6 months when fed on high fat diet (Figure 3.7C). The fasting insulin levels were similar in the wild type and mutant mice at various age points. However, glucose stimulated insulin secretion was more in *Wdr13* knockout mice (Figure 3.7D).

3.2.10 Metabolic parameters in *Wdr13* knockout mice

Given the age dependent obesity in *Wdr13* knockout mice, various metabolic parameters were analysed including triglycerides, cholesterol, LDL cholesterol, HDL cholesterol, VLDL, blood urea, serum creatinine, T3, T4, TSH, bilirubin and various liver function parameters (Table. 3.4) at 12 months age in fed condition. Serum triglycerides were significantly lower in mutant mice; where as other parameters were similar in both mutant and wild type mice.

Table 3.4 - Various metabolic parameters from *Wdr13* mutant and their wild type littermates at the age of 12 months on normal chow

| S.No. | Metabolic Parameters | Wdr13 +/0 | Wdr13 -/0 |
|-------|-------------------------------------|-----------------|----------------|
| 1. | Serum Triglycerides (mg/dl)* | 169.5 ± 22.57 | 121.5 5 ± 6.97 |
| 2. | Serum Cholesterol (mg/dl) | 219.66 ± 15.92 | 243.5 ± 11.05 |
| 3. | L D L Cholesterol (mg/dl) | 74.16 ± 10.93 | 91.5 ± 7.61347 |
| 4. | H D L Cholesterol (mg/dl) | 111.83 ± 6.49 | 127.83 ± 5.38 |
| 5. | V L D L (mg/dl) | 33.66 ± 4.54 | 24.16 ± 1.45 |
| 6. | Blood Urea (mg/dl) | 43.33 ± 2.66 | 34.16 ± 1.58 |
| 7. | Serum Creatinine (mg/dl) | 0.416 ± 0.016 | 0.383 ± 0.030 |
| 8. | T3 (ng/ml) | 1.92 ± 0.115 | 1.86 ± 0.060 |
| 9. | T4 (µg/dl) | 5.94 ± 0.409 | 5.56 ± 0.487 |
| 10. | T.S.H. (UIU/ml) | 0.0116 ± 0.0016 | 0.01 ± 0 |
| 11. | Total Bilirubin (mg/dl) | 0.12 ± 0.0221 | 0.141 ± 0.014 |
| 12. | Conjugated Bilirubin (mg/dl) | 0.043 ± 0.003 | 0.035 ± 0.002 |
| 13. | Unconjugated Bilirubin (mg/dl) | 0.076 ± 0.020 | 0.106 ± 0.012 |
| 14. | Serum Alanine Trans Aminase (U/L) | 48 ± 7.41 | 40.83 ± 1.01 |
| 15. | Serum Aspartate Trans Aminase (U/L) | 72.5 ± 10.81 | 60.33 ± 2.14 |
| 16. | Serum Alkaline phosphatase (U/L) | 80.16 ± 4.11 | 88 ± 7.53 |
| 17. | Total proteins (gms/dl) | 5.80 ± 0.103 | 5.83 ± 0.168 |
| 18. | Serum albumin (gms/dl) | 1.26 ± 0.021 | 1.35 ± 0.072 |
| 19. | Serum Globulin (gms/dl) | 4.55 ± 0.080 | 4.49 ± 0.100 |

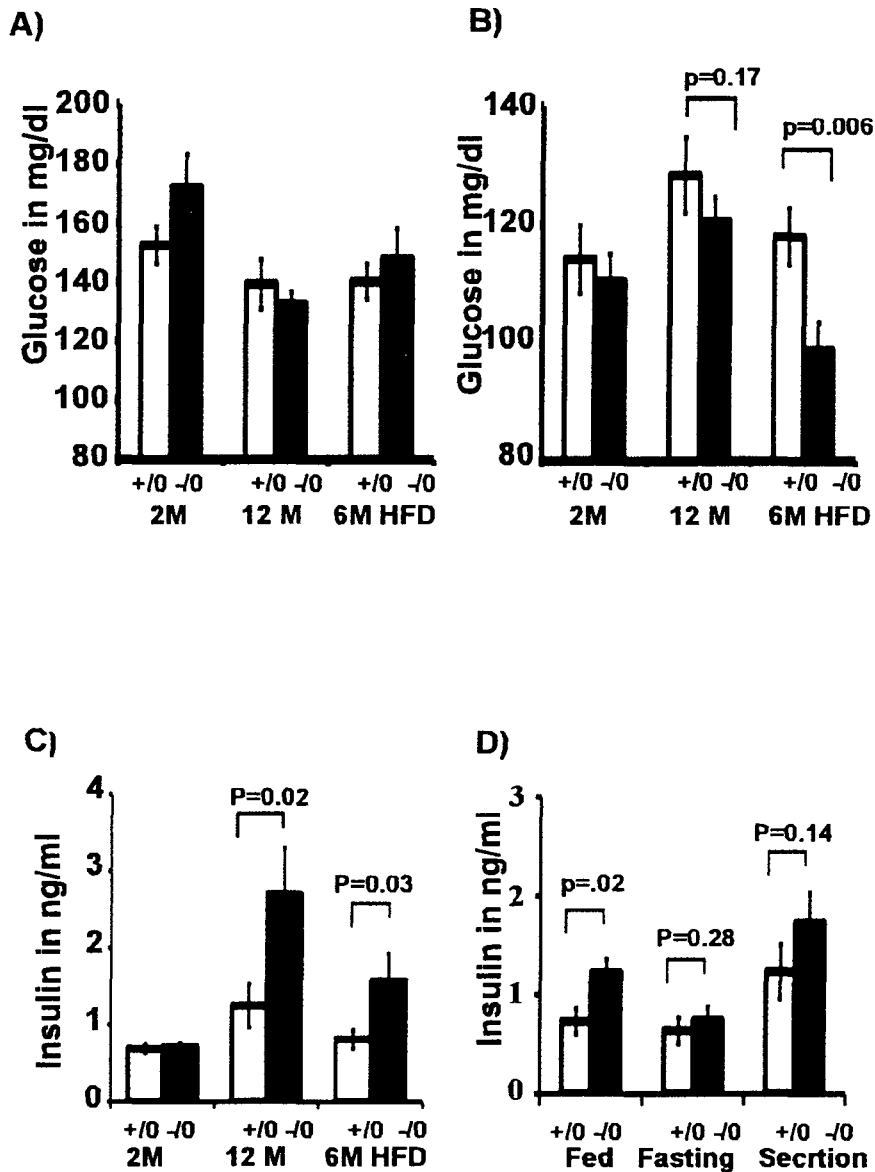


Figure 3.7 Glucose homeostasis in *Wdr13* knockout mice. A) Fed glucose level at 2 months, 12 months on normal chow and 6 months on high fat diet (n= 10 to 12). B) Fasting glucose levels at 2 months, 12 months on normal chow and 6 months on high fat diet (n= 10 to 12). C) Insulin level at 2 months, 12 months on normal chow and 6 months on high fat diet in fed condition (n= 8 to 10). D) Insulin level at 6 months on high fat diet in fed, fasting and secreted after 30 min in response to glucose (n=3 to 6).

3.2.11 Better glucose clearance in *Wdr13* knockout mice

Given the high level of random insulin levels in *Wdr13* deficient mice, these mice were challenged with glucose to determine their glucose clearance at various ages. Mutant mice showed similar glucose clearance at age of 2 months (Figure 3.8A). However mutant mice showed consistently better glucose clearance at age of 6 month on High fat diet (Figure 3.8B) and at age of 12 months on normal chow in-spite of having higher body weight.

3.2.12 Unaltered insulin sensitivity in *Wdr13* knockout mice

The increase in insulin level may be due to increase in insulin resistance to peripheral tissues such as liver, muscle and adipose. To check that possibility, exogenous insulin was injected to both mutant and wild type mice and glucose was monitored at various time points. The mutant mice responded to extraneous insulin in a manner similar to that of wild type indicating no evidence for insulin resistance in mutant mice at age of two months on normal chow (Figure 3.8C) and 6 months on high fat diet (Figure 3.8D).

3.2.13 Histopathological examination of various tissues

The *Wdr13* knockout mice and wild type mice were dissected and various tissues including liver, pancreas, testis and fat pad were collected at the age of 2 months on normal chow and 6 months on high fat diet. The histology of various tissues was examined by H&E staining. At age of 2 months, there was no structural difference between various tissues analyzed. However at age of 6 months, there was hypertrophy in adipocytes of *wdr13* knockout mice in both fat pad as well as in subcutaneous fat (Figure 3.9C).

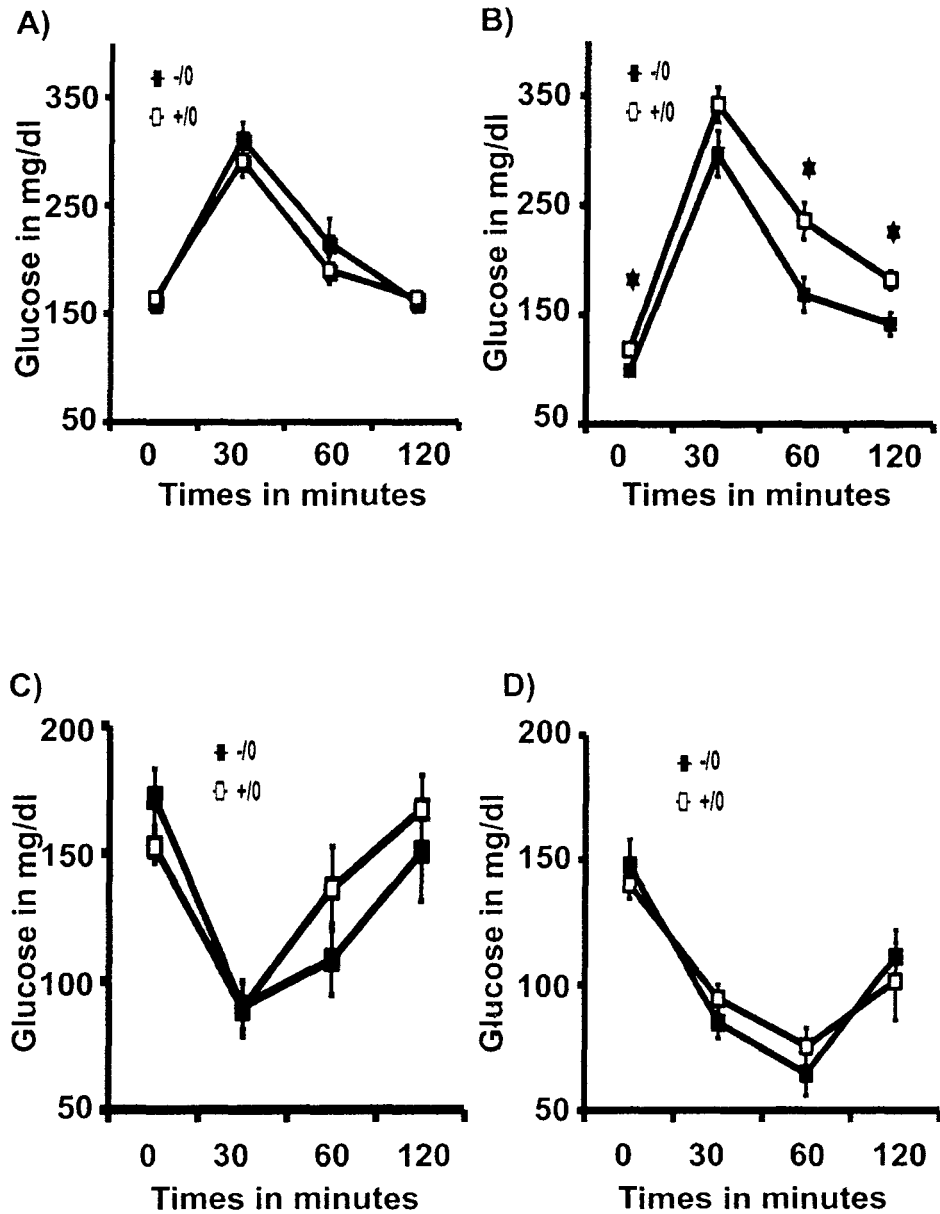


Figure 3.8 Glucose tolerance test (GTT) and Insulin tolerance test (ITT) of *Wdr13* knockout mice. A) GTT at age of 2 months shows similar glucose clearance in mutant mice. B) GTT at age of 6 months on high fat diet shows better glucose clearance in mutant mice compare to their wildtype littermates.. C) ITT at age of 2 months shows similar insulin sensitivity in mutant mice. D) ITT at age of 6 months on high fat diet shows similar insulin sensitivity in mutant mice.

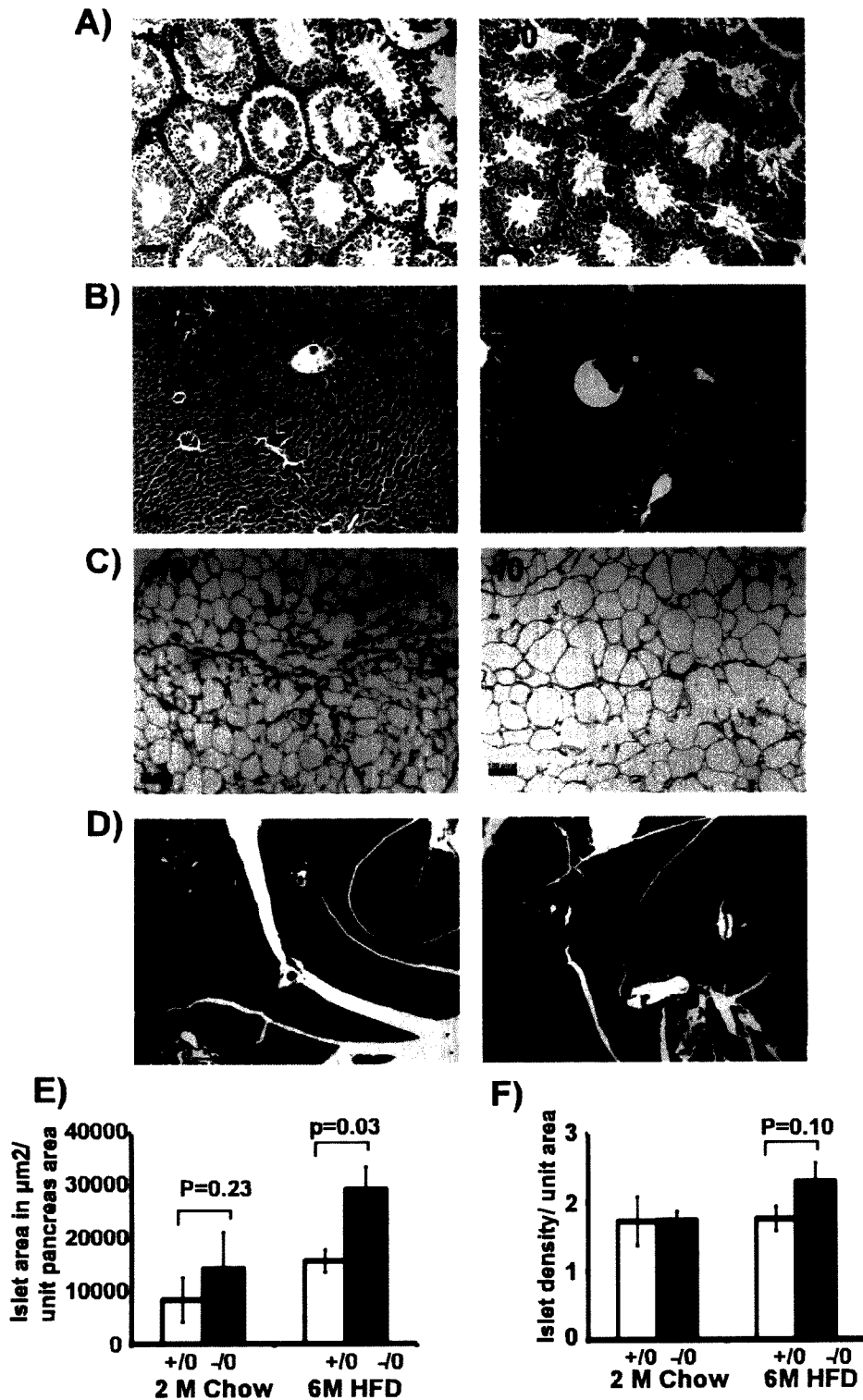


Figure 3.9 Histological examination of testis, liver, adipocytes and pancreas from *Wdr13* knockout mice (-/-) and their wild type littermates (+/+). H&E staining of A) Testis, B) Liver, C) Adipocytes, and D) Pancreas at 6 months on high fat diet. E) Islet area per unit pancreas area at age of 2 months on normal chow and 6 months on HFD. F) Islet density per unit pancreas area at age of 2 months on normal chow and 6 months on HFD.

Since *Wdr13* mutant mice were hyperinsulinemic and mildly obese, pancreatic histology was analyzed at two months and at 6 months on high fat diet. Interestingly, islet density was more ($p < 0.10$) at 6 months on high fat diet (Figure 3.9F). Total Islet mass was more in *Wdr13* knockout mice (Figure 3.9E) at 6 months on high fat diet. Histological examination of testis and liver did not reveal any changes in mutant mice with age (Figure 3.9A,B).

3.2.14 Increased pancreatic beta cell and spermatogonial cell proliferation in *Wdr13* knockout mice

To understand the increased islet mass, beta cell proliferation was measured by BrdU labelling. At the age of 2 months on normal chow there was no significant difference in beta cell proliferation of both mutant and wild type littermates. Interestingly, when one month-old mice were kept on high fat diet for three weeks, there was two fold more proliferation of beta cells in *Wdr13* mutant mice as compared to their wild type littermates (Figure 3.10A). These results suggest that in response to higher demand for insulin, the beta cell proliferation is more in *Wdr13* knockout mice. This leads to increased islet mass.

Given the expression of *wdr13* in various tissues, cell proliferation in yet one more type of tissue, i.e., testis was analyzed and it was observed that spermatogonial cell proliferation was more in *Wdr13* knockout mice compare to their wild type littermates. This result suggested that the phenomenon of enhanced cell proliferation is present in the various tissues of *Wdr13* knockout mice (Figure 3.11A,B). However, there could be some compensatory mechanism that controls the increased cell proliferation.

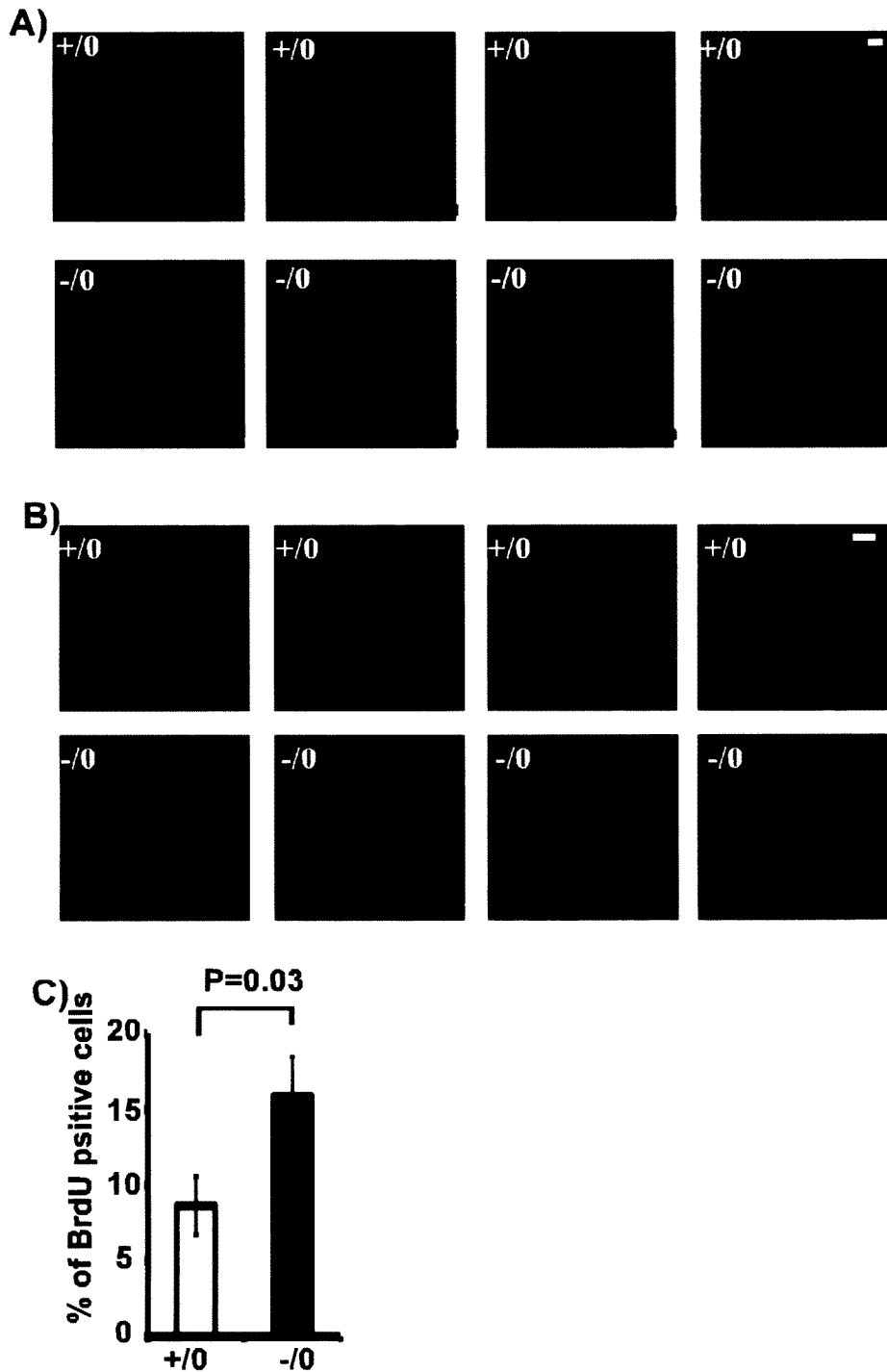


Figure 3.10 Pancreatic beta cell proliferation and apoptosis in *Wdr13* knockout mice A) Pancreatic beta cells proliferation analysis by BrdU labeling in mutant mice and their wild type littermates. B) TUNEL assay for beta cell apoptosis in mutant mice and their wild type littermates C) Percentage of dividing cells in islet by BrdU labeling (n=309-517) shows increased beta cell proliferation in mutant mice.

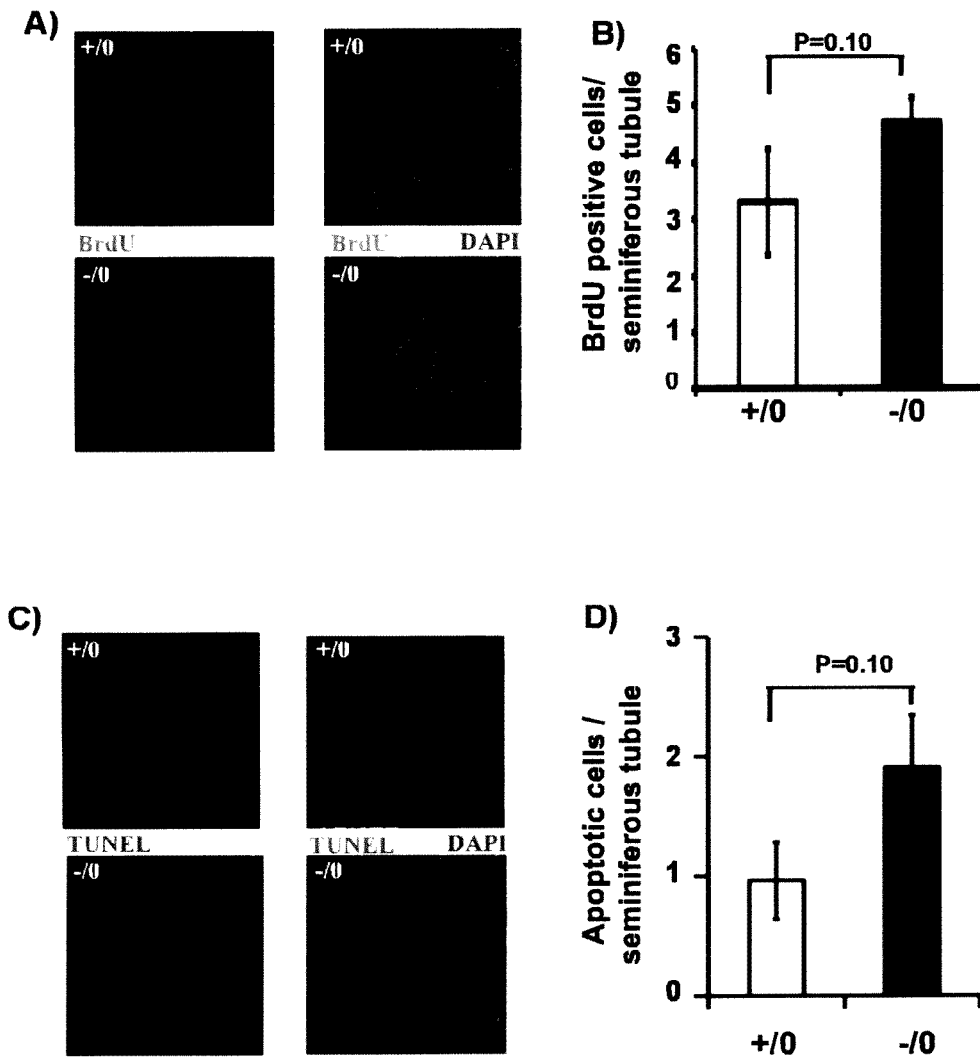


Figure 3.11 Spermatogonial cell proliferation and apoptosis in *Wdr13* $-/-$ mice. A) Spermatogonial cell proliferation in seminiferous tubule by BrdU labelling in mutant mice and their wild-type littermates. B) BrdU labeling index in seminiferous tubules shows enhanced cell proliferation in mutant mice. C) Apoptotic cells in seminiferous tubule by TUNEL staining in mutant mice and their wildtype littermates. D) Apoptotic index in seminiferous tubule shows increased apoptosis in mutant mice.

3.2.15 Apoptotic index of pancreatic beta cell and spermatogonial cell

It was suspected that *Wdr13* knockout mice would develop spontaneous tumors due to hyperplasia. But there was no overt tumor in *Wdr13* knockout mice till one year of age. To understand this phenomenon, apoptosis was measured in pancreatic beta cells as well as in spermatogonial cells. In spermatogonial cells, the number of apoptotic cells were more compared to their wild type littermates (Figure 3.11C,D). However, in pancreatic beta cells, due to their slow cell division, the number of apoptotic cells were minimal and *Wdr13* knockout mice had similar number of apoptotic cells compared to their wild type littermates (Figure 3.10B). This result suggests that increased cell proliferation was compensated by increased apoptosis.

3.2.16 Cell cycle marker analysis in *Wdr13* knockout mice

Various cyclins expression was analyzed by real time PCR in pancreatic islets isolated from 2 month old mice, which was kept on high fat diet for last 3 weeks to understand the pancreatic beta cell proliferation (Figure 3.12A). Cyclin E1 transcript level was 1.5-fold upregulated in *Wdr13* mutant mice whereas cyclin D1 transcript level was down regulated and cyclin D2 transcript level remained unaltered. Cell cycle inhibitor P21 transcript was upregulated in mutant pancreatic islets where as P27 transcript level was not affected. Other cell cycle markers were unaffected at transcript level. Similarly, various cell cycle regulators were analyzed from testis tissue. In testis transcript level of cyclin D2 and P21 was upregulated, whereas other cell cycle regulators were unaltered (Figure 3.12B).

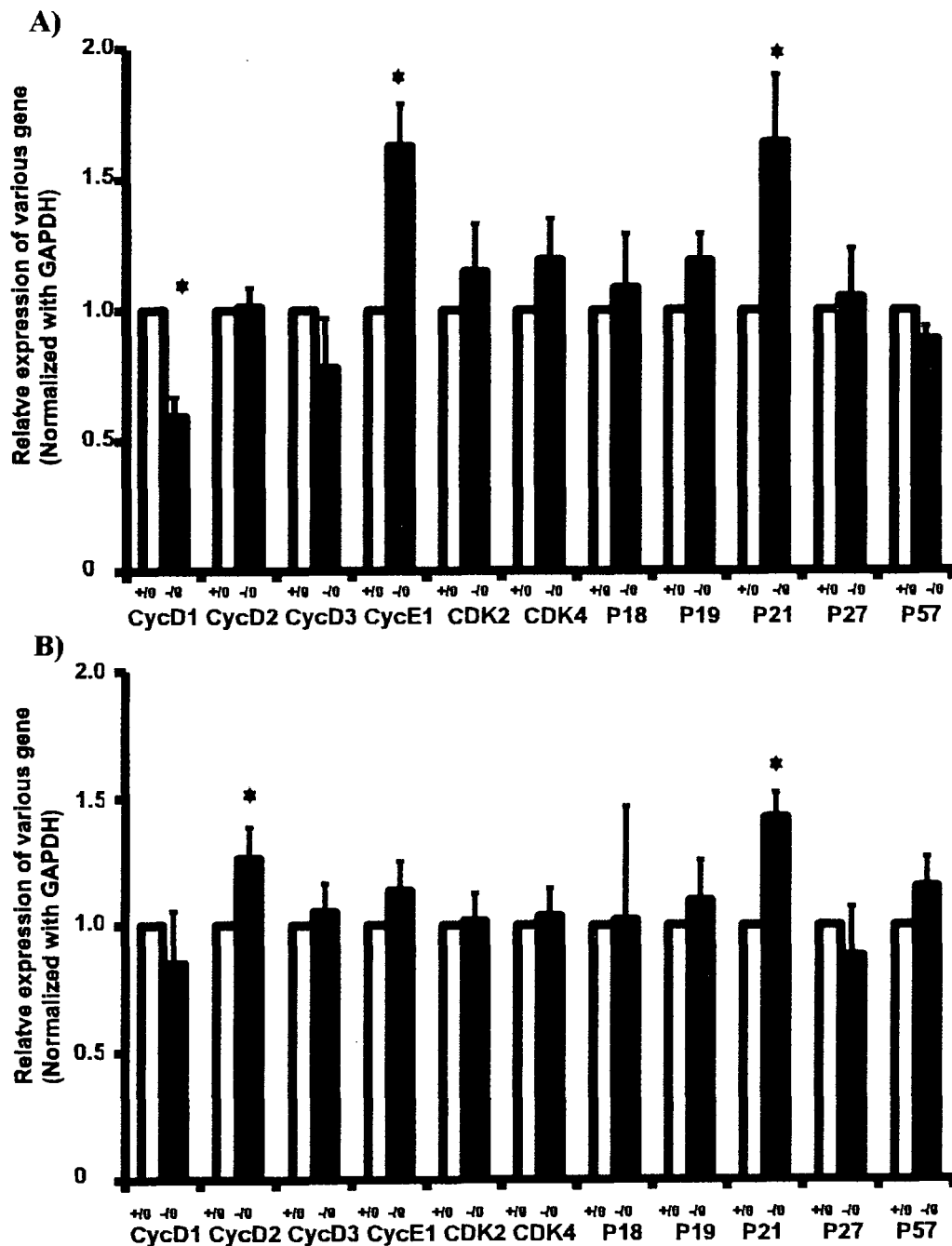


Figure 3.12 Relative expression of cell cycle regulator from *Wdr13* knockout mice compare to their wild type littermates in pancreatic islet and testis. A) Relative expression of cyclin D1, D2, D3, E1, cyclin dependent kinase 2, 4, and cell cycle inhibitors p18 p19, p21, p27, p57 from pancreatic islet of *Wdr13* knockout mice compared with their wild type littermates after keeping mice on high fat diet for three weeks, shows upregulation of cyclin E1, p21 and downregulation of cyclin D1. B) Relative expression of cyclin D1, D2, D3, E1, cyclin dependent kinase 2, 4, and cell cycle inhibitors p18 p19, p21, p27, p57 from testis of *Wdr13* knockout mice compared with their wild type littermates shows upregulation of cyclin D2 and p21.

3.2.17 Overexpression of *wdr13* causes cell growth retardation

To further clarify that increase in insulin level is not a feedback response to obesity but it is due to enhanced beta cell proliferation, *wdr13* protein was overexpressed in MIN-6 cell line using pAd Easy system. MIN-6 cells were transfected with AdGFP and Ad*wdr13* with 200 MOI each in 24 well plates. Overexpression of *wdr13* was confirmed by western blot (Figure 3.13A) using anti *wdr13* antibody after 48 hours post transfection. Further, growth curve was prepared using MTT assay at various time points (Figure 3.13B). After 48 hours of post transfection *wdr13* overexpressing cells showed growth retardation. However the effect was significant at 72 hours post transfection. This result suggests that the overexpression of *wdr13* causes cell growth retardation in MIN-6 cell lines.

3.2.18 Overexpression of *wdr13* causes down regulation of cyclin D2 and cyclin E1

To understand the effect of *wdr13* overexpression on cell proliferation, various cell cycle regulators were analyzed. Overexpression of *wdr13* protein causes reduction of cyclin D2 and cyclin E1 transcript in MIN-6 as well as in NIH3T3 cells (Figure 3.13 C, D). Whereas overexpression of *wdr13* had no effect on transcripts level of cyclin D1, P27. In Min-6 cells P21 transcript level was unaltered whereas P21 transcript was down regulated in NIH3T3 cells due to overexpression of *wdr13* (Figure 3.13 C, D). These results suggest that Cyclin D2 and Cyclin E1 transcripts may be regulated directly or indirectly by *wdr13*.

3.2.19 Overexpression of *wdr13* protein in ES cells

The overexpression of *wdr13* in MIN-6 cells causes cell growth retardation. To understand the *in vivo* phenotype of *wdr13* overexpression it would be interesting to generate transgenic mice overexpressing *wdr13*. For this purpose, a conditional *Wdr13* transgenic vector was constructed for *HPRT*

locus (Figure 2.4). Targeting strategy has been given in figure 3.14A. After targeting at *HPRT* locus, *HPRT* gene was disrupted and cells were resistant to neomycin and 6TG. The resistant clones were analyzed by southern blot. After digestion with BamHI, the wild type allele of *HPRT* showed 6.83kb band ($HPRT^+ Neo^- Wdr13^-$) using 339bp HincII-HpaI fragment of mouse *HPRT* cDNA clone pHPT5 (Kumar and Simons, 1993), which was essentially specific for exons 2 and 3 of *HPRT*. After targeting with pHPT-CMV-LNL-*Wdr13* vector at *HPRT* locus the size of band shifted to 10.93kb (Figure. 3.14B). A total of 5 clones were positive for *HPRT* targeting ($HPRT^- Neo^+ Wdr13^-$). Two clones were karyotyped and 70-80% cells showed normal chromosome number. The neomycin was removed from those two clones by transient cre recombinase expression and neo removal was confirmed by southern blot, which showed 9.83 kb band ($HPRT^- Neo^- Wdr13^+$) size (Figure 3.14B). The expression of *Wdr13* gene was further confirmed at transcript level by real time PCR that showed two to five fold overexpression of *Wdr13* gene in neomycin removed clones (Figure. 3.14C).

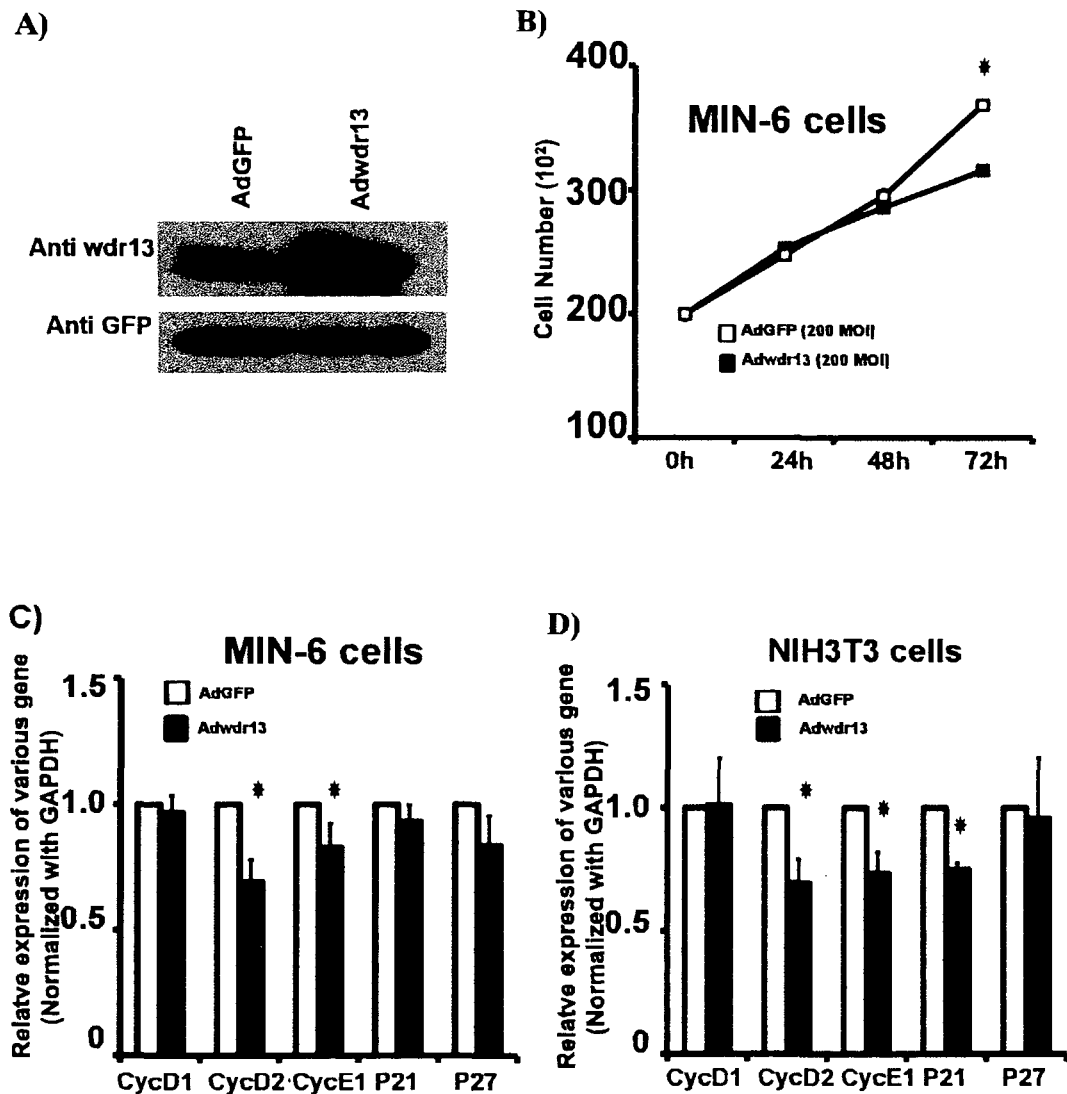


Figure 3.13 Overexpression of wdr13 protein in MIN-6 and NIH3T3 cell lines and cell cycle regulation. A) Transfection with Adwdr13 shows overexpression of wdr13 protein in MIN6 cells by immunoblot with anti wdr13 antibody. Lower panel shows GFP as loading control. B) Overexpression of wdr13 protein causes cell growth retardation in MIN-6 cell line after transfection of 72 hours. C) Overexpression of wdr13 protein with Adwdr13 in MIN-6 cells causes reduction in cyclin D2 and cyclin E1 levels compared to control AdGFP adenovirus transfected cells. Where as cyclin D1, p21 and p27 levels are unaffected. D) Overexpression of wdr13 protein with Adwdr13 in NIH3T3 cells causes reduction in cyclin D2, cyclin E1 and P21 levels compared to control AdGFP adenovirus transfected cells. Where as cyclin D1 and p27 levels are unaffected.

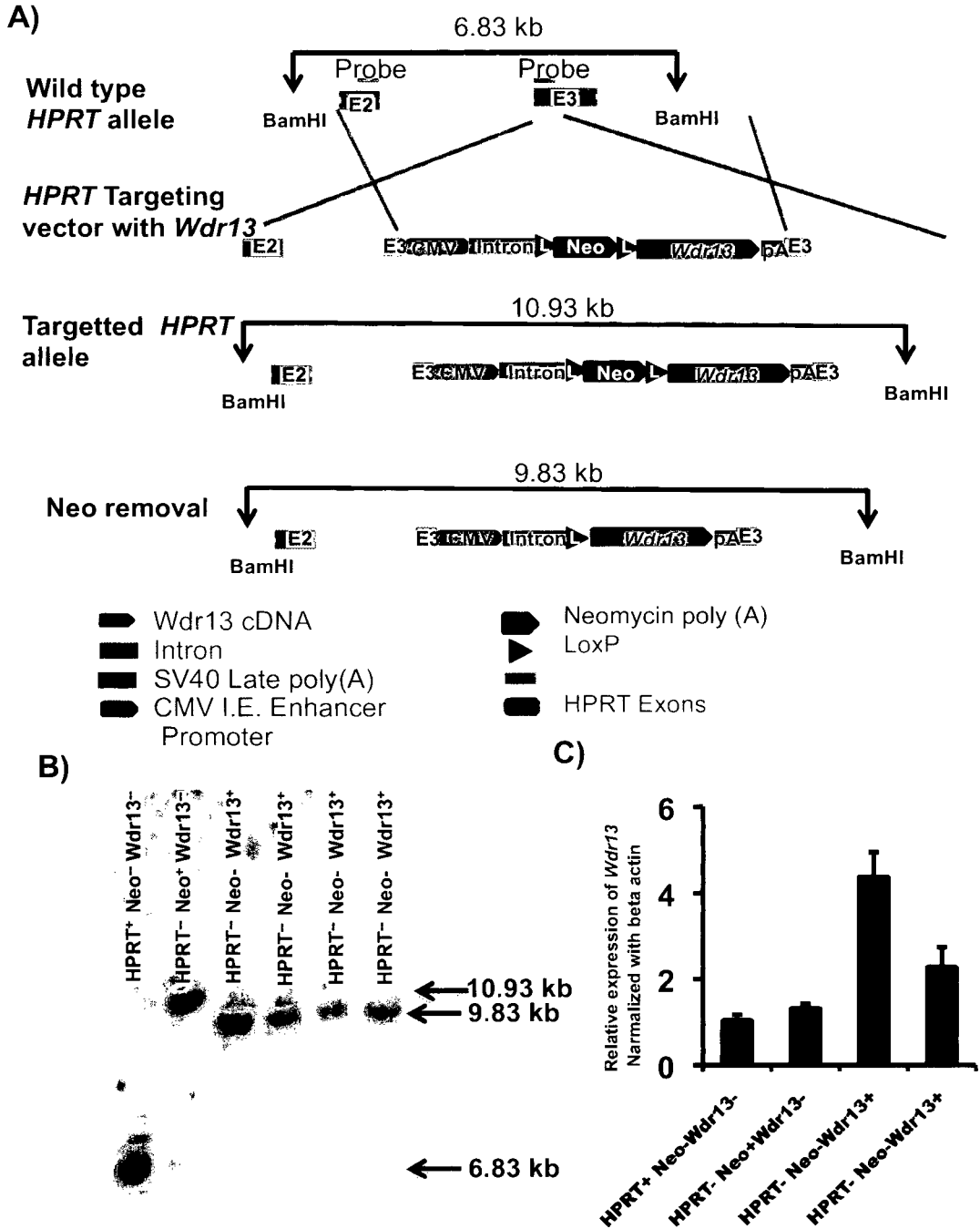


Figure 3.14 Over expression of *wdr13* protein in ES cells. A) Targeting strategy of *Wdr13* transgene at *HPRT* locus. B) After BamHI digestion the size of wild type allele is 6.83 kb, *HPRT* targeted allele is 10.93 kb, which after neo removal results in 9.83 kb. C) Expression of *Wdr13* by real time PCR in wild type ES cells, *HPRT* targeted ES cells as well as in neo removed clones, shows overexpression of *Wdr13* transcript in neo removed clones compare to their parent clone.

3.3 DISCUSSION

To study the functional significance of *Wdr13* gene, the phenotype of *Wdr13* knockout mice was analyzed. Mutant mice were viable and fertile. As proposed previously by Suresh *et al.*, and Julie *et al.*, (Cocquet *et al.*, 2010; Suresh *et al.*, 2005) the role of *Wdr13* in germ cell and spermatid differentiation, structural alteration in germ cell and spermatid differentiation was not observed. Sperm number and all sperm motility parameters analyzed by CASA of mutant mice were similar to their wild type littermates.

3.3.1 Hyperinsulinemia and obesity in *Wdr13* knockout mice

Body weight, pancreatic islet mass and insulin production are inter-related (Bouwens and Rooman, 2005; Rhodes, 2005). Insulin levels have been positively correlated with obesity in humans (Lustig *et al.*, 2004) rodents (Rohner-Jeanrenaud and Jeanrenaud, 1985) and avian models (Simon and Leclercq, 1985). Generally, obesity leads to higher demand for insulin production and the same is met by increase in beta cell mass and insulin levels. Obesity is also a major risk factor for the onset of peripheral insulin resistance (Muoio and Newgard, 2008). Insulin resistance leads to further higher demand for insulin from beta cells triggering beta cell failure. This leads to beta cell survival defects, insufficient beta cell mass and deterioration of key beta cell function such as glucose stimulated insulin secretion and ultimately leading to type 2 diabetes. In type 1 diabetes, beta cell mass is lost due to autoimmune destruction resulting into hypoinsulinemia.

On the other hand, obesity may be a consequence of higher insulin levels (Song *et al.*, 2008; Wen *et al.*, 2009; Willing *et al.*, 1990) as insulin has stimulatory effect on adipogenesis by increasing the lipid accumulation in adipocytes (Bluher *et al.*, 2002; Bruning *et al.*, 1998; Girard *et al.*, 1994). Insulin is also involved in adipocyte survival (Loftus *et al.*, 1998). Adipose tissue specific insulin receptor knockout protects against obesity emphasizing that

insulin signaling to adipocytes is important for development of obesity (Bluher et al., 2002). Hyper insulin secretion in MOR-1 opioid receptor knockout mice results in more body weight gain with age (Wen et al., 2009) whereas CHOP knockout mice become obese by increasing insulin secretion although without affecting glucose tolerance in the latter (Ariyama et al., 2007).

Insulin, a pancreatic hormone is one of the major factors involved in these disease conditions. Insulin has major role in glucose and lipid homeostasis (Saltiel and Kahn, 2001). The binding of insulin to insulin receptor (IR) causes autophosphorylation of the IR, leading to the binding of various scaffold proteins (Taniguchi et al., 2006), which include insulin receptor substrate (IRS), Src-homology-2-containing protein (SHC) and c-Cbl proto-oncogene. Phosphorylation of these scaffold proteins by the IR initiates various signaling pathways. The IRS1 is the key mediator of insulin mediated glucose uptake and activation of anabolic pathways in muscle and adipose tissues whereas anabolic effect of insulin in liver is mainly mediated by IRS2. The phosphorylation of IRS1 and IRS2 leads to their association with p85 subunit of phosphatidylinositol 3-kinase (PI3K), which recruits p110 catalytic subunit of PI3K (Taniguchi et al., 2006). This results in conversion of phosphatidylinositol-4,5-bisphosphate to phosphatidylinositol-3,4,5 trisphosphate (PtdIns(3,4,5)P₃). PtdIns(3,4,5)P₃ facilitates additional signaling events by the binding to the phosphoinositide-dependent protein kinase-1 (PDK1), PDK2 and AKT (Muoio and Newgard, 2008). This results in phosphorylation of AKT and subsequent phosphorylation of glycogen synthase kinase-3 (GSK3) and AS160 Rab GTPase-activating protein, which interact with small GTPase RAB10 to facilitate translocation of glucose transporter-4 (GLUT4) to the cell surface and promote glucose uptake (Sano et al., 2007). The phosphorylation of GSK3 causes its inactivation, which ultimately leads to decrease rate of phosphorylation of glycogen synthase, thus increasing its active state and promoting glycogen synthesis.

Insulin inhibits the production and release of glucose by the liver by

blocking gluconeogenesis and glycogenolysis. It inhibits the transcription of the gene encoding phosphoenolpyruvate carboxylase, which is the rate-limiting step in gluconeogenesis. Insulin also decreases transcription of the gene fructose-1,6-bisphosphatase and glucose-6-phosphatase and increases transcription of glycolytic enzyme such as glucokinase and pyruvate kinase and lipogenic enzymes such as fatty acid synthase and acetyl-CoA carboxylase. Insulin also inhibits lipolysis in adipocytes, primarily through inhibition of the enzyme hormone sensitive lipase (Pilkis and Granner, 1992).

The effect of insulin can be regulated at several nodes. The autophosphorylation of IRs can be reverted back by protein tyrosin phosphatases-1B (PTB1B). Tyrosin phosphorylation and activation of IRS can be further inhibited by ser-phosphorylation of these proteins by activation of stress pathways. The lipid phosphatase PTEN (phosphatase and tenin homolog) activity can convert PtdIns(3,4,5)P₃ to PtdIns(4,5)P₂ and reduce AKT activity (Lazar and Saltiel, 2006).

The *Wdr13* knockout mice were significantly heavier than their wild-type littermates at around nine months and continued to weigh more till the termination of the growth experiment at 12-months when fed on normal chow. This age dependent higher body weight of mutant mice was preponed to five months when these mice were fed on high fat diet. Anatomical and histological examination revealed that the increased body weights of mutant animals were primarily due to increase in the adipose tissue volume/ weight as a result of hypertrophy of adipocytes without any indication of change in adipocyte numbers. The lack of evidence for any difference in the extent of *in vitro* generation of adipocytes from MEFs of the mutant and wild type mice was consistent with the histological data suggesting that the obesity of *Wdr13* knockout mice was not due to altered adipogenesis (Rosen and MacDougald, 2006).

Wdr13 knockout mice had mild obesity and were hyperinsulinimic at 12 months on normal diet and at 6 months on high fat diet, whereas fasting

insulin levels were normal. Dynamic change in insulin producing pancreatic beta cell mass according to metabolic conditions and a positive correlation between body weight, insulin production and islet mass are well documented (Bouwens and Rومان, 2005; Lee and Nielsen, 2009). Various studies have shown that increase in insulin level may be a compensatory mechanism to the decreased peripheral insulin sensitivity, which finally leads to islet failure, and lead to diabetes (Gerich, 1998). On the other hand, as discussed above, the higher insulin level results in higher glucose uptake by adipose tissues, which would in turn alter the lipid metabolism and adipogenesis (Rosen and Spiegelman, 2000). Consistent with the latter findings, insulin receptor knockout mice exhibited decreased adipose tissue finally leading to neonatal lethality (Cinti et al., 1998).

In *Wdr13* knockout mice, obesity and insulin levels increased with age along with body weight. Glucose stimulated insulin secretion at six months was also more in *Wdr13* knockout mice kept on high fat diet. In spite of having more weight at 6 month and onwards, these mice were having better glucose clearance, whereas insulin sensitivity was normal as evident from ITT results. These results suggest that the body weight gain in *Wdr13* knockout mice may be related to the general growth stimulatory effect of insulin rather than higher insulin levels being a feedback to the increased adipose tissue mass. Insulin stimulates hepatic lipogenesis as well as lipid absorption by adipocytes leading to the increased adipose tissue formation (Girard et al., 1994). Moreover, insulin receptor glucose transporter-4 pathway helps to convert glucose to lipid in adipose tissues (Rosen and Spiegelman, 2000). Insulin sensitivity was similar upto 12 months in mutant mice. As discussed above glucose clearance was better in *Wdr13* knockout mice, suggesting that higher insulin secretion in these animals is responsible for low glucose and triglyceride levels. Therefore, given that the insulin sensitivity is normal in knockout mice, insulin hyper secretion appears less likely to be a compensatory response of the islets as a consequence of obesity. Hyperinsulinemia, accompanied by mild obesity in *Wdr13* knockout mice are

reminiscent of *MOR1* (Wen et al., 2009) and *chop* (Ariyama et al., 2007; Song et al., 2008) knockout mice where adiposity is enhanced by higher insulin secretion. There was a tendency among *Wdr13* knockout mice to eat more as compared to wild type mice. However, this difference was not statistically significant. Since *Wdr13* expresses in hypothalamus and other parts of the brain (D'Agata et al., 2003), the possibility of *Wdr13* gene having a role in feeding behaviour and or in general metabolism cannot be ruled out.

3.3.2 Increased pancreatic islet mass and beta cell proliferation in *Wdr13* knockout mice

Wdr13 knockout mice had more pancreatic islet mass and islet density when fed on high fat diet for five months after weaning at one month. To understand the phenomenon of increased islet mass, beta cell proliferation was assayed after one-month old mice were fed high fat diet for three weeks. *Wdr13* knockout mice had more beta cell proliferation as compared to their wild type littermates. It appears that increase in beta cell mass in *Wdr13* knockout mice is due to the enhanced beta cell proliferation.

The beta cell mass is regulated by the balance between neogenesis/proliferation and apoptosis/necrosis (Hanley et al., 2010; Ritzel et al., 2006). In mice, differentiation of islet precursor and expansion are responsible for beta cell neogenesis until the first week of life (Bouwens and Rooman, 2005; Finegood et al., 1995). Thereafter, expansion of existing beta cells is the main source of newly formed beta cells (Bonner-Weir, 2000; Dor et al., 2004). In pathological conditions there can be alpha to beta cell trans-differentiation (Thorel et al., 2010). Various extrinsic and intrinsic factors responsible for beta cell proliferation have been reported (Bouwens and Rooman, 2005; Heit et al., 2006b). Many positive regulators of beta cells exist which include incretins (Xu et al., 1999), EGF (Suarez-Pinzon et al., 2005), lactogens and growth hormones (Nielsen et al., 2001), HNF-4a (Gupta et al., 2007), calcineurin/NFAT (Heit et al., 2006a), Wnt3a (Rulifson et al., 2007) and integrins (Nikolova et al., 2006). Glucose is also one of the major factors

involved in promoting the expansion of beta cell mass during adult life (Terauchi et al., 2007). Various cell cycle inhibitors (P15, P16, P18, P19, P21, P27 and P57) have been identified, which target either various cyclins or cyclin dependent kinases to inhibit progression at various stages of cell cycle (Heit et al., 2006b). Several WD repeat proteins have been identified which express in pancreatic beta cells and have roles in beta cell proliferation (Honore et al., 2002; Podcheko et al., 2007). Earlier studies have shown that *wdr13* is a nuclear protein suggesting (Suresh et al., 2005) the possibility that this protein has a role in gene regulation. In *Wdr13* knockout mice, islet cyclin E1 was upregulated. However, cyclin E1 knockout mice develop normally with no defects in beta cells. But it is not known whether these mice had lower insulin level and or impaired glucose metabolism leading to diabetes at a later age. It appears that the overexpression of cyclin E1 may be leading to higher beta cell proliferation in *Wdr13* knockout mice, although there is no direct evidence in the literature showing the effect of over expression of cyclin E1 on beta cell proliferation. The effect of *wdr13* on cyclin E1 gene expression may be direct or indirect. The down regulation of cyclin D1 and up regulation of P21 observed in *Wdr13* knockout mice might be a feed back response to the enhanced beta cell proliferation. It is well established that P21 expression increases in response to mitogens in various cells types (Cozar-Castellano et al., 2006).

The phenotype of enhanced cell proliferation is not limited to pancreatic beta cells only. We also observed the enhanced cell proliferation in spermatogonial cells accompanied by upregulation of cyclin D2 and p21 in testis. However, it may be noted that the increased spermatogonial cell proliferation in testis did not translate into the increased sperm concentration. It appears that the higher apoptosis in testis of knockout mice might be responsible for such an outcome as shown by other workers that enhanced spermatogonial cell proliferation resulted in higher apoptosis (DeJong, 2006; Matzuk and Lamb, 2002; Roy and Matzuk, 2006; Sinha Hikim and Swerdloff, 1999).

3.3.3 Overexpression of *wdr13* causes cell growth retardation

The overexpression of *wdr13* protein causes growth retardation in MIN6 cell lines, which was supported by down regulation of cyclin D2 and cyclin E1 in Min-6 as well as in NIH3T3 cells. However, expression of cyclin D1 transcript was unaffected. The overexpressions of cyclin D2 and cyclin E1 have been reported in many tumors (Deshpande et al., 2005). These results suggest that, *Wdr13* is a negative regulator of cell cycle. The overexpression studies suggest that overexpression of cyclin D2 in testis and cyclin E1 in pancreatic beta cells of *Wdr13* knockout mice may be responsible for enhanced cell proliferation.

In conclusion, the knockout of *Wdr13* gene in mouse led to the enhanced proliferative activity in pancreatic beta cells, hyperinsulinemia and mild obesity with no evidence of impaired glucose metabolism till 12 months of age in CD1 genetic background. The enhanced cell proliferation phenotype was not restricted to beta cells only since we also observed higher cell proliferation in spermatogonia. However, overexpression of *wdr13* protein causes inhibition of cell proliferation. It may be hypothesized that *wdr13* protein is a negative regulator of cell cycle. Given the enhanced beta cell proliferation accompanied by higher insulin levels and the absence of insulin resistance in *Wdr13* knockout mice, it is possible that this protein may be a candidate drug target for ameliorating the impaired glucose metabolism in disease conditions. Similarly, *wdr13* protein may represent a drug target for oligozoospermatic individuals.

Chapter 4

CHAPTER 4: IDENTIFICATION OF PROTEIN(S) INTERACTING WITH wdr13

4.1 INTRODUCTION

Differentiation of a fertilized egg into a multicellular organism is the result of complex integration of various signaling pathways followed by the precise and co-ordinated regulation of gene expression (Perissi et al., 2010). The differential regulation of these pathways in a given cell type determine its fate. An understanding of the regulation of the different genes in a given pathway will illustrate the mechanism of gene expression. The eukaryotic system has evolved complex mechanism to regulate gene expression that operate at various levels including, transcriptional, post-transcriptional, translational and post translational control. Regulation of the transcription is the primary control.

The binding of trans-acting factors (transcription factors) to the cis-acting regulatory DNA sequences (promoters, silencers, enhancers) control the transcription (Riethoven, 2010). The *cis*-regulatory sequences act as component of genetic switch by serving as recognition sites for the binding of specific proteins. These elements consist of several composite and/or individual binding sites for transcription factors. The *cis*-sequences have been classified as promoters, silencers, enhancers and response elements according to their mechanism of transcriptional regulation.

The function of a promoter is to recruit the minimal transcriptional initiation complex which includes RNA polymerase II and transcriptional factors like TFIID, TFIIB, TFIIF and further elongation units like TFIIIE and TFIIH (Buratowski, 1994; Gnatt, 2002). The binding of regulatory proteins to the upstream sequences regulates the formation of initiation complex (Lee et al., 1993). The transcriptions of a number of genes are also affected due to the presence of sequence elements at distant positions. These elements are

called enhancers or silencers or response elements based on their respective effect on transcription of the gene.

The numbers of *trans*-acting factors have been identified such as homeodomain transcription factors, basic helix-loop-helix transcription factors and zinc-finger proteins, which have regulatory role in gene expression. The nuclear receptors are transcription factors that are hormone regulated and control many physiological and developmental processes in animals and humans (Privalsky, 2004). However, there are some orphan nuclear receptors for which either the ligand has not been identified or may not exist. The nuclear receptors contain DNA binding domains as well as ligand binding domains. Nuclear receptors can be classified into three broad classes according to their mechanism of action (Aranda and Pascual, 2001). Type I nuclear receptors are generally present in cytoplasm and move inside the nucleus in the presence of ligands. The example for Type I nuclear receptors are androgen, estrogen, progesterone and glucocorticoid nuclear receptors. In contrast to Type I nuclear receptors, Type II nuclear receptors are retained in the nucleus. In the presence of ligand they bind with coactivator and in the absence of ligand they bind with corepressors. The examples for Type II receptors are retinoic acid receptor, retinoid X receptor and thyroid hormone receptor. Type III nuclear receptors are orphan nuclear receptor such as NR2E1 where there are no known ligands. Generally nuclear receptors along with coactivators and corepressors have major role in gene expression by histone modifications (Perissi et al., 2010).

Coactivators bind to the nuclear receptors in ligand dependent manner (Rosenfeld et al., 2006). Many coactivators have been identified which have been shown to have histone acetyltransferase (HAT) activity such as p300/cyclic-AMP-response - element binding protein (CBP) - associated factors (PCAF) and have role in transcriptional activation (Marmorstein, 2001; Marmorstein and Roth, 2001). HAT activity has also been reported to TAFII250—a TATA–box binding protein (TBP)—associated factor that is present

in the TFIID general transcription factor complex and activating transcription factor 2 (ATF2) a sequence specific transcription factor (Sterner and Berger, 2000). Transcriptional activation requires the action of many multisubunit coactivator complexes that are recruited in a parallel or sequential manner. The enzymatic activity associated with coactivator, which leads to histone modification can be of multiple type including H3K4 methylation, H3K9 and H3K14 acetylation, H4K20 acetylation and phosphorylation of the linker histone H1b 9 (Rosenfeld et al., 2006).

The corepressors can be recruited to various nuclear receptors in both ligand dependent and ligand independent manner (Rosenfeld et al., 2006). The corepressor, which had been extensively studied are NCoR (nuclear receptor corepressor) and SMRT (silencing mediator for retinoid and thyroid hormone receptors) (Li et al., 2000; Oberoi et al., 2011). These corepressors bind to nuclear receptor in absence of ligand and recruit histone deacetylase (HDAC1, 2 and 3) for repression (Gray and Ekstrom, 2001). Some corepressors like LCoR (Fernandes et al., 2003) and RIP140 (Cavailles et al., 1995) interact with nuclear receptor in ligand dependent manner and recruit histone deacetylase.

The wdr13 protein is a negative regulator of cell cycle as illustrated by the present study (chapter 3). Although wdr13 is localized into the nucleus (Suresh et al., 2005), so far no DNA binding domain has been demonstrated in this protein. WD repeat proteins provide platform for protein-protein interactions and therefore, it was hypothesized that wdr13 may have a role in regulation of gene expression through facilitating interactions among other proteins. This chapter describes the experiments undertaken to identify interacting partners of wdr13 protein, and the probable mechanisms of wdr13 action in gene regulations have been discussed in the light of these experiments.

4.2 RESULTS

4.2.1 Overexpression of *wdr13* protein in mammalian cells

To perform immunoprecipitation experiments endogenous expression of *wdr13* protein was analyzed in various experimental cell lines. Western blot analysis showed expression of *wdr13* protein in HELA and HEK293 cells (Figure 4.1A). Transient overexpression of *wdr13* protein was performed in HELA cells using pCMV-FLAG-*Wdr13* and pCMV-FLAG vectors and the overexpression of *wdr13* protein was confirmed by western blot analysis (Figure 4.1B) which was further strengthened by immunolocalization (Figure 4.1C). As reported previously (Singh et al., 2003; Suresh et al., 2005) the *wdr13* protein was localized in the nucleus.

4.2.2 Immunoprecipitation of interacting proteins with *wdr13* and their identification by LC-MS/MS

Ten 10-cm dishes of HELA cells were transfected with either pCMV-FLAG vector or pCMV-FLAG-*Wdr13* each and the cells were allowed to grow for 48 hours. The cells were lysed and immunoprecipitated with anti FLAG antibody conjugated with agarose beads and interacting proteins were eluted with FLAG peptide. The eluate was separated on SDS-PAGE and stained with silver stain (Figure 4.1D) or digested in solution with trypsin for protein identification. The trypsin-digested peptides were separated by liquid chromatography with a 90-minute linear gradient from 0 to 90% of acetonitrile and identified by MS-MS. The peptide which were having peptide ion score ≥ 15 were considered as significant ID. The number of proteins identified from three independent experiments is summarized in table 4.1.

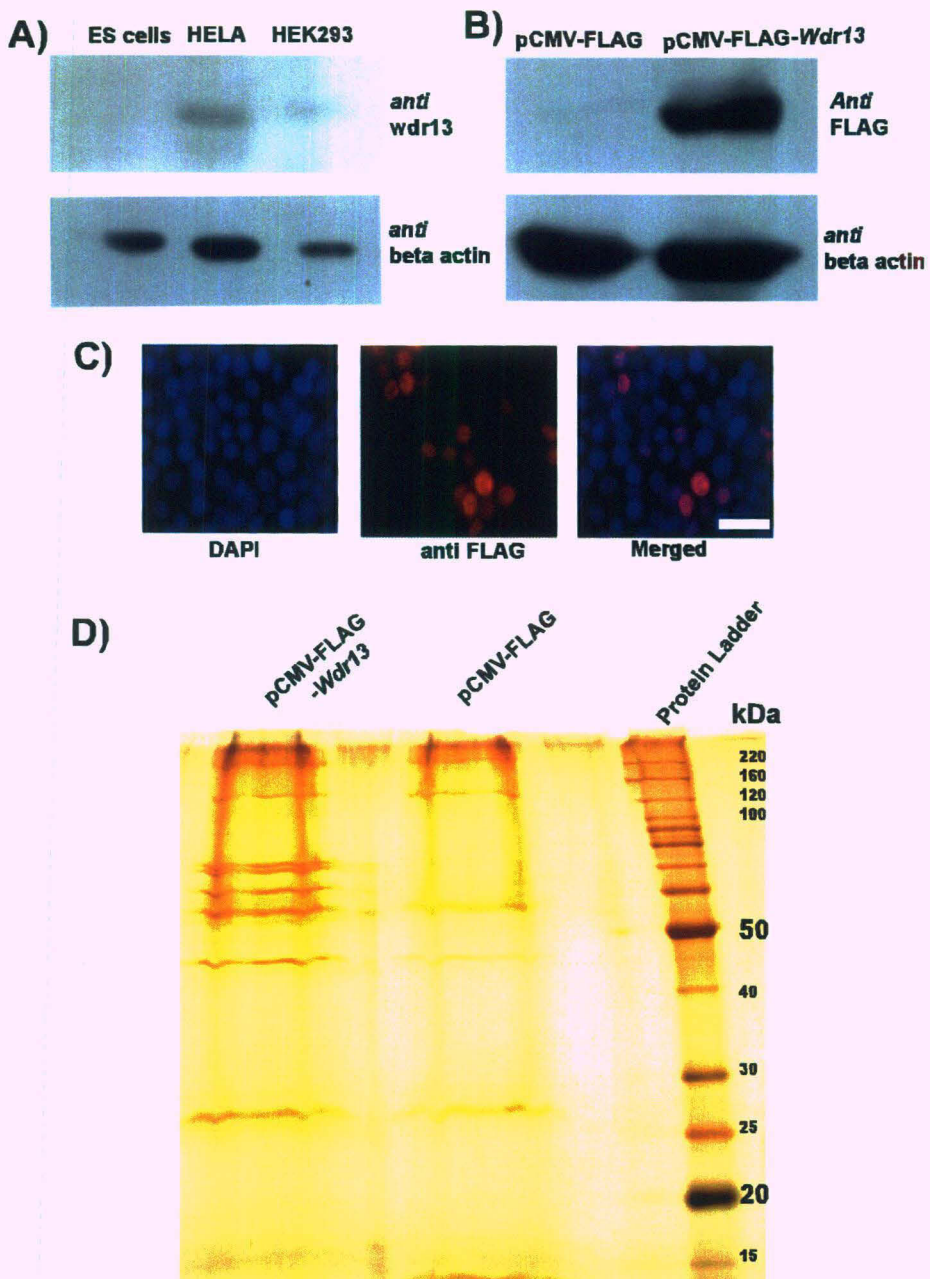


Figure 4.1 Identification of interacting protein of wdr13 by immunoprecipitation. A) Endogenous expression of wdr13 protein by western blot from various cell lines using anti wdr13 antibody. Lower panel shows beta actin as loading control. B) Western blot using anti FLAG antibody shows overexpression of wdr13 protein in HELA cells transfected by pCMV-FLAG control vector and pCMV-FLAG-*Wdr13* vector. Lower panel shows beta actin as loading control. C) Immunolocalization of wdr13 protein in HELA cells transfected with pCMV-FLAG-*Wdr13* vector using anti FLAG antibody. D) Silver stained gel of immunoprecipitated proteins using anti FLAG antibody from HELA cells transfected with pCMV-FLAG control and pCMV-FLAG-*Wdr13* vectors.

Table 4.1 - List of protein identified by LC-MS/MS

| Rank | Protein Name | Accession No. | Ion Score | Peptides sequences |
|------|---|-----------------------|---|---|
| 1 | WD repeat-containing protein 13 | sp Q9H1Z4 WDR13_HUMAN | 48 45 33 75 20 7 35 56 | AYSNSIVR IWASEDGR TPTFPQFR YGPLSEPGSAR MEDFEDDPR GSYQLQAQMNR LWVHEGSPVTSISAR MAAVWQQVLAVDAR |
| 2 | Heat shock cognate 71 kDa protein | sp P11142 HSP7C_HUMAN | 39 42 58 38 26 22 46 35 7 36 | LLQDFNNGK VQVEYKGETK DAGTIAGLNVLRL VEIANDQGNR FEELNADLFR NSLESYAFNMK TTPSYVAFTDTER STAGDTHLGGEDFDNR NQVAMNPTNTVFDAGR QTQTFTTYSNDQPGVLIQYEGER |
| 3 | PH-interacting protein | sp Q8WWQ0 PHIP_HUMAN | 37 1 15 10 13 17 | IWATDDGR KQQTNQHNRYR VTMVAWDR RVVPELSAGVASR VTMVAWDR RVVPELSAGVASR |
| 4 | Heat shock 70 kDa protein 1 | sp P08107 HSP71_HUMAN | 28 6 3 | LLQDFNNGR LVNHFVEEFKR TTPSYVAFTDTER |
| 5 | Nuclear receptor subfamily 2 group E member 1 | sp Q9Y466 NR2E1_HUMAN | 25 | LDATEFACKL |
| 6 | Histone deacetylase 7a (HD7a) | HDAC7_HUMAN | 3 16 | SAKPSEKPR TVHPNSPGIPYR |

Ion score more than 15 are significant.

4.2.3 PHIP1 interacts with *wdr13* by coimmunoprecipitation and colocalization

LC-MS/MS results (Table 4.1) indicated that PHIP1 interacts with *wdr13*. The interaction of PHIP1 with *wdr13* was further confirmed by co-immunoprecipitation. HEK293 cells were co-transfected with pCMV-FLAG-*Wdr13*, pCMV-Myc-PHIP1 and pCMV-FLAG, pCMV-Myc-PHIP1 vectors and allowed to grow for 48 hours before lysis. The immunoprecipitation of cell lysate using anti FLAG antibody followed by immunoblotting with anti Myc antibody showed interaction of *wdr13* and PHIP1 (Figure 4.2A). The interaction of PHIP1 and *wdr13* was further strengthened by immunocolocalization (Figure 4.2B) of these proteins in the nucleus.

PHIP1 contains WD domain at N-terminal and bromodomain at C-terminal. To obtain further insights into mechanistic details of PHIP1 and *wdr13* interaction, two domains of PHIP1 were cloned separately in Myc tagged expression vector. Cotransfection of HEK 293 cells with pCMV-FLAG-*Wdr13*, pCMV-Myc-PHIP-WD and pCMV-FLAG, pCMV-Myc-PHIP-WD vectors followed by immunoprecipitation with anti FLAG antibody and immunoblotting with anti Myc antibody showed interaction of PHIP WD domain with *wdr13* (Figure 4.2C). However, cotransfection of HEK293 cells with pCMV-FLAG-*Wdr13*, pCMV-Myc-PHIP-Bromo and pCMV-FLAG, pCMV-Myc-PHIP-Bromo vectors followed by immunoprecipitation with anti FLAG antibody and immunoblotting with anti Myc antibody did not show any interaction between *wdr13* and bromodomain of PHIP1 (Figure 4.2C). These results suggested that *wdr13* interacts with PHIP1 through WD domain of the latter.

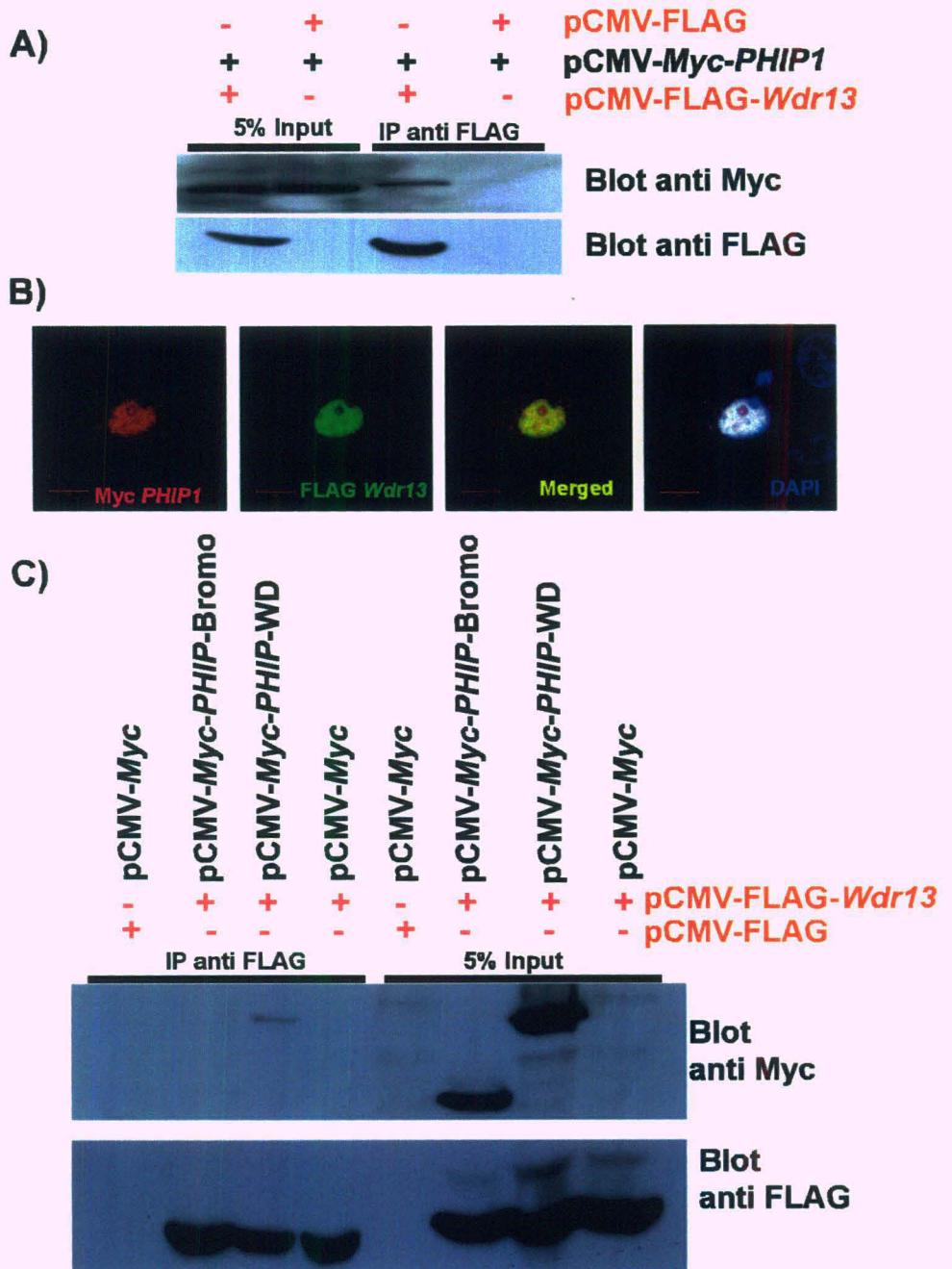


Figure 4.2 Interaction of wdr13 with PHIP1 by coimmunoprecipitation and immuno-colocalization. A) HEK 293 cell lysate of FLAG-wdr13 and Myc- PHIP1 transfected cells were immunoprecipitated with anti FLAG antibody, followed by immunoblotting with anti Myc antibody shows interaction of PHIP1 with wdr13 protein. 5% input shows protein expression in cell lysate with FLAG or Myc specific antibody. B) Immuno colocalization of Myc-PHIP1 and FLAG-wdr13 by immunofluorescence shows interaction of PHIP1 with wdr13. C) HEK 293 cell lysate of FLAG-wdr13 and Myc-PHIP-WD or Myc-PHIP-Bromo transfected cells were immunoprecipitated with anti FLAG antibody, followed by immunoblotting with anti Myc antibody shows interaction of PHIP WD domain with wdr13 protein. 5% input shows protein expression in cell lysate with FLAG or Myc specific antibody.

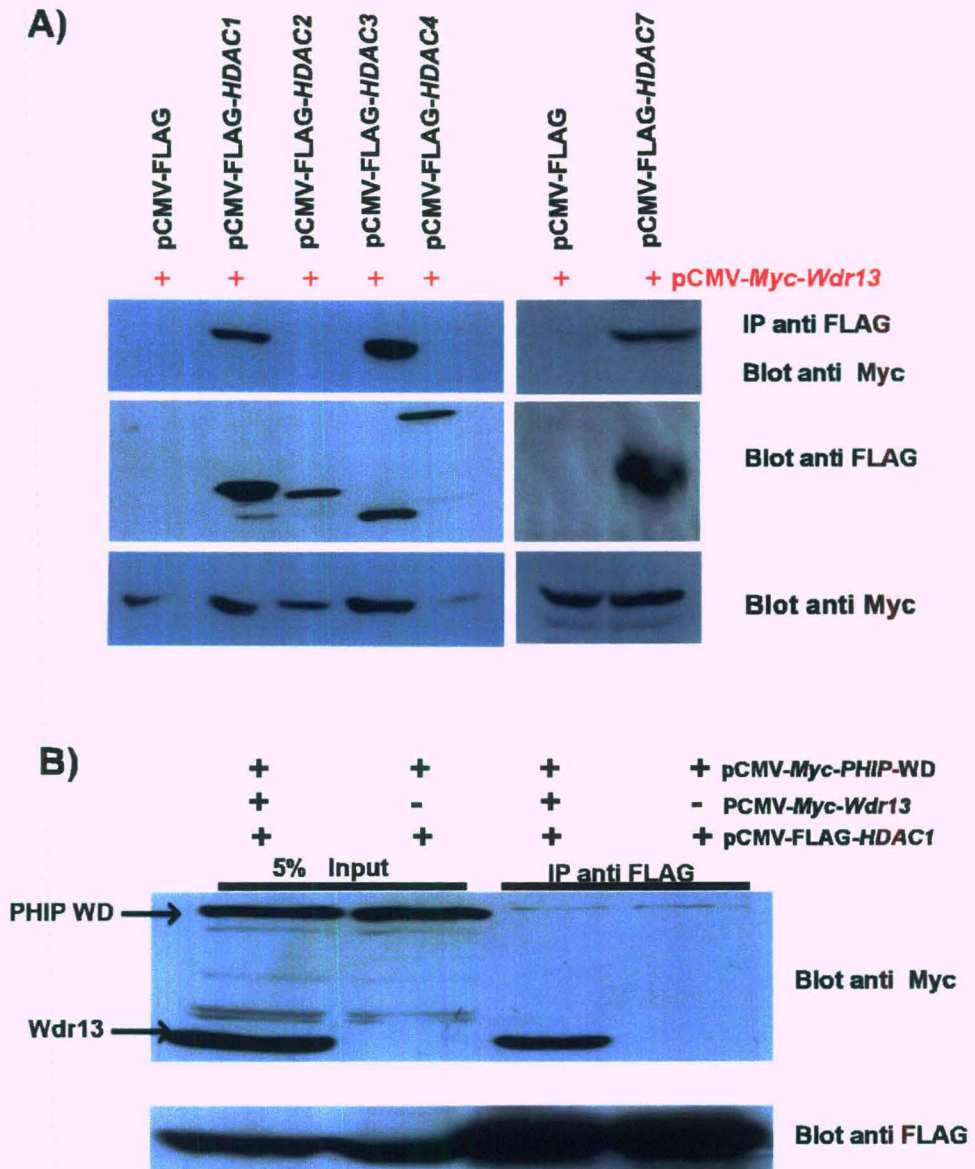


Figure 4.3 The interaction of wdr13, HDACs and PHIP1. A) HEK 293 cells lysate of *Myc-Wdr13* and FLAG-HDACs transfected cells were immunoprecipitated with anti FLAG antibody, followed by immunoblotted with anti Myc antibody shows interaction with HDAC1, HDAC3 and HDAC7. 5% input shows protein expression in cell lysate with FLAG or Myc specific antibody in the lower pannels. B) Cells lysate of FLAG -HDAC1, *Myc-Wdr13* and *Myc-PHIP-WD* domain, transfected cells were immunoprecipitated with anti FLAG antibody, followed by immunoblotted with anti Myc antibody shows no interaction of HDAC1 and PHIP WD domain through wdr13 protein. 5% input shows protein expression in cell lysate with FLAG or Myc specific antibody

4.2.4 HDAC 1, 3 and 7 interact with *wdr13*

LC-MS/MS results (Table 4.1) also indicated that HDAC7 protein was interacting with *wdr13*. The interaction of HDAC7 and *wdr13* was further validated by coimmunoprecipitation experiment. HEK293 cells were co-transfected with pCMV-FLAG-*HDAC7*, pCMV-*Myc-Wdr13* and pCMV-FLAG, pCMV-*Myc-Wdr13* vectors and allowed to grow for 48 hours before lysis. The immunoprecipitation of cell lysate using anti FLAG antibody followed by immunoblotting with anti Myc antibody showed interaction of *wdr13* and HDAC7 (Figure 4.3A).

Given the structural and functional similarities of various HDACs (Gregorette et al., 2004), the interaction of HDAC7 with *wdr13* opened the possibility that *wdr13* may interact with other HDACs. To test this hypothesis, both class I and class II HDACs were coimmunoprecipitated with *wdr13*. HEK293 cells cotransfected with pCMV-FLAG-*HDACs(1,2,3,4)*, pCMV-*Myc-Wdr13* and pCMV-FLAG, pCMV-*Myc-Wdr13* vectors followed by immunoprecipitation with anti FLAG antibody and immunoblotting with anti Myc antibody showed interaction of *wdr13* with HDAC1 and HDAC3 (Figure 4.3A).

4.2.5 HDAC1 and 3 do not interact with PHIP1

Bromodomain containing proteins bind with acetylated histones and can work as coactivator or corepressor depending on recruitment of various complexes (Denis, 2010). Interaction of *wdr13* with PHIP1 and HDACs opened the possibility that PHIP1 may act like corepressor by recruiting HDACs through *wdr13*. To test this hypothesis coimmunoprecipitation experiments were performed. HEK293 cells cotransfected with pCMV-FLAG-*HDACs(1,3)*, pCMV-*Myc-Wdr13*, pCMV-*Myc-PHIP-WD* and pCMV-FLAG-*HDACs(1,3)*, pCMV-*Myc*, pCMV-*Myc-PHIP-WD* vectors followed by immunoprecipitation with anti FLAG antibody and immunoblotting with anti

Myc antibody did not show interaction of HDAC1 and HDAC3 with PHIP1 WD domain (Figure 4.3B). Similar type of immunoprecipitation experiments were also performed in presence of PHIP1 bromodomain but did not show any interaction with HDAC1 and HDAC3. These results suggest that either the presence or absence of *wdr13* did not affect interaction of HDAC1 and HDAC3 with PHIP1.

4.2.6 *wdr13* protein contains nuclear receptor box (LxxLL)

Eukaryotic Linear Motif resource for functional sites in proteins showed that *wdr13* protein contains five WD repeats and a nuclear receptor box (LNKLL) at position 378-382 (Figure 4.4A) along with various casein kinase and GSK3 phosphorylation sites. The presence of LxxLL motif opens the possibility that *wdr13* may interact with a nuclear receptor in a ligand dependent manner.

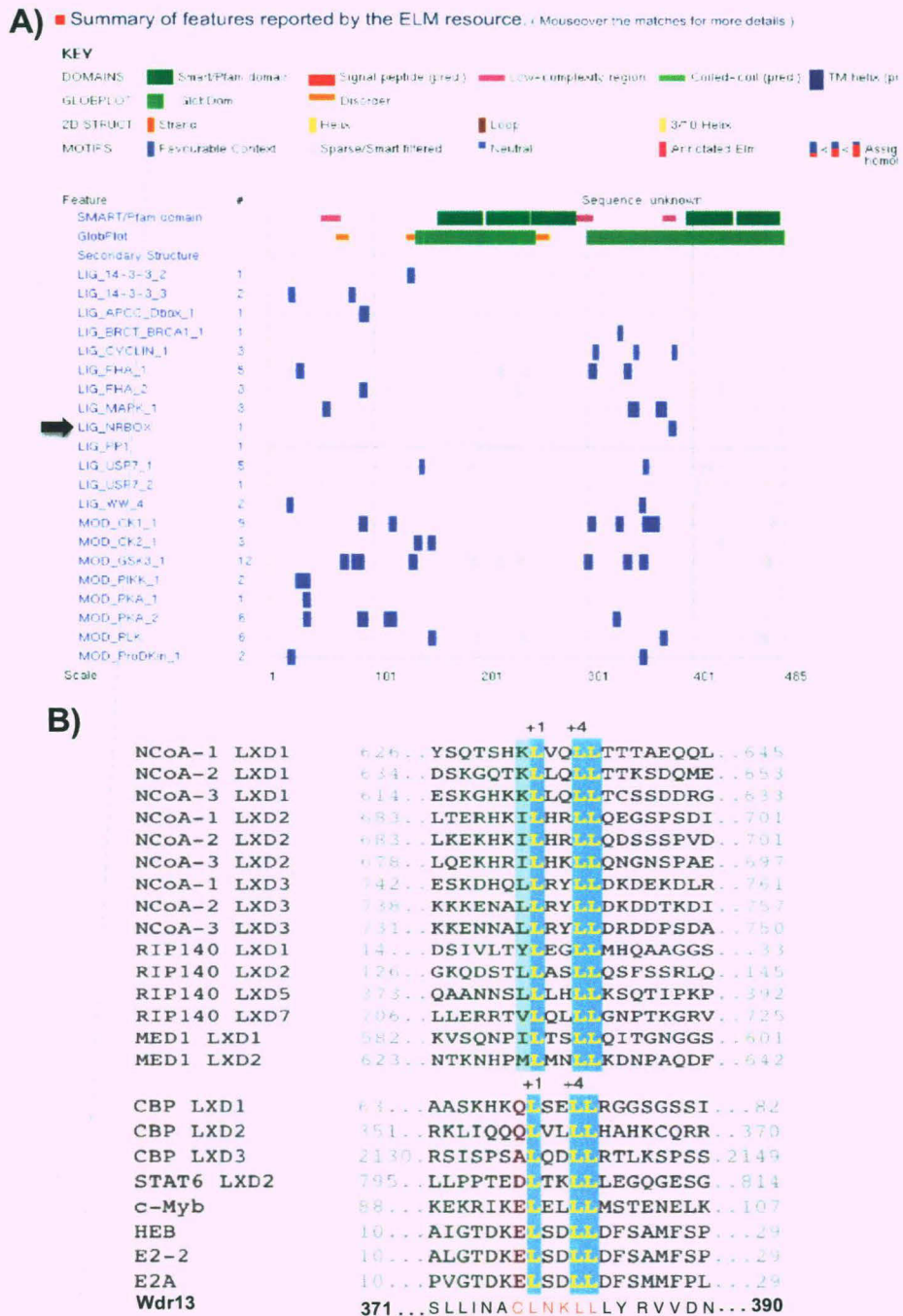


Figure 4.4 Presence of LxxLL motif in wdr13 protein A) Results of ELM motif search after globular domain filtering, structural filtering and context filtering shows NRBOX [377-383] CLNKLIII in wdr13 protein B) Co-activator and co-repressors containing LxxLL motif along with wdr13 protein.

4.3 DISCUSSION

The *Wdr13* is a member of WD repeats protein family and has proposed to have role in protein–protein interactions (Smith et al., 1999). The coimmunoprecipitation experiment showed that *wdr13* interacts with PHIP1, HDAC1, HDAC3, and HDAC7. The interaction of *wdr13* with PHIP1 (contains bromodomain) and histone deacetylases suggests its role in chromatin regulations.

The WD repeat proteins have important role in chromatin organization and are associated to nuclear receptor either as an activator or repressors (Suganuma et al., 2008b). WDR5, RbBp5, RbAp48/46 are the four WD repeat proteins which have been identified as components of histone modifying complexes. WDR5 is associated with SET domain containing methyltransferases, such as Set1, MLL, MLL2 and MLL3/4 (Dou et al., 2006; Wysocka et al., 2005). In addition to its role in histone methylation, WDR5 is associated with several histone acetyltransferase (HAT) complexes (Mendjan et al., 2006; Suganuma et al., 2008a). The other WD repeat protein RbAp48/46 and its *Drosophila* homolog p55 are associated with variety of chromatin regulating complexes including chromatin assembly factor CAF-1 (Tyler et al., 1996), HDAC1, the NuRD ATP dependent chromatin remodelling complex (Hassig et al., 1997; Xue et al., 1998; Zhang et al., 1999) and Extra sex combs (ESC) and Enhancer of zeste [E(Z)] complex, which is a type of poly comb group (PcG) histone methyltransferase complex (Czermin et al., 2002; Muller et al., 2002). The *Drosophila* WD repeat protein Groucho and its mammalian homolog TLE1 are transcriptional corepressors involved in various signaling pathways (Pickles et al., 2002).

The pleckstrin homology domain-interacting protein1 contains WD domain at N-terminal and bromodomain at C-terminals. PHIP1 also contains bipartite nuclear localization signal, resulting in nuclear localization of protein

(Podcheko et al., 2007). The overexpression of PHIP1 has been shown to stimulate cell proliferation by enhancing the cyclin D2 overexpression in MIN6 and NIH3T3 cells, where as knockdown of PHIP1 had reverse effect (Podcheko et al., 2007). However, these studies had not mentioned the effect of overexpression and knockdown on other cyclins and CDKIs. The overexpression of wdr13 showed down-regulation of cyclin D2 and cyclin E1 in MIN6 and NIH3T3 cells and knockout mice of wdr13 showed upregulation of cyclin E1 in pancreatic beta cells and cyclin D2 in testis (see chapter 3). The regulation of cyclin D2 by PHIP1 is not yet known to be either a direct or indirect effect. The interaction of wdr13 with PHIP1 WD domain gives us one possibility that wdr13 may be inhibiting PHIP1 action.

The other classes of proteins, which interact with wdr13 are histone deacetylases (HDACs). The co-immunoprecipitation experiments showed the interaction of wdr13 with HDAC1, HDAC3 and HDAC7. The HDACs are a large protein family, which mediate transcription repression by deacetylation of chromatin (Gray and Ekstrom, 2001). In vertebrates eleven HDACs have been identified. These can be divided into four subclasses: Class I (HDAC1, HDAC2, HDAC3 and HDAC8), Class II (HDAC4, HDAC5, HDAC6, HDAC7, HDAC9 and HDAC10), Class III (deacetylase are NAD⁺ dependent sirtuin family) and Class IV (HDAC11) (Gregoretta et al., 2004). In general, removal of acetyl group from histones by HDACs causes condensation of chromatin and repression of genes. The interaction of wdr13 with HDACs open the possibility that wdr13 may be acting like repressors. However, further studies will be required to confirm this repression activity.

Genome wide mapping of histone acetyltransferases and histone deacetylases of CD4⁺ cells have shown that HDAC1 and HDAC3 occupied promoter of cyclin D2, cyclin D3, cyclin E1 and p21 but not the promoter of cyclin D1 (Wang et al., 2009). These results suggest that HDACs may have role in expression of cell cycle regulators. The wdr13 may be having a role in repression of these genes. Consistent with genome wide occupancy of

various promoters of cyclins by HDACs, the overexpression of *wdr13* causes repression of cyclin D2, cyclin E1 transcript and unaltered cyclin D1 transcript.

The bromodomain containing proteins have been reported to perform dual function (coactivator and corepressor) (Denis, 2010). Immunoprecipitation with HDAC1 and HDAC3 in the presence or in the absence of *wdr13* failed to immunoprecipitate PHIP1. This result showed that PHIP1 does not interact with HDAC1 and HDAC3 through *wdr13*. However, these results indirectly indicate that both HDACs and PHIP1 are interacting with same domain of *wdr13*. But this needs to be further verified. It is possible that on one hand *wdr13* is inhibiting the function of PHIP1 and on other hand, the protein is working as repressors through HDACs and thus regulating the the cyclin D2 and Cyclin E1 expression.

The LxxLL motifs participate in many protein-protein interactions and are associated with different aspects of transcriptional regulation (Plevin et al., 2005). Originally LxxLL motif was identified in cofactor proteins that interact with hormone activated nuclear receptor through ligand binding domain (Heery et al., 1997). In many cases where LxxLL motif interacts with nuclear receptor contains hydrophobic residue at -1 position and binds with higher affinity like RIP140 and NcoA. The proteins containing polar residues at -1 position bind with lower affinity like CBP/p300 (Heery et al., 2001). The binding of cofactor containing LxxLL motif either enhances or suppresses target genes of nuclear receptor, depending on associated proteins (Plevin et al., 2005). The absence of DNA binding domain in *wdr13* and interaction with HDACs open the possibility that *wdr13* may have interactions with some nuclear receptors. However, we could not identify nuclear receptor in LC/MS-MS experiment probably due to weak interaction or absence of ligand except NR2E1. However, coimmunoprecipitation from HEK293 in our lab failed to immunoprecipitate *wdr13* with NR2E1. This may be either due to absence of ligand for NR2E1 in HEK293 cells or this was a case of false positive

interaction obtained during LC-MS/MS. Further studies will help to understand whether the *wdr13* interacts with NR2E1 or other nuclear receptors.

Many coactivators contain multiple LxxLL motif, which may be used in nuclear receptor specific manner. The interaction of LxxLL motif is ligand dependent (McInerney et al., 1998). Similarly, corepressors contain cornr-box (LXXI/HIXXXI/L) (Hu and Lazar, 1999). This motif occupied the same hydrophobic pocket contacted by LxxLL motif in the absence of agonist. The agonist binding reduces the affinity of nuclear receptor for cornr-box containing corepressors and increases affinity with LxxLL motif containing coactivators (Webb et al., 2000). Some ligand dependent corepressors are also recruited to nuclear receptor through same motif. The examples are LCoR (Ligand dependent nuclear corepressor) (Fernandes et al., 2003), RIP 140 (receptor interacting protein 140) (Cavailles et al., 1995), REA (repressor of estrogen receptor activity) (Delage-Mourroux et al., 2000), and human tumor antigen PRAME (Epping et al., 2005). These proteins interact with nuclear receptor through LxxLL motif but exert corepressor function.

In conclusion, *wdr13* interacts with PHIP1, HDAC1, HDAC3 and HDAC7. It appears that *wdr13* helps in recruitment of HDACs at some genomic loci and may have a role in gene repression.

Chapter 5

CHAPTER 5: OVERVIEW

With the advancement of scientific information, the knowledge about functional diversity of WD repeat protein family has increased and will continue to increase further. Majority of WD repeat proteins are found in eukaryotes and their number increases with the complexity of system. This indicates that functional diversity of WD repeat protein is important in complex systems. WD repeat proteins have diverse functions that include cell cycle, vesicular trafficking, chromatin organization, cytoskeleton assembly and apoptosis.

Wdr13 is a conserved member of WD repeat protein family and expresses ubiquitously in majority of the tissues analyzed. Expression of *Wdr13* in unfertilized egg and neural stem cell as reported earlier (Suresh et al., 2005), suggested its role during normal development. The *Wdr13* deficient mice reported in this study were viable and fertile with no overt phenotype till the age of 2 months. However, these mice developed mild obesity in age dependent manner. These results suggest that *Wdr13* is dispensable for development and fertility. *In vitro* adipogenesis experiments did not reveal any difference in the adipogenesis of wild type and *Wdr13* knockout MEFs suggesting that enhanced adipogenesis is not the primary cause of obesity in *Wdr13* knockout mice. However, the increased islet mass, followed by hyperinsulinemia leads to obesity. This phenotype is preponed on high fat diet. The increase in the islet mass is not due to peripheral insulin resistance as suggested by ITT. The phenomenon of increased islet mass in absence of *wdr13* protein can be further understood by transferring *Wdr13* null mutation in some diabetic genetic background such as non-obese diabetic model (NOD) and obese diabetic model (db/db).

Increase in spermatogonial cell proliferation and beta cell proliferation, in *Wdr13* knockout mice suggested the role of *Wdr13* in cell proliferation in testis. The effect of enhanced cell proliferation in testis was compensated by

enhanced cell apoptosis. The *Wdr13* expression has been reported in cancers like colon adenocarcinoma, neuroblastoma, Ewing's sarcoma, Larynx sarcoma, pancreatic ductal carcinoma, signet ring cell carcinoma, ovary teratocarcinoma, and lung tumors on the basis of differential gene expression (Suresh et al., 2005). The identification of *Wdr13* in these cancer cells may be due to feedback response to increased cell proliferation. Several tumor suppressor genes have been identified namely; *p53*, *p21*, *p27*, *BRCA1* and *BRCA2*, which have role in cell proliferation and mutations in these genes develop various types of tumors. The enhanced cell proliferation is compensated by apoptosis in testis of *Wdr13* knockout mice. This could be the reason for us not to observe development of spontaneous tumor till the age of 12 months. However, it will be interesting to observe these mice further. The upregulation of *p21* may be the main cause of this compensation. It will be interesting to transfer *Wdr13* null mutation in *p21* or *p53* knockout mice genetic background. In these double knockout mice since one would expect lack of *p21* upregulation through feedback mechanisms, it may be possible that the phenotype of *Wdr13* will be enhanced.

It may be noted that I have studied the phenotype of *Wdr13* knockout mice in pancreas, testis and adipose tissues only. The *Wdr13* gene expresses at high levels in brain, liver, kidney, eye and ovary. The phenotypes of these tissues have not been analyzed in detail in *Wdr13* knockout mice. In the present study it has been shown that *Wdr13* knockout mice have tendency to eat more. This would be interesting to study the behavioural phenotype of *Wdr13* knockout mice. Agatha *et al*, has shown that the down-regulation of *Wdr13* after classical conditioning in brain hippocampus (D'Agata et al., 2003) suggesting *wdr13* role in memory and learning process. Liver is a major organ for glucose homeostasis. The knockdown of class II HDACs in liver has been shown to ameliorate hyperglycemia in diabetic mouse models (Mihaylova et al., 2011) and these researchers have suggested that HDAC inhibitors can be used to ameliorate hyperglycemia. The interaction of *wdr13* with HDACs and *Wdr13* knockout mice's hypoglycemic conditions suggest that *Wdr13* knockout

can be used as model organism to understand glucose homeostasis in liver. It is possible that some of the target genes of HDACs may be regulated through *Wdr13* and thus, are being hyperacetylated and getting upregulated in liver of *Wdr13* knockout mice.

The overexpression of *wdr13* protein causes inhibition of cell proliferation by targeting repression of cyclin D2 and cyclin E1 in various cell lines. The cyclin D and cyclin E have been reported to be upregulated in many types of tumors. The generation of transgenic mice (Figure 3.14) over expressing *wdr13* protein in tissue specific manner in the background of some tumor suppressor null mutations (p53, BRCA1) may help us to understand the role of *wdr13* protein in tumor suppression.

The nuclear localization and interaction of *wdr13* with HDAC1, HDAC3, HDAC7 and PHIP1 provide strong possibility that *wdr13* is acting through chromatin regulation. The presence of LxxLL motif gives possibility that *wdr13* may be regulating chromatin through nuclear receptor in ligand dependent manner. Various co-activators and co-repressors have been identified having LxxLL motif and they interact with nuclear receptors in ligand-dependent manner (Plevin et al., 2005). The identification of nuclear receptor like estrogen receptor, progesterone receptor, retinoic acid receptor and liver X receptor will help to illustrate the *Wdr13* function in great detail. Further immunoprecipitation experiment will help to understand the interaction of *wdr13* with various nuclear receptors in presence and absence of ligands. However, the nuclear receptor may be acting in tissue specific manner. The target genes of *wdr13* are not known; it would be interesting to understand the promoter occupancy by *wdr13* at genome level.

Genome wide occupancy of HDACs and HATs in CD4+ cells (Wang et al., 2009) had showed that both binds to the promoter of active genes, suggesting the dynamic change by chromatin acetylation. The study also showed that HDAC1 and HDAC3 bind with promoter and HDAC2 binds only

with intragenic region. The interaction of wdr13 protein with HDAC1 and HDAC3 but not with HDAC2 indicated that wdr13 regulates gene expression at promoter sequences. However, there is no direct evidence to suggest the repression activity of wdr13 protein. The chromatin immunoprecipitation study of various genes using antibody against various histone modifications will give insight on the repression activity of wdr13 protein.

The work described in my thesis suggests that *Wdr13* knockout mice have enhanced beta cell proliferation followed by increased islet mass and hyperinsulinemia resulting in better glucose clearance. By inhibiting *Wdr13*, it may be possible to ameliorate diabetic conditions in humans. On the other side overexpression of wdr13 causes suppression of cell proliferation in various cell lines. Overexpression of this protein in mouse model may help to understand the tumor suppression activity of wdr13 protein. This may help to develop wdr13 agonist(s) as tumor suppressors.

Appendix

APPENDIX

A.1 20X SSC

3.0M NaCl, 0.3M sodium acetate

A.2 1M Phosphate buffer (pH 7.2)

684 ml 1M Na₂HPO₄ and 316 ml 1M NaH₂PO₄

A.3 Avertin

A stock of 100% avertin was prepared by mixing 10 gram of 2,2,2-tribromomethyl alcohol with 10 ml of *tert*-amyl alcohol by heating at 50°C overnight. The solution was diluted to 1.25% in saline for final use.

A.4 Luria-Bertani Medium (LB Medium)

LB Medium was prepared by dissolving 10g tryptone, 5g Yeast extract, 10g NaCl in one liter MilliQ H₂O and pH was adjusted with 5N NaOH.

For LB agar 2% agar-agar was added to LB Medium.

A.5 TBST

50mM Tris.Cl (pH 7.5), 150mM NaCl, 0.05% Tween-20

A.6 PBST

137 mM NaCl, 2.7 mM MKCl, 10 mM Na₂HPO₄, 2mM KH₂PO₄, 0.05% Tween-20

A.7 Inoue Transformation Buffer (TFB)

Inoue transformation buffer was prepared by dissolving all of the solutes listed below in 800 ml of MilliQ H₂O and then 20 ml of 0.5 M PIPES (pH 6.7) was added.

Reagent Amount per Liter Final Concentration

MnCl₂.4H₂O 10.88 g (55 mM)

CaCl₂.2H₂O 2.20 g (15 mM)

KCl 18.65 g (250 mM)

PIPES (0.5 M, pH 6.7) 20 ml (10 mM)

The final volume of the transformation buffer was adjusted to 1 liter with MilliQ H₂O.

A.8 Cracking Buffer

Two ml of 5 M NaOH, 2.5 ml of 10 % SDS and 10 gm of sucrose was added into 40 ml of ddH₂O and mixed well and the volume was made up to 50 ml

A.9 List of primers used for Real Time PCR

| S.N. | Primer Name | Primer sequences 5'-3' |
|------|------------------------------------|--|
| 1 | Wdr13E2F Wdr13E2R | aacgcctaccgtacaccaac tgctataggcagcagcactg |
| 2 | NeoF NeoR | gatcggccattgaacaagat atactttctcggcaggagca |
| 3 | PPAR γ F PPAR γ R | gagtcctctcagctgttcgc gtagatctcctggagcaggg |
| 4 | EBP α F EBP α R | aatggcagtggtcacgtcta cccaaacatccctaaaccaa |
| 5 | Cyclin D1F Cyclin D1R | cccttggggacatgttgta ccctactctcagggtgatgc |
| 6 | Cyclin D2F Cyclin D2R | ctagtgcataatgccccctt cgtttctgattcctcctgg |
| 7 | Cyclin D3F Cyclin D3R | ccctcccttctgtctcc tgaaagcccttggtctgagt |
| 8 | Cyclin E1F Cyclin E1R | ccattgcctcaaagacagt cacttccatccaaggcatct |
| 9 | CDK2F CDK2R | tggctgttcatcgtgggtc gaggccctctgacaactcaa |
| 10 | CDK4F CDK4R | cagcactcctacctgcacaa aggagaggtggggacttgtt |
| 11 | P15F P15R | gggatcaccaaggagattt tttcagttcacaggggaagg |
| 12 | P18F P18R | caccagtaactcccgccta cgctcctactccaagacc |
| 13 | P19F P19R | gccactgtctccagccttac aacacacaaaaggggtgag |
| 14 | P21F P21R | cggtggaacttgacttcgt cagggcagaggaagtactgg |
| 15 | P27F P27R | cagaatcataagcccctgga ggctctcagagttgcctga |
| 16 | P57F P57R | aagagaactgcgaggagaa cccagagtcttccatcgtc |
| 17 | GAPDHF GAPDHR | accagaagactgtggatgg cacattgggggtaggaacac |
| 18 | BetaF BetaR | tgttaccactgggacgaca ccatcacaatgcctgtggta |

A.10 List of Antibodies used in this study

| Antibody | Source |
|------------------------|-------------------------------|
| Anti-Brdu | BD Biosciences, Cat No-347580 |
| Anti-Insulin | R&D systems, Cat No- MAB1417 |
| Anti-wdr13 | Sigma, Cat No-HPA000913 |
| Anti-FLAG | Sigma, Cat No-F3165 |
| Anti-Myc | Santacruz, Cat No-sc-2091 |
| Anti-Beta | Abcam, Cat No-8226 |
| Anti-myc-HRP | Invitrogen, Cat No-R951-25 |
| Anti-mouse HRP | Amersham, Cat No-NA9310V |
| Anti-rat HRP | Amersham, Cat No-NA9350V |
| Anti- rabbit HRP | Amersham, Cat No-NA9340V |
| Anti- rabbit rhodamine | Santacruz, Cat No -sc-2091 |
| Anti- mouse FITC | Sigma, Cat No-F-5262 |
| Anti-rat Cy5 | Santacruz, Cat No-sc-45100 |

References

REFERENCES

Abou-Haila, A., and Tulsiani, D.R. (2003). Evidence for the capacitation-associated membrane priming of mouse spermatozoa. *Histochem Cell Biol* 119, 179-187.

Adams, D.J., Biggs, P.J., Cox, T., Davies, R., van der Weyden, L., Jonkers, J., Smith, J., Plumb, B., Taylor, R., Nishijima, I., *et al.* (2004). Mutagenic insertion and chromosome engineering resource (MICER). *Nat Genet* 36, 867-871.

Aranda, A., and Pascual, A. (2001). Nuclear hormone receptors and gene expression. *Physiol Rev* 81, 1269-1304.

Ariyama, Y., Shimizu, H., Satoh, T., Tsuchiya, T., Okada, S., Oyadomari, S., and Mori, M. (2007). Chop-deficient mice showed increased adiposity but no glucose intolerance. *Obesity (Silver Spring)* 15, 1647-1656.

Baribault, H., and Kemler, R. (1989). Embryonic stem cell culture and gene targeting in transgenic mice. *Mol Biol Med* 6, 481-492.

Bluher, M., Michael, M.D., Peroni, O.D., Ueki, K., Carter, N., Kahn, B.B., and Kahn, C.R. (2002). Adipose tissue selective insulin receptor knockout protects against obesity and obesity-related glucose intolerance. *Dev Cell* 3, 25-38.

Bonner-Weir, S. (2000). Perspective: Postnatal pancreatic beta cell growth. *Endocrinology* 141, 1926-1929.

Bouwens, L., and Rooman, I. (2005). Regulation of pancreatic beta-cell mass. *Physiol Rev* 85, 1255-1270.

- Bradley, A., Evans, M., Kaufman, M.H., and Robertson, E. (1984). Formation of germ-line chimaeras from embryo-derived teratocarcinoma cell lines. *Nature* 309, 255-256.
- Bruning, J.C., Michael, M.D., Winnay, J.N., Hayashi, T., Horsch, D., Accili, D., Goodyear, L.J., and Kahn, C.R. (1998). A muscle-specific insulin receptor knockout exhibits features of the metabolic syndrome of NIDDM without altering glucose tolerance. *Mol Cell* 2, 559-569.
- Buehr, M., Meek, S., Blair, K., Yang, J., Ure, J., Silva, J., McLay, R., Hall, J., Ying, Q.L., and Smith, A. (2008). Capture of authentic embryonic stem cells from rat blastocysts. *Cell* 135, 1287-1298.
- Buratowski, S. (1994). The basics of basal transcription by RNA polymerase II. *Cell* 77, 1-3.
- Capecchi, M.R. (1989). Altering the genome by homologous recombination. *Science* 244, 1288-1292.
- Castets, F., Bartoli, M., Barnier, J.V., Baillat, G., Salin, P., Moqrigh, A., Bourgeois, J.P., Denizot, F., Rougon, G., Calothy, G., *et al.* (1996). A novel calmodulin-binding protein, belonging to the WD-repeat family, is localized in dendrites of a subset of CNS neurons. *J Cell Biol* 134, 1051-1062.
- Castets, F., Rakitina, T., Gaillard, S., Moqrigh, A., Mattei, M.G., and Monneron, A. (2000). Zinedin, SG2NA, and striatin are calmodulin-binding, WD repeat proteins principally expressed in the brain. *J Biol Chem* 275, 19970-19977.

Cavaillès, V., Dauvois, S., L'Horset, F., Lopez, G., Hoare, S., Kushner, P.J., and Parker, M.G. (1995). Nuclear factor RIP140 modulates transcriptional activation by the estrogen receptor. *EMBO J* 14, 3741-3751.

Chow, V.T., and Quek, H.H. (1996). HEP-COP, a novel human gene whose product is highly homologous to the alpha-subunit of the yeast coatmer protein complex. *Gene* 169, 223-227.

Cinti, S., Eberbach, S., Castellucci, M., and Accili, D. (1998). Lack of insulin receptors affects the formation of white adipose tissue in mice. A morphometric and ultrastructural analysis. *Diabetologia* 41, 171-177.

Cocquet, J., Ellis, P.J., Yamauchi, Y., Riel, J.M., Karacs, T.P., Rattigan, A., Ojarikre, O.A., Affara, N.A., Ward, M.A., and Burgoyne, P.S. (2010). Deficiency in the multicopy Sycp3-like X-linked genes Slx and Slx1 causes major defects in spermatid differentiation. *Mol Biol Cell* 21, 3497-3505.

Cozar-Castellano, I., Weinstock, M., Haught, M., Velazquez-Garcia, S., Sipula, D., and Stewart, A.F. (2006). Evaluation of beta-cell replication in mice transgenic for hepatocyte growth factor and placental lactogen: comprehensive characterization of the G1/S regulatory proteins reveals unique involvement of p21cip. *Diabetes* 55, 70-77.

Czermin, B., Melfi, R., McCabe, D., Seitz, V., Imhof, A., and Pirrotta, V. (2002). Drosophila enhancer of Zeste/ESC complexes have a histone H3 methyltransferase activity that marks chromosomal Polycomb sites. *Cell* 111, 185-196.

D'Agata, V., Schreurs, B.G., Pascale, A., Zohar, O., and Cavallaro, S. (2003). Down regulation of cerebellar memory related gene-1 following classical conditioning. *Genes Brain Behav* 2, 231-237.

- deFazio, A., Leary, J.A., Hedley, D.W., and Tattersall, M.H. (1987). Immunohistochemical detection of proliferating cells in vivo. *J Histochem Cytochem* 35, 571-577.
- DeJong, J. (2006). Basic mechanisms for the control of germ cell gene expression. *Gene* 366, 39-50.
- Delage-Mourroux, R., Martini, P.G., Choi, I., Kraichely, D.M., Hoeksema, J., and Katzenellenbogen, B.S. (2000). Analysis of estrogen receptor interaction with a repressor of estrogen receptor activity (REA) and the regulation of estrogen receptor transcriptional activity by REA. *J Biol Chem* 275, 35848-35856.
- Deng, X.W., Matsui, M., Wei, N., Wagner, D., Chu, A.M., Feldmann, K.A., and Quail, P.H. (1992). COP1, an Arabidopsis regulatory gene, encodes a protein with both a zinc-binding motif and a G beta homologous domain. *Cell* 71, 791-801.
- Denis, G.V. (2010). Bromodomain coactivators in cancer, obesity, type 2 diabetes, and inflammation. *Discov Med* 10, 489-499.
- Denis, G.V., McComb, M.E., Faller, D.V., Sinha, A., Romesser, P.B., and Costello, C.E. (2006). Identification of transcription complexes that contain the double bromodomain protein Brd2 and chromatin remodeling machines. *J Proteome Res* 5, 502-511.
- Deshpande, A., Sicinski, P., and Hinds, P.W. (2005). Cyclins and cdks in development and cancer: a perspective. *Oncogene* 24, 2909-2915.

- Dor, Y., Brown, J., Martinez, O.I., and Melton, D.A. (2004). Adult pancreatic beta-cells are formed by self-duplication rather than stem-cell differentiation. *Nature* 429, 41-46.
- Dou, Y., Milne, T.A., Ruthenburg, A.J., Lee, S., Lee, J.W., Verdine, G.L., Allis, C.D., and Roeder, R.G. (2006). Regulation of MLL1 H3K4 methyltransferase activity by its core components. *Nat Struct Mol Biol* 13, 713-719.
- Duden, R., Griffiths, G., Frank, R., Argos, P., and Kreis, T.E. (1991). Beta-COP, a 110 kd protein associated with non-clathrin-coated vesicles and the Golgi complex, shows homology to beta-adaptin. *Cell* 64, 649-665.
- EI-Hattab, A., Bournat, J., Eng, P.A., Wu, J.B., Walker, B.A., Stankiewicz, P., Cheung, S.W., and Brown, C.W. (2010). Microduplication of Xp11.23p11.3 with effects on cognition, behavior, and craniofacial development. *Clin Genet*.
- Epping, M.T., Wang, L., Edel, M.J., Carlee, L., Hernandez, M., and Bernards, R. (2005). The human tumor antigen PRAME is a dominant repressor of retinoic acid receptor signaling. *Cell* 122, 835-847.
- Evans, M.J., and Kaufman, M.H. (1981). Establishment in culture of pluripotential cells from mouse embryos. *Nature* 292, 154-156.
- Fernandes, I., Bastien, Y., Wai, T., Nygard, K., Lin, R., Cormier, O., Lee, H.S., Eng, F., Bertos, N.R., Pelletier, N., *et al.* (2003). Ligand-dependent nuclear receptor corepressor LCoR functions by histone deacetylase-dependent and -independent mechanisms. *Mol Cell* 11, 139-150.
- Finegood, D.T., Scaglia, L., and Bonner-Weir, S. (1995). Dynamics of beta-cell mass in the growing rat pancreas. Estimation with a simple mathematical model. *Diabetes* 44, 249-256.

- Francia, G., Cruz-Munoz, W., Man, S., Xu, P., and Kerbel, R.S. (2011). Mouse models of advanced spontaneous metastasis for experimental therapeutics. *Nat Rev Cancer* 11, 135-141.
- Gerich, J.E. (1998). The genetic basis of type 2 diabetes mellitus: impaired insulin secretion versus impaired insulin sensitivity. *Endocr Rev* 19, 491-503.
- Girard, J., Perdereau, D., Foufelle, F., Prip-Buus, C., and Ferre, P. (1994). Regulation of lipogenic enzyme gene expression by nutrients and hormones. *FASEB J* 8, 36-42.
- Gnatt, A. (2002). Elongation by RNA polymerase II: structure-function relationship. *Biochim Biophys Acta* 1577, 175-190.
- Gray, S.G., and Ekstrom, T.J. (2001). The human histone deacetylase family. *Exp Cell Res* 262, 75-83.
- Gregorette, I.V., Lee, Y.M., and Goodson, H.V. (2004). Molecular evolution of the histone deacetylase family: functional implications of phylogenetic analysis. *J Mol Biol* 338, 17-31.
- Gu, H., Marth, J.D., Orban, P.C., Mossmann, H., and Rajewsky, K. (1994). Deletion of a DNA polymerase beta gene segment in T cells using cell type-specific gene targeting. *Science* 265, 103-106.
- Gupta, R.K., Gao, N., Gorski, R.K., White, P., Hardy, O.T., Rafiq, K., Brestelli, J.E., Chen, G., Stoeckert, C.J., Jr., and Kaestner, K.H. (2007). Expansion of adult beta-cell mass in response to increased metabolic demand is dependent on HNF-4alpha. *Genes Dev* 21, 756-769.

Handschug, K., Sperling, S., Yoon, S.J., Hennig, S., Clark, A.J., and Huebner, A. (2001). Triple A syndrome is caused by mutations in AAAS, a new WD-repeat protein gene. *Hum Mol Genet* 10, 283-290.

Hanley, S.C., Austin, E., Assouline-Thomas, B., Kapeluto, J., Blaichman, J., Moosavi, M., Petropavlovskaja, M., and Rosenberg, L. (2010). β -Cell mass dynamics and islet cell plasticity in human type 2 diabetes. *Endocrinology* 151, 1462-1472.

Hassig, C.A., Fleischer, T.C., Billin, A.N., Schreiber, S.L., and Ayer, D.E. (1997). Histone deacetylase activity is required for full transcriptional repression by mSin3A. *Cell* 89, 341-347.

He, T.C., Zhou, S., da Costa, L.T., Yu, J., Kinzler, K.W., and Vogelstein, B. (1998). A simplified system for generating recombinant adenoviruses. *Proc Natl Acad Sci U S A* 95, 2509-2514.

Heery, D.M., Hoare, S., Hussain, S., Parker, M.G., and Sheppard, H. (2001). Core LXXLL motif sequences in CREB-binding protein, SRC1, and RIP140 define affinity and selectivity for steroid and retinoid receptors. *J Biol Chem* 276, 6695-6702.

Heery, D.M., Kalkhoven, E., Hoare, S., and Parker, M.G. (1997). A signature motif in transcriptional co-activators mediates binding to nuclear receptors. *Nature* 387, 733-736.

Heine, P.A., Taylor, J.A., Iwamoto, G.A., Lubahn, D.B., and Cooke, P.S. (2000). Increased adipose tissue in male and female estrogen receptor-alpha knockout mice. *Proc Natl Acad Sci U S A* 97, 12729-12734.

Heit, J.J., Apelqvist, A.A., Gu, X., Winslow, M.M., Neilson, J.R., Crabtree, G.R., and Kim, S.K. (2006a). Calcineurin/NFAT signalling regulates pancreatic beta-cell growth and function. *Nature* 443, 345-349.

Heit, J.J., Karnik, S.K., and Kim, S.K. (2006b). Intrinsic regulators of pancreatic beta-cell proliferation. *Annu Rev Cell Dev Biol* 22, 311-338.

Henning, K.A., Li, L., Iyer, N., McDaniel, L.D., Reagan, M.S., Legerski, R., Schultz, R.A., Stefanini, M., Lehmann, A.R., Mayne, L.V., *et al.* (1995). The Cockayne syndrome group A gene encodes a WD repeat protein that interacts with CSB protein and a subunit of RNA polymerase II TFIIH. *Cell* 82, 555-564.

Holsberger, D.R., Buchold, G.M., Leal, M.C., Kiesewetter, S.E., O'Brien, D.A., Hess, R.A., Franca, L.R., Kiyokawa, H., and Cooke, P.S. (2005). Cell-cycle inhibitors p27Kip1 and p21Cip1 regulate murine Sertoli cell proliferation. *Biol Reprod* 72, 1429-1436.

Honore, B., Baandrup, U., Nielsen, S., and Vorum, H. (2002). Endonuclein is a cell cycle regulated WD-repeat protein that is up-regulated in adenocarcinoma of the pancreas. *Oncogene* 21, 1123-1129.

Hu, X., and Lazar, M.A. (1999). The CoRNR motif controls the recruitment of corepressors by nuclear hormone receptors. *Nature* 402, 93-96.

Inoue, H., Nojima, H., and Okayama, H. (1990). High efficiency transformation of *Escherichia coli* with plasmids. *Gene* 96, 23-28.

Kumar, S., and Simons, J.P. (1993). The effects of terminal heterologies on gene targeting by insertion vectors in embryonic stem cells. *Nucleic Acids Res* 21, 1541-1548.

- Laemmli, U.K. (1970). Cleavage of structural proteins during the assembly of the head of bacteriophage T4. *Nature* 227, 680-685.
- Laird, P.W., Zijderveld, A., Linders, K., Rudnicki, M.A., Jaenisch, R., and Berns, A. (1991). Simplified mammalian DNA isolation procedure. *Nucleic Acids Res* 19, 4293.
- Lazar, D.F., and Saltiel, A.R. (2006). Lipid phosphatases as drug discovery targets for type 2 diabetes. *Nat Rev Drug Discov* 5, 333-342.
- Lee, J.S., Galvin, K.M., and Shi, Y. (1993). Evidence for physical interaction between the zinc-finger transcription factors YY1 and Sp1. *Proc Natl Acad Sci U S A* 90, 6145-6149.
- Lee, Y.C., and Nielsen, J.H. (2009). Regulation of beta cell replication. *Mol Cell Endocrinol* 297, 18-27.
- Li, D., and Roberts, R. (2001). WD-repeat proteins: structure characteristics, biological function, and their involvement in human diseases. *Cell Mol Life Sci* 58, 2085-2097.
- Li, J., Wang, J., Nawaz, Z., Liu, J.M., Qin, J., and Wong, J. (2000). Both corepressor proteins SMRT and N-CoR exist in large protein complexes containing HDAC3. *EMBO J* 19, 4342-4350.
- Li, P., Tong, C., Mehrian-Shai, R., Jia, L., Wu, N., Yan, Y., Maxson, R.E., Schulze, E.N., Song, H., Hsieh, C.L., *et al.* (2008). Germline competent embryonic stem cells derived from rat blastocysts. *Cell* 135, 1299-1310.
- Lijnen, H.R. (2011). Murine models of obesity and hormonal therapy. *Thromb Res* 127 Suppl 3, S17-20.

- Liu, C., Szurek, P.F., and Yu, Y.E. (2011). MICER targeting vectors for manipulating the mouse genome. *Methods Mol Biol* 693, 245-256.
- Liu, C.Z., Chen, Y., and Sui, S.F. (2006). The identification of a new actin-binding region in p57. *Cell Res* 16, 106-112.
- Lo Nigro, C., Chong, C.S., Smith, A.C., Dobyns, W.B., Carrozzo, R., and Ledbetter, D.H. (1997). Point mutations and an intragenic deletion in LIS1, the lissencephaly causative gene in isolated lissencephaly sequence and Miller-Dieker syndrome. *Hum Mol Genet* 6, 157-164.
- Loftus, T.M., Kuhajda, F.P., and Lane, M.D. (1998). Insulin depletion leads to adipose-specific cell death in obese but not lean mice. *Proc Natl Acad Sci U S A* 95, 14168-14172.
- Lubahn, D.B., Moyer, J.S., Golding, T.S., Couse, J.F., Korach, K.S., and Smithies, O. (1993). Alteration of reproductive function but not prenatal sexual development after insertional disruption of the mouse estrogen receptor gene. *Proc Natl Acad Sci U S A* 90, 11162-11166.
- Lustig, R.H., Sen, S., Soberman, J.E., and Velasquez-Mieyer, P.A. (2004). Obesity, leptin resistance, and the effects of insulin reduction. *Int J Obes Relat Metab Disord* 28, 1344-1348.
- Marmorstein, R. (2001). Structure and function of histone acetyltransferases. *Cell Mol Life Sci* 58, 693-703.
- Marmorstein, R., and Roth, S.Y. (2001). Histone acetyltransferases: function, structure, and catalysis. *Curr Opin Genet Dev* 11, 155-161.

- Matzuk, M.M., Finegold, M.J., Su, J.G., Hsueh, A.J., and Bradley, A. (1992). Alpha-inhibin is a tumour-suppressor gene with gonadal specificity in mice. *Nature* 360, 313-319.
- Matzuk, M.M., and Lamb, D.J. (2002). Genetic dissection of mammalian fertility pathways. *Nat Cell Biol* 4 *Suppl*, s41-49.
- McInerney, E.M., Rose, D.W., Flynn, S.E., Westin, S., Mullen, T.M., Krones, A., Inostroza, J., Torchia, J., Nolte, R.T., Assa-Munt, N., *et al.* (1998). Determinants of coactivator LXXLL motif specificity in nuclear receptor transcriptional activation. *Genes Dev* 12, 3357-3368.
- Mendjan, S., Taipale, M., Kind, J., Holz, H., Gebhardt, P., Schelder, M., Vermeulen, M., Buscaino, A., Duncan, K., Mueller, J., *et al.* (2006). Nuclear pore components are involved in the transcriptional regulation of dosage compensation in *Drosophila*. *Mol Cell* 21, 811-823.
- Meng, Z.X., Nie, J., Ling, J.J., Sun, J.X., Zhu, Y.X., Gao, L., Lv, J.H., Zhu, D.Y., Sun, Y.J., and Han, X. (2009). Activation of liver X receptors inhibits pancreatic islet beta cell proliferation through cell cycle arrest. *Diabetologia* 52, 125-135.
- Mihaylova, M.M., Vasquez, D.S., Ravnskjaer, K., Denechaud, P.D., Yu, R.T., Alvarez, J.G., Downes, M., Evans, R.M., Montminy, M., and Shaw, R.J. (2011). Class IIa Histone Deacetylases Are Hormone-Activated Regulators of FOXO and Mammalian Glucose Homeostasis. *Cell* 145, 607-621.
- Muller, J., Hart, C.M., Francis, N.J., Vargas, M.L., Sengupta, A., Wild, B., Miller, E.L., O'Connor, M.B., Kingston, R.E., and Simon, J.A. (2002). Histone methyltransferase activity of a *Drosophila* Polycomb group repressor complex. *Cell* 111, 197-208.

- Muller, U. (1999). Ten years of gene targeting: targeted mouse mutants, from vector design to phenotype analysis. *Mech Dev* 82, 3-21.
- Muoio, D.M., and Newgard, C.B. (2008). Mechanisms of disease: molecular and metabolic mechanisms of insulin resistance and beta-cell failure in type 2 diabetes. *Nat Rev Mol Cell Biol* 9, 193-205.
- Naaz, A., Holsberger, D.R., Iwamoto, G.A., Nelson, A., Kiyokawa, H., and Cooke, P.S. (2004). Loss of cyclin-dependent kinase inhibitors produces adipocyte hyperplasia and obesity. *FASEB J* 18, 1925-1927.
- Neer, E.J., Schmidt, C.J., and Smith, T. (1993). LIS is more. *Nat Genet* 5, 3-4.
- Nielsen, J.H., Galsgaard, E.D., Moldrup, A., Friedrichsen, B.N., Billestrup, N., Hansen, J.A., Lee, Y.C., and Carlsson, C. (2001). Regulation of beta-cell mass by hormones and growth factors. *Diabetes* 50 Suppl 1, S25-29.
- Nikolova, G., Jabs, N., Konstantinova, I., Domogatskaya, A., Tryggvason, K., Sorokin, L., Fassler, R., Gu, G., Gerber, H.P., Ferrara, N., *et al.* (2006). The vascular basement membrane: a niche for insulin gene expression and Beta cell proliferation. *Dev Cell* 10, 397-405.
- Oberoi, J., Fairall, L., Watson, P.J., Yang, J.C., Czimmerer, Z., Kampmann, T., Goult, B.T., Greenwood, J.A., Gooch, J.T., Kallenberger, B.C., *et al.* (2011). Structural basis for the assembly of the SMRT/NCoR core transcriptional repression machinery. *Nat Struct Mol Biol* 18, 177-184.
- Perissi, V., Jepsen, K., Glass, C.K., and Rosenfeld, M.G. (2010). Deconstructing repression: evolving models of co-repressor action. *Nat Rev Genet* 11, 109-123.

- Pfleger, C.M., and Kirschner, M.W. (2000). The KEN box: an APC recognition signal distinct from the D box targeted by Cdh1. *Genes Dev* 14, 655-665.
- Philipp, J., Vo, K., Gurley, K.E., Seidel, K., and Kemp, C.J. (1999). Tumor suppression by p27Kip1 and p21Cip1 during chemically induced skin carcinogenesis. *Oncogene* 18, 4689-4698.
- Philipps, D.L., Wigglesworth, K., Hartford, S.A., Sun, F., Pattabiraman, S., Schimenti, K., Handel, M., Eppig, J.J., and Schimenti, J.C. (2008). The dual bromodomain and WD repeat-containing mouse protein BRWD1 is required for normal spermiogenesis and the oocyte-embryo transition. *Dev Biol* 317, 72-82.
- Pickles, L.M., Roe, S.M., Hemingway, E.J., Stifani, S., and Pearl, L.H. (2002). Crystal structure of the C-terminal WD40 repeat domain of the human Groucho/TLE1 transcriptional corepressor. *Structure* 10, 751-761.
- Pilkis, S.J., and Granner, D.K. (1992). Molecular physiology of the regulation of hepatic gluconeogenesis and glycolysis. *Annu Rev Physiol* 54, 885-909.
- Plevin, M.J., Mills, M.M., and Ikura, M. (2005). The LxxLL motif: a multifunctional binding sequence in transcriptional regulation. *Trends Biochem Sci* 30, 66-69.
- Podcheko, A., Northcott, P., Bikopoulos, G., Lee, A., Bommareddi, S.R., Kushner, J.A., Farhang-Fallah, J., and Rozakis-Adcock, M. (2007). Identification of a WD40 repeat-containing isoform of PHIP as a novel regulator of beta-cell growth and survival. *Mol Cell Biol* 27, 6484-6496.
- Price, M., Lang, M.G., Frank, A.T., Goetting-Minesky, M.P., Patel, S.P., Silveira, M.L., Krady, J.K., Milner, R.J., Ewing, A.G., and Day, J.R. (2003).

Seven cDNAs enriched following hippocampal lesion: possible roles in neuronal responses to injury. *Brain Res Mol Brain Res* 117, 58-67.

Privalsky, M.L. (2004). The role of corepressors in transcriptional regulation by nuclear hormone receptors. *Annu Rev Physiol* 66, 315-360.

Reiner, O., Carrozzo, R., Shen, Y., Wehnert, M., Faustinella, F., Dobyns, W.B., Caskey, C.T., and Ledbetter, D.H. (1993). Isolation of a Miller-Dieker lissencephaly gene containing G protein beta-subunit-like repeats. *Nature* 364, 717-721.

Rhodes, C.J. (2005). Type 2 diabetes-a matter of beta-cell life and death? *Science* 307, 380-384.

Riethoven, J.J. (2010). Regulatory regions in DNA: promoters, enhancers, silencers, and insulators. *Methods Mol Biol* 674, 33-42.

Ritzel, R.A., Butler, A.E., Rizza, R.A., Veldhuis, J.D., and Butler, P.C. (2006). Relationship between beta-cell mass and fasting blood glucose concentration in humans. *Diabetes Care* 29, 717-718.

Roberts, S.G. (2000). Mechanisms of action of transcription activation and repression domains. *Cell Mol Life Sci* 57, 1149-1160.

Rohner-Jeanrenaud, F., and Jeanrenaud, B. (1985). Involvement of the cholinergic system in insulin and glucagon oversecretion of genetic preobesity. *Endocrinology* 116, 830-834.

Ron, D., Chen, C.H., Caldwell, J., Jamieson, L., Orr, E., and Mochly-Rosen, D. (1994). Cloning of an intracellular receptor for protein kinase C: a homolog of the beta subunit of G proteins. *Proc Natl Acad Sci U S A* 91, 839-843.

- Rosen, E.D., and MacDougald, O.A. (2006). Adipocyte differentiation from the inside out. *Nat Rev Mol Cell Biol* 7, 885-896.
- Rosen, E.D., and Spiegelman, B.M. (2000). Molecular regulation of adipogenesis. *Annu Rev Cell Dev Biol* 16, 145-171.
- Rosenfeld, M.G., Lunyak, V.V., and Glass, C.K. (2006). Sensors and signals: a coactivator/corepressor/epigenetic code for integrating signal-dependent programs of transcriptional response. *Genes Dev* 20, 1405-1428.
- Roy, A., and Matzuk, M.M. (2006). Deconstructing mammalian reproduction: using knockouts to define fertility pathways. *Reproduction* 131, 207-219.
- Rulifson, I.C., Karnik, S.K., Heiser, P.W., ten Berge, D., Chen, H., Gu, X., Taketo, M.M., Nusse, R., Hebrok, M., and Kim, S.K. (2007). Wnt signaling regulates pancreatic beta cell proliferation. *Proc Natl Acad Sci U S A* 104, 6247-6252.
- Sadlack, B., Merz, H., Schorle, H., Schimpl, A., Feller, A.C., and Horak, I. (1993). Ulcerative colitis-like disease in mice with a disrupted interleukin-2 gene. *Cell* 75, 253-261.
- Saltiel, A.R., and Kahn, C.R. (2001). Insulin signalling and the regulation of glucose and lipid metabolism. *Nature* 414, 799-806.
- Sano, H., Egeuz, L., Teruel, M.N., Fukuda, M., Chuang, T.D., Chavez, J.A., Lienhard, G.E., and McGraw, T.E. (2007). Rab10, a target of the AS160 Rab GAP, is required for insulin-stimulated translocation of GLUT4 to the adipocyte plasma membrane. *Cell Metab* 5, 293-303.

Shirayama, M., Zachariae, W., Ciosk, R., and Nasmyth, K. (1998). The Polo-like kinase Cdc5p and the WD-repeat protein Cdc20p/fizzy are regulators and substrates of the anaphase promoting complex in *Saccharomyces cerevisiae*. *EMBO J* 17, 1336-1349.

Simon, J., and Leclercq, B. (1985). Fat and lean chickens: prefattening period and in vivo sensitivity to insulin, atropine, and propranolol. *Am J Physiol* 249, R393-401.

Singh, B.N., Suresh, A., UmaPrasad, G., Subramanian, S., Sultana, M., Goel, S., Kumar, S., and Singh, L. (2003). A highly conserved human gene encoding a novel member of WD-repeat family of proteins (WDR13). *Genomics* 81, 315-328.

Sinha Hikim, A.P., and Swerdloff, R.S. (1999). Hormonal and genetic control of germ cell apoptosis in the testis. *Rev Reprod* 4, 38-47.

Smith, A.G., Heath, J.K., Donaldson, D.D., Wong, G.G., Moreau, J., Stahl, M., and Rogers, D. (1988). Inhibition of pluripotential embryonic stem cell differentiation by purified polypeptides. *Nature* 336, 688-690.

Smith, T.F. (2008). Diversity of WD-repeat proteins. *Subcell Biochem* 48, 20-30.

Smith, T.F., Gaitatzes, C., Saxena, K., and Neer, E.J. (1999). The WD repeat: a common architecture for diverse functions. *Trends Biochem Sci* 24, 181-185.

Song, B., Scheuner, D., Ron, D., Pennathur, S., and Kaufman, R.J. (2008). Chop deletion reduces oxidative stress, improves beta cell function, and

promotes cell survival in multiple mouse models of diabetes. *J Clin Invest* 118, 3378-3389.

Southern, E.M. (1975). Detection of specific sequences among DNA fragments separated by gel electrophoresis. *J Mol Biol* 98, 503-517.

Steimle, P.A., Naismith, T., Licate, L., and Egelhoff, T.T. (2001). WD repeat domains target dictyostelium myosin heavy chain kinases by binding directly to myosin filaments. *J Biol Chem* 276, 6853-6860.

Sterner, D.E., and Berger, S.L. (2000). Acetylation of histones and transcription-related factors. *Microbiol Mol Biol Rev* 64, 435-459.

Stewart, C.L., Kaspar, P., Brunet, L.J., Bhatt, H., Gadi, I., Kontgen, F., and Abbondanzo, S.J. (1992). Blastocyst implantation depends on maternal expression of leukaemia inhibitory factor. *Nature* 359, 76-79.

Suarez-Pinzon, W.L., Yan, Y., Power, R., Brand, S.J., and Rabinovitch, A. (2005). Combination therapy with epidermal growth factor and gastrin increases beta-cell mass and reverses hyperglycemia in diabetic NOD mice. *Diabetes* 54, 2596-2601.

Suganuma, T., Gutierrez, J.L., Li, B., Florens, L., Swanson, S.K., Washburn, M.P., Abmayr, S.M., and Workman, J.L. (2008a). ATAC is a double histone acetyltransferase complex that stimulates nucleosome sliding. *Nat Struct Mol Biol* 15, 364-372.

Suganuma, T., Pattenden, S.G., and Workman, J.L. (2008b). Diverse functions of WD40 repeat proteins in histone recognition. *Genes Dev* 22, 1265-1268.

Suresh, A., Shah, V., Rani, D.S., Singh, B.N., Prasad, G.U., Subramanian, S., Kumar, S., and Singh, L. (2005). A mouse gene encoding a novel member of the WD family of proteins is highly conserved and predominantly expressed in the testis (Wdr13). *Mol Reprod Dev* 72, 299-310.

Takagaki, Y., and Manley, J.L. (1992). A human polyadenylation factor is a G protein beta-subunit homologue. *J Biol Chem* 267, 23471-23474.

Takahashi, K., and Yamanaka, S. (2006). Induction of pluripotent stem cells from mouse embryonic and adult fibroblast cultures by defined factors. *Cell* 126, 663-676.

Tang, Q.Q., Otto, T.C., and Lane, M.D. (2003). CCAAT/enhancer-binding protein beta is required for mitotic clonal expansion during adipogenesis. *Proc Natl Acad Sci U S A* 100, 850-855.

Taniguchi, C.M., Emanuelli, B., and Kahn, C.R. (2006). Critical nodes in signalling pathways: insights into insulin action. *Nat Rev Mol Cell Biol* 7, 85-96.

Terauchi, Y., Takamoto, I., Kubota, N., Matsui, J., Suzuki, R., Komeda, K., Hara, A., Toyoda, Y., Miwa, I., Aizawa, S., *et al.* (2007). Glucokinase and IRS-2 are required for compensatory beta cell hyperplasia in response to high-fat diet-induced insulin resistance. *J Clin Invest* 117, 246-257.

Thorel, F., Nepote, V., Avril, I., Kohno, K., Desgraz, R., Chera, S., and Herrera, P.L. (2010). Conversion of adult pancreatic alpha-cells to beta-cells after extreme beta-cell loss. *Nature* 464, 1149-1154.

Troelstra, C., van Gool, A., de Wit, J., Vermeulen, W., Bootsma, D., and Hoeijmakers, J.H. (1992). ERCC6, a member of a subfamily of putative

helicases, is involved in Cockayne's syndrome and preferential repair of active genes. *Cell* 71, 939-953.

Tullio-Pelet, A., Salomon, R., Hadj-Rabia, S., Mugnier, C., de Laet, M.H., Chaouachi, B., Bakiri, F., Brottier, P., Cattolico, L., Penet, C., *et al.* (2000). Mutant WD-repeat protein in triple-A syndrome. *Nat Genet* 26, 332-335.

Tulsiani, D.R., Yoshida-Komiya, H., and Araki, Y. (1997). Mammalian fertilization: a carbohydrate-mediated event. *Biol Reprod* 57, 487-494.

Tyler, J.K., Bulger, M., Kamakaka, R.T., Kobayashi, R., and Kadonaga, J.T. (1996). The p55 subunit of *Drosophila* chromatin assembly factor 1 is homologous to a histone deacetylase-associated protein. *Mol Cell Biol* 16, 6149-6159.

Verreault, A., Kaufman, P.D., Kobayashi, R., and Stillman, B. (1996). Nucleosome assembly by a complex of CAF-1 and acetylated histones H3/H4. *Cell* 87, 95-104.

Wall, M.A., Coleman, D.E., Lee, E., Iniguez-Lluhi, J.A., Posner, B.A., Gilman, A.G., and Sprang, S.R. (1995). The structure of the G protein heterotrimer Gi alpha 1 beta 1 gamma 2. *Cell* 83, 1047-1058.

Wang, Z., Zang, C., Cui, K., Schones, D.E., Barski, A., Peng, W., and Zhao, K. (2009). Genome-wide mapping of HATs and HDACs reveals distinct functions in active and inactive genes. *Cell* 138, 1019-1031.

Waters, M.G., Serafini, T., and Rothman, J.E. (1991). 'Coatomer': a cytosolic protein complex containing subunits of non-clathrin-coated Golgi transport vesicles. *Nature* 349, 248-251.

Webb, P., Anderson, C.M., Valentine, C., Nguyen, P., Marimuthu, A., West, B.L., Baxter, J.D., and Kushner, P.J. (2000). The nuclear receptor corepressor (N-CoR) contains three isoleucine motifs (I/LXXII) that serve as receptor interaction domains (IDs). *Mol Endocrinol* 14, 1976-1985.

Welch, M.D., DePace, A.H., Verma, S., Iwamatsu, A., and Mitchison, T.J. (1997). The human Arp2/3 complex is composed of evolutionarily conserved subunits and is localized to cellular regions of dynamic actin filament assembly. *J Cell Biol* 138, 375-384.

Welcker, M., and Clurman, B.E. (2008). FBW7 ubiquitin ligase: a tumour suppressor at the crossroads of cell division, growth and differentiation. *Nat Rev Cancer* 8, 83-93.

Wen, T., Peng, B., and Pintar, J.E. (2009). The MOR-1 opioid receptor regulates glucose homeostasis by modulating insulin secretion. *Mol Endocrinol* 23, 671-678.

Whibley, A.C., Plagnol, V., Tarpey, P.S., Abidi, F., Fullston, T., Choma, M.K., Boucher, C.A., Shepherd, L., Willatt, L., Parkin, G., *et al.* (2010). Fine-scale survey of X chromosome copy number variants and indels underlying intellectual disability. *Am J Hum Genet* 87, 173-188.

Willing, A.E., Walls, E.K., and Koopmans, H.S. (1990). Insulin infusion stimulates daily food intake and body weight gain in diabetic rats. *Physiol Behav* 48, 893-898.

Wu, C.L., and Melton, D.W. (1993). Production of a model for Lesch-Nyhan syndrome in hypoxanthine phosphoribosyltransferase-deficient mice. *Nat Genet* 3, 235-240.

Wysocka, J., Swigut, T., Milne, T.A., Dou, Y., Zhang, X., Burlingame, A.L., Roeder, R.G., Brivanlou, A.H., and Allis, C.D. (2005). WDR5 associates with histone H3 methylated at K4 and is essential for H3 K4 methylation and vertebrate development. *Cell* 121, 859-872.

Xu, G., Stoffers, D.A., Habener, J.F., and Bonner-Weir, S. (1999). Exendin-4 stimulates both beta-cell replication and neogenesis, resulting in increased beta-cell mass and improved glucose tolerance in diabetic rats. *Diabetes* 48, 2270-2276.

Xue, Y., Wong, J., Moreno, G.T., Young, M.K., Cote, J., and Wang, W. (1998). NURD, a novel complex with both ATP-dependent chromatin-remodeling and histone deacetylase activities. *Mol Cell* 2, 851-861.

Zhang, Y., Ng, H.H., Erdjument-Bromage, H., Tempst, P., Bird, A., and Reinberg, D. (1999). Analysis of the NuRD subunits reveals a histone deacetylase core complex and a connection with DNA methylation. *Genes Dev* 13, 1924-1935.

Zou, H., Henzel, W.J., Liu, X., Lutschg, A., and Wang, X. (1997). Apaf-1, a human protein homologous to *C. elegans* CED-4, participates in cytochrome c-dependent activation of caspase-3. *Cell* 90, 405-413.

TH-1976

